Development and application of a porcine model of deep venous thrombosis

Adeline Schwein

UNIVERSITÉ DE STRASBOURG

Ecole doctorale Sciences de la Vie et de la Santé

Mitochondries, Stress Oxydant et Protection Musculaire – EA 3072

Thèse présentée pour obtenir le grade de

Docteur de l'Université de Strasbourg

***Discipline** : Sciences de la vie et de la santé*

MISE AU POINT ET APPLICATIONS D'UN MODELE PORCIN DE THROMBOSE VEINEUSE PROFONDE

Présentée et soutenue publiquement par

Adeline SCHWEIN

Le 28 novembre 2022

Membres du jury :

Rapporteur Externe : Professeur Philippe KOLH, Liège
Rapporteur Externe : Professeur Raphaël COSCAS, Boulogne Billancourt
Rapporteur Interne : Docteur Pierre MANGIN, Strasbourg
Examinateur Externe : Docteur Marianne DE MAESENEER, Rotterdam
Examinateur Interne : Professeur Anne LEJAY, Strasbourg
Directeur de Thèse : Professeur Nabil CHAKFE, Strasbourg
Co-directeur de Thèse : Professeur Jean BISMUTH, Houston

Invité :
Examinateur Interne : Professeur Frédéric HEIM, Mulhouse

REMERCIEMENTS

Je profite de ces quelques lignes pour remercier et rendre hommage à tous ceux qui, plus ou moins directement, ont participé à la réalisation de ce travail.

Je souhaiterais tout d'abord remercier mes deux directeurs de thèse, Messieurs les Professeurs Jean Bismuth et Nabil Chakfé, et leur exprimer toute ma gratitude. Vous avez su éveiller ma curiosité pour la recherche, me guider tout au long de ce travail, et me soutenir dans mes décisions ; grâce à vos conseils, votre rigueur et votre bienveillance, j'ai pu avancer sereinement et enfin arriver au bout de ce beau projet.

Je souhaite également remercier mes rapporteurs pour le temps qu'ils ont consacré à la lecture de cette thèse et à la rédaction de leur rapport : Monsieur le Professeur Philippe Kolh, Monsieur le Professeur Raphaël Coscas et Monsieur le Docteur Pierre Mangin. J'éprouve un profond respect pour vos travaux et vos parcours, ancrés dans différentes disciplines, et je vous remercie d'avoir accepté de juger cette thèse.

A Madame le Docteur Marianne De Maesenneer, je suis très reconnaissante et heureuse que vous ayez accepté de faire partie de ce jury de thèse. Vous avez grandement participé à l'amélioration de la connaissance et de la prise en charge de la pathologie veineuse. J'ai beaucoup appris en étudiant vos travaux et c'est un honneur pour moi de pouvoir bénéficier de votre expertise.

A Monsieur le Professeur Frédéric Heim, je te remercie chaleureusement d'avoir accepté de juger ce travail. J'ai pu apprécier de nombreuses fois tes qualités professionnelles, pédagogiques, et humaines. C'est un honneur pour moi de te compter parmi les membres du jury.

Je tiens également tout particulièrement à remercier Madame le Professeur Anne Lejay. Merci infiniment pour tes conseils, ton écoute, ta disponibilité et ta gentillesse. Merci pour toute la confiance et les encouragements que tu me témoignes au quotidien ; travailler avec toi est un plaisir immense, et une chance incroyable.

Je remercie également toutes les personnes formidables que j'ai rencontrées grâce à ce travail, toute l'équipe du Houston Methodist Research Institute et du département de bio-ingénierie de Rice University : Ponraj, Tony, Judit, Kyle, Rebecca, Leslie, Dessy, Jane, Dipan, Hector, Marta, CJ, Maga and Courtney. Merci pour votre gentillesse, vos sourires et votre aide au quotidien face à tous les défis.

Que cette thèse soit également le reflet de toute mon affection pour mes collègues et amis du Service de Chirurgie Vasculaire : au Professeur Yannick Georg, tu connais toute l'estime que j'ai pour toi ; je suis heureuse de te compter comme ami.

Au Docteur Anne-Florence Rouby, merci de tout cœur pour ces deux années de clinicat passées à tes côtés ; je chéris tous les moments que nous avons partagés, nos premières et nos galères... Je n'aurais pas pu espérer meilleure co-chef, merci pour ton soutien sans faille, merci pour ton amitié.

Une dédicace particulière et un grand merci aux Docteurs Benjamin Del Tatto, Vincenzo Vento, Bogdan Bratu, Salomé Kuntz, Louis Magnus, Jonathan Grandhomme, et Ioan Gogeneata qui ont fait vivre notre bureau des chefs ; j'emporte avec moi les fous rires, les citations, les conseils et tous les beaux moments partagés.

Je voudrais également remercier tous ceux qui ont illuminés mes années de médecine, d'internat et de clinicat : Sophie, Stéphanie, Agathe, Thibault, Justine, Phiphi, Elvira, Urji, Mickaël, Guillaume, Charline, Gabrielle, Arielle, Sarah et tant d'autres.

Merci au FBB, aux copains d'Ohna, à Alma, Linette et Elisabeth : mes amis de toujours, à tous les beaux moments qui nous attendent.

Au moment de clore cette thèse, qui représente un chapitre important de ma vie professionnelle mais aussi personnelle, je souhaite remercier ceux qui m'ont accompagné et soutenu à chaque instant, dès le premier jour ; je dédie donc particulièrement cette thèse à mes Parents et à mon Frère. Je suis fière d'être votre fille et sœur, et je vous aime de tout mon cœur.

Et à Jacques, toi qui a déménagé ma vie.
Je chéris chaque instant à tes côtés, merci pour la vie que nous construisons et pour les belles aventures qui nous attendent.

TABLE OF CONTENTS

TABLE OF ILLUSTRATIONS

FIGURES

TABLES

ABBREVIATIONS

ANOVA	Analisys Of Variance
BMT	Best Medical Therapy
CBCT	Cone Beam Computed Tomography
CDT	Catheter Directed Thrombolysis
CIV	Common Iliac Vein
CVD	Chronic Venous Disease
DIC	Digital Image Correlation
DVT	Deep Venous Thrombosis
DW	Diffusion Weighted
EC	Endothelial Cell
ESVS	European Society for Vascular Surgery
FDA	Food and Drug Administration
IACUC	Institutional Animal Care and Use Committee
IVC	Inferior Vena Cava
MRI	Magnetic Resonance Imaging
MRV	Magnetic Resonance Venography
MT	Magnetization Transfer
NIH	National Institute of Health
PE	Pulmonary Embolism
PBS	Phosphate Buffered Saline
PMCDT	PharmacoMechanical Catheter Directed Thrombolysis
PTS	Post Thrombotic Syndrome
SD	Standard Deviation
SMC	Smooth Muscle Cell
TRS	Thrombus Removal Strategies
VTE	Venous ThromboEmbolism

PUBLICATIONS RELATED TO THE THESIS

Published original articles

- **Schwein A**, Magnus L, Markovits J, Chinnadurai P, Autry K, Jenkins L, Barnes R, Vekilov DP, Shah D, Chakfé N, Bismuth J. Endovascular porcine model of iliocaval venous thrombosis. *Eur J Vasc Endovasc Surg. 2022 Apr;63(4):623-630.*

Published review article

- **Schwein A**, Magnus L, Chakfé N, Bismuth J. Critical review of large animal models for central deep venous thrombosis. *Eur J Vasc Endovasc Surg. 2020 Aug;60(2):243-252.*
- **Schwein A**, Georg Y, Lejay A, Nicolini P, Hartung O, Contassot D, Thaveau F, Heim F, Chakfé N. Endovascular treatment for venous diseases: where are the venous stents? *Methodist Debakey Cardiovasc J. 2018 Jul-Sep(3);208-213.*

Submitted original article

- Vekilov DP, **Schwein A**, Magnus L, Bismuth J, Grande Allen KJ. Venous wall mechanical properties change after deep vein thrombosis: an experimental model (submitted)

Oral communication

- **Schwein A**, Markovits J, Chinnadurai P, Autry K, Jenkins L, Barnes R, Shah D, Chakfé N, Bismuth J. An innovative porcine model of acute and chronic central venous thrombosis mimicking human pathology. 10th European Symposium on Vascular Biomaterials, Strasbourg, France, 2017.

Book chapter

- Vekilov DP, **Schwein A**, Magnus L, Bismuth J, Grande Allen KJ. Venous wall mechanical properties change after deep vein thrombosis: an experimental model

INTRODUCTION

Venous thromboembolism (VTE) is a major healthcare issue in western countries, due to its frequency, its long-term complications and the costs generated. While best medical therapy (BMT) involving anticoagulation and elastic compression stockings is the recommended treatment of deep venous thrombosis (DVT) occurring in femoropopliteal and calf veins, BMT offers only suboptimal results, especially on post thrombotic syndrome (PTS), when DVT occurs in the common femoral vein, in the iliac veins or in the inferior vena cava (IVC)[1]. Therefore, the latest clinical practice guidelines from the European Society for Vascular Surgery (ESVS) recommend early thrombus removal strategies (TRS) in case of symptomatic acute iliofemoral DVT (Class IIa, Level A)[2].

TRS involves thrombolytic therapies and/or mechanical thrombectomy. Ideal timing of TRS after DVT symptoms onset is unclear. An objective and non-invasive method capable of identifying thrombus age or thrombus susceptibility to lysis is therefore needed and should help defining which group of patients will benefit the most from early TRS.

While both arteries and veins have a 3-layer architecture, their precise structural composition largely varies, affording completely different mechanical properties and function. Few studies have looked specifically at venous properties, and even less is known on the venous wall modifications occurring during DVT and after venous recanalisation, both in terms of structural composition and mechanical properties. Such knowledge is however needed for the design of specific endovascular devices for the treatment of persistent venous outflow obstruction after TRS or in patients with severe PTS.

Many animal models of venous thrombosis have been described in the literature[3–5]. Most of these models use small animals and focused mainly on studying the biology behind DVT and on developing pharmaceutical approaches[6,7].
Large animal models of DVT are indispensable to advance our knowledge on the natural history and the optimal management of the disease, as well as to provide adequate vehicles for the development, testing and evaluation of dedicated endovascular devices.

In this context, our objectives were as follows:

1. Review the existing literature on large animal models of DVT to select the ideal one, which should be technically simple, fast to perform, reproducible and form a consistent size of thrombosed vein with analogous characteristics to clinical human DVT.

2. Create acute and subacute iliocaval DVT in a large animal that should allow clinical imaging, management and follow-up, and that could be used for the development and evaluation of interventional management.

3. Use the model to further study non-invasive methods of thrombus characterization as well as the evolution of the mechanical properties of the thrombosed veins over time:

    a. Use magnetic resonance imaging (MRI) capabilities to characterize the created thrombus and its evolution over time, focusing on morphometric, image texture, and analysis of fibrin content.

b. Characterize the mechanical properties of healthy veins to serve as baseline values and conduct mechanical analysis of the venous wall of a porcine model of iliocaval DVT.

After having reminded important notions for the understanding of our problematics (current management of DVT, thrombus removal potential and mechanical properties of veins), we will present our research with dedicated discussions and perspectives, before a general conclusion.

STATE OF THE ART

1. DEEP VENOUS THROMBOSIS

The term of DVT describes the presence of thrombus within a deep vein of the body as proven by diagnostic imaging, more often in the leg and pelvic veins. Although often considered as a benign condition, inadequate management may lead to either short-term pulmonary embolism (PE) and death, or to long-term disabling venous obstruction and reflux, called PTS.
BMT, involving anticoagulation and elastic compression, has long been the only recommended management for DVT, whatever its anatomical location. Its results are however largely suboptimal for the prevention of PTS in case of DVT occurring in the ilio-femoral segment, opening the door for a new interventional paradigm of care for these patients[1].

1.1. Definitions

For the sake of standardization, specific terms have been defined to classify DVT according to their age and location[8].

1.1.1. Temporal definition

Acute DVT refers to venous thrombosis for which symptoms have been present for less than 14 days. Subacute DVT refers to venous thrombosis for which symptoms have been present for 15-28 days. Chronic DVT refers to venous thrombosis for which symptoms have been present for more than 28 days.
The term “recurrent DVT” should be used in case of DVT involving a new venous segment or a previously involved venous segment for which symptomatic and imaging improvement had been obtained in a patient with at least one prior episode of DVT.

1.1.2. Anatomical definition

The old term “proximal” DVT referred to the partial or complete occlusion of one or more of the following veins: popliteal vein, femoral vein, deep femoral vein, common femoral vein, iliac vein and IVC. Due to the large diversity of thrombus distribution and their different management, this term should be abandoned and replaced with femoropopliteal DVT, involving the popliteal, femoral and or deep femoral vein, or iliofemoral DVT, involving any part of the iliac and/or common femoral vein[9].
Distal or calf DVT refers to thrombosis of one or more deep calf veins (anterior tibial, posterior tibial, peroneal and/or deep muscular veins).

1.2. Epidemiology

VTE including DVT and PE is a major world-wide healthcare issue, with an estimated average annual incidence ranging from 104 to 183 per 100 000 persons in western countries, similar

incidence to that of stroke. Estimated incidence rates for symptomatic leg DVT alone range from 45 to 117 per 100 000 persons annually[10].
With an estimated total annual cost ranging from 1.5 to 13.2 billion of euros, VTE results in a considerable burden to healthcare systems; better preventive and treatment measures could lead to significant savings[11].
A recent observational study on 1338 patients presenting with acute DVT found a median age of DVT occurrence of 62 years old, with a ratio male/female of 1/1. Left sided DVT was predominant with 57% of the cases. Distal DVT limited to the calf veins happened in 28%, iliofemoral DVT occurred in 38% of the patients[9].

1.3. Pathophysiology

The Virchow's triad describes the three main pathophysiological factors implicated in venous thrombosis: increased blood procoagulant state, vein wall damage and venous stasis.

In the acute phase, the thrombotic process leads to physiological modifications (increased outflow resistance, increased venous pressure, changes in blood velocity, arterial inflow modification and hemodynamic changes in the microcirculation) as well as a complex inflammatory state[12]. The combination of altered hemodynamics and inflammation explains the clinical symptoms of acute DVT: swelling, pain and tenderness.
The anatomical level and extent of venous occlusion will influence the hemodynamic disturbances, which will determine the degree of symptoms; these are usually more severe as the thrombosis extends more proximally, translating to a greater degree of outflow obstruction.
Following acute DVT, spontaneous clot lysis over weeks and recanalization over months or years can be observed; the recanalization rate varies between DVT location: around 80% in calf veins but only 20% in the iliac segment[2]. Involvement of the iliac and common femoral veins is frequent and represent 28% to 38% of patients presenting with DVT[9,13].
Prolonged venous thrombosis will result in chronic venous outflow obstruction as well as secondary venous valve damage and reflux, possibly leading to the development of PTS.

1.4. Risk factors of DVT

When no clear precipitating risk factor can be identified, DVT is considered unprovoked.
Risk factors can either be hereditary, including non-O blood type, factor V Leiden gene polymorphism, deficiency of antithrombin, protein C or protein S, or more often acquired: cancer, immobility, surgery, trauma, acute medical illness, infection inflammatory diseases, pregnancy, long distance travel, hormone therapy and antiphospholipid syndrome[2].

1.5. Post-thrombotic syndrome

The PTS is a chronic complication of DVT affecting 20% to 50% of patients one to two years after DVT[14–17]. Symptoms are the result of chronic venous outflow caused by a combination of deep venous obstruction, valvular reflux and vein wall remodelling following a DVT. Its clinical

presentation includes all stages of the CEAP (Clinical Etiological Anatomical Pathophysiological) chronic venous disease (CVD) classification (Table 1)[18] and gathers pain, heaviness, discomfort, swelling and cramping in the leg; skin changes and venous ulcers are the most severe manifestations.

Class	Description
Clinical (C) class	
C0	No visible or palpable signs of venous disease
C1	Telangiectasia or reticular veins
C2	Varicose veins
C2r	Recurrent varicose veins
C3	Oedema
C4	Changes in skin and subcutaneous tissue secondary to CVD
C4a	Pigmentation or eczema
C4b	Lipodermatosclerosis or atrophie blanche
C4c	Corona phlebectatica
C5	Healed ulcer
C6	Active venous ulcer
C6r	Recurrent venous ulceration
Symptomatic or not: subscript 'S' or subscript 'A'	S: symptomatic, including ache, pain, tightness, skin irritation, heaviness, and muscle cramps, and other complaints attributable to venous dysfunction A: asymptomatic
Etiological (E) class	
Ep	Primary
Es	Secondary
Esi	Secondary – intravenous
Ese	Secondary – extravenous
Ec	Congenital
En	None identified
Anatomical (A) class	
As	Superficial
Ad	Deep
Ap	Perforators
An	No identifiable venous location
*Pathophysiological (P) class**	
Pr	Reflux
Po	Obstruction
Pr,o	Reflux and obstruction
Pn	No pathophysiology identified

* Reporting of pathophysiological class must be accompanied by the relevant anatomical location (see Table 4). CVD = chronic venous disease.

Table 1 : Clinical Etiological Anatomical Pathophysiological (CEAP) classification

Source: Lurie et al. J Vasc Surg: Venous and Lym Dis 2020;8:342-352

Many risk factors have been associated with the occurrence and severity of PTS: older age, obesity, history of ipsilateral DVT, proximal DVT affecting the ilio-femoral junction, pre-existing primary venous incompetence and inadequate anticoagulation during the first 3 months of treatment[19].

Prevention consists in optimizing anticoagulant treatment, adequate compression treatment, and also recently included TRS when indicated, as it has been demonstrated that BMT alone is not sufficient for the prevention and treatment of PTS[1].

The Villalta scale is a clinical tool based on these subjective and objective signs to diagnose and assess the severity of PTS (Table 2)[20,21].

A Villalta score ≥5 or the presence of venous ulcer in a leg with previous DVT defines the presence of PTS. The severity of the disease has been categorized in: mild for a Villalta score 5-9, moderate for a Villalta score 10-14 and severe for a Villalta score ≥15. In order to avoid confusion between PTS and acute symptoms of DVT, a time threshold of 3 months after symptom's onset has been established for PTS diagnosis[22].

Symptoms and Clinical signs	None	Mild	Moderate	Severe
Symptoms				
Pain	0 points	1 point	2 points	3 points
Cramps	0 points	1 point	2 points	3 points
Heaviness	0 points	1 point	2 points	3 points
Paresthesia	0 points	1 point	2 points	3 points
Pruritus	0 points	1 point	2 points	3 points
Clinical signs				
Pretibial edema	0 points	1 point	2 points	3 points
Skin induration	0 points	1 point	2 points	3 points
Hyperpigmentation	0 points	1 point	2 points	3 points
Redness	0 points	1 point	2 points	3 points
Venous ectasia	0 points	1 point	2 points	3 points
Pain on calf compression	0 points	1 point	2 points	3 points
Venous ulcer	Absent	Present		

Table 2 : Villalta's PTS scale

Source : Villalta et al. Haemostasis 1994;24:158a

Conservative management is the first line treatment and consists in supervised exercise training, compression treatment and pharmacotherapy.
Following the last ESVS clinical practice guidelines on the management of CVD, patients with severe PTS and iliac vein outflow obstruction should be considered for endovascular treatment[23].

1.6. Thrombus removal strategies in acute DVT

The aim of TRS is to remove the largest amount of venous thrombus to both avoid chronic venous outflow obstruction and venous valve damage, with the ultimate goal being to prevent PTS.
Clinical practice guidelines on the management of acute DVT suffer from a lack of consensus between countries and medical societies.

In 2012, the American Society for Vascular Surgery and the American Venous Forum published the first guidelines mentioning TRS. They suggest a strategy of early thrombus removal in selected patients with a first episode of acute iliofemoral DVT, with symptoms onset less than 14 days,

with a low risk of bleeding and good functional capacity and acceptable life expectancy[24]. They recommend the use of adjunctive self-expanding metallic stents for treatment of chronic iliocaval compression or obstructive lesions.

The ESVS published its first Guidelines on DVT in 2021; they recommend that early TRS be considered in selected patients with symptomatic iliofemoral deep vein thrombosis (Class IIa, Level A), whereas such strategies are not recommended for DVT limited to femoropopliteal or calf veins (Class III, Level B)[2]. The choice of TRS should be based on physician's judgement (Class IIa. Level C).

On the contrary, the American Society of Hematology 2020 guidelines suggest that, in most patients with proximal DVT, anticoagulation therapy alone should be used over thrombolytic therapy in addition to anticoagulation[25].
The 2019 guidelines on VTE management from the Thrombosis and Haemostasis Society of Australia and New Zealand state that catheter directed thrombolysis (CDT) may be considered in selected patients with extensive proximal DVT involving the common iliac vein (CIV) and low bleeding risk[26].

1.6.1. Techniques of TRS

Several techniques of TRS have been described over the years, with an increased proportion of minimally invasive and rapid management.

1.6.1.1. Surgical thrombectomy

Surgical thrombectomy of acute iliofemoral DVT is usually performed under general anaesthesia through a groin cut down. After common femoral venotomy, embolectomy of the iliac and/or IVC is performed using a Fogarty catheter. If DVT extends to the femoropopliteal or calf veins, manual massage of the whole leg, starting from the foot, should be enough to extract the thrombus.
The creation of a temporary arteriovenous fistula is usually indicated to maintain patency in the first postoperative weeks.

1.6.1.2. Percutaneous mechanical thrombectomy

This procedure uses mechanical forces to remove thrombus while avoiding surgical cutdowns and thrombolystic therapies; it thus remains a minimally invasive technique using either standard endovascular material (large sheeths and/or catheters to perform thrombo-aspiration of the clot), or dedicated endovascular catheters i. e. the Indigo Aspiration System (Penumbra, Inc., Alameda, CA, USA) or the FlowTriever (Inari Medical, Irvine, CA, USA).

1.6.1.3. Catheter directed thrombolysis

CDT has been practiced for the last 20 years and is considered to be a minimally invasive procedure for acute thrombus removal in comparison to surgical thrombectomy. The technique consists in placing a multiple perforated catheter directly within the thrombosed venous segment in order to infuse thrombolytics.
The puncture site should usually be thrombus free, either the popliteal vein, the great saphenous vein, the jugular vein or the contralateral common femoral vein. Local thrombolytics are administrated in addition to systemic anticoagulation. The duration of lysis is dependent on radiological disappearance of thrombus in daily venograms.

1.6.1.4. Pharmacomechanical catheter directed thrombolysis

This procedure combines local infusion of thrombolytic therapies with catheter-based devices for mechanical retrieval of the thrombus, in order to accelerate thrombus removal, from several days with CDT to one single procedure with pharmacomechanical catheter directed thrombolysis (PMCDT). Several pharmacomechanical catheters are currently available and differ by their mechanical aspects: pulsatile saline jets via Venturi effect (Angiojet peripheral thrombectomy system, Boston Scientific, Natick, MA, USA); low-energy high-frequency ultrasound (Ekos Endovascular System, Boston Scientific, Natick, MA, USA).

1.6.1.5. Adjunct endovascular stenting

For all the above-mentioned techniques, additional stenting may be needed depending on the presence of remaining iliac obstruction on venograms, caused either by extrinsic venous compression or residual non-resolved thrombus material.

1.6.2. Results of early TRS

The effectiveness of CDT and PMCDT versus anticoagulation alone in reducing PTS after DVT has been evaluated in four randomized clinical trials (RCT): (TORPEDO [Thrombus Obliteration by Rapid Percutaneous Endovenous Intervention in Deep Venous Occlusion], CaVenT [Catheter-Directed Venous Thrombolysis in Acute Iliofemoral Vein Thrombosis], ATTRACT [Acute Venous Thrombosis: Thrombus Removal with Adjunctive Catheter-Directed Thrombolysis], and CAVA [CAtheter Versus Anticoagulation Alone for Acute Primary Iliofemoral DVT]); all of them unfortunately had severe methodological and technological flaws[27–31].

CaVenT and TORPEDO showed significant reduction in PTS occurrence after CDT/PMCDT strategies for acute DVT; CaVenT, being the most significant study, reported an absolute risk reduction of PTS occurrence of 14.4% and 28% at 2 and 5 years of follow-up respectively when comparing CDT to anticoagulation alone.

On the contrary, ATTRACT and CAVA did not show a significant difference between CDT/PMCDT and anticoagulation for acute DVT alone at 1 and 2 years of follow-up, but demonstrated an increased risk of major bleeding following PMCDT.
Results of these four RCTs are contradictory; above all, limitations are multiple and relevant: inclusion of femoropopliteal DVTs, very long inclusion periods, lack of statistical power, high rate of consent withdraw, market retrieval of the used PMCDT, no clear postoperative surveillance, low rate of stenting…

A meta-analysis of the four RCTs showed evidence of better results of CDT/PMCDT strategies than anticoagulation alone in preventing any PTS (p = 0.05) and, particularly in preventing moderate to severe PTS (p = 0.02), with however an increased risk of major bleeding (RR = 5.68, p = 0.02) (Figure 1 and 2)[2].
The following factors have been associated with better outcomes of TRS: symptoms duration less than 14 days, pulse-spray infusion strategy and the absence of previous post-thrombotic lesions[32].

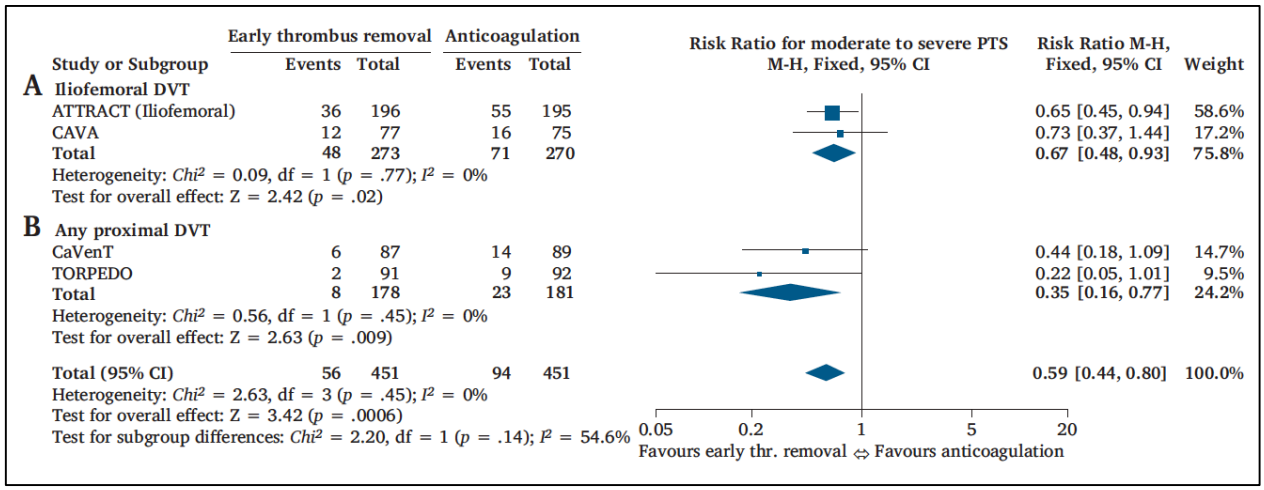

Figure 1: Randomized controlled trials results of TRS on PTS outcome

Forest plot analysis of randomized controlled trials comparing early TRS with anticoagulation alone regarding the outcome of moderate to severe PTS in patients with (A) iliofemoral DVT or (B) any proximal DVT.
Source: Kakkos et al, EJVES 2020 ;63 :184-267

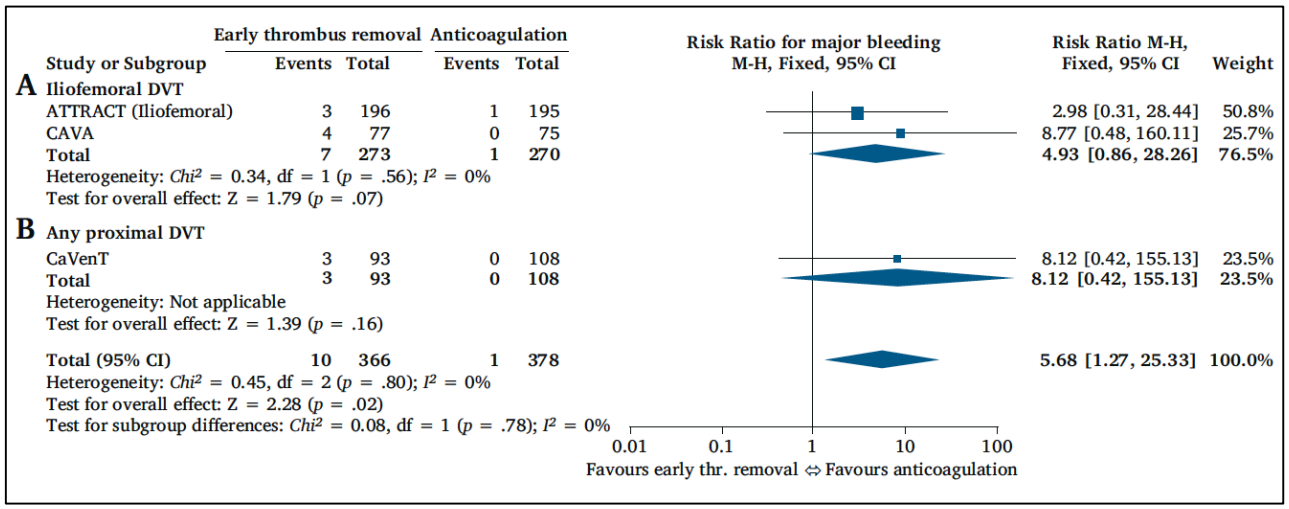

Figure 2 : **Randomized controlled trials results of TRS on major bleeding outcome**

Forest plot analysis of randomized controlled trials comparing early TRS with anticoagulation alone regarding the outcome major bleeding in patients with (A) iliofemoral DVT or (B) any proximal DVT.

Source: Kakkos et al, EJVES 2020 ;63 :184-267

1.7. Endovascular treatment for obstructive venous disease

Following the last European clinical practice guidelines on the management of CVD, patients with severe PTS and iliac vein outflow obstruction should be considered for endovascular treatment (Class IIa, Level B)[23].

The use of adjunctive balloon angioplasty and stenting for the treatment of persistent iliocaval compression or obstructive lesions after TRS for acute DVT is also recommended.

There are innumerable devices and tools available to treat arterial pathologies (e.g., angioplasty balloons, stents, stent grafts, drug-eluting devices, atherectomy devices, guidewires and catheters), but, back in 2018, not a single FDA-approved balloon or stent had been specifically designed for venous purposes.

As a result, surgeons routinely use arterial devices to treat all types of venous pathologies.

Although veins and arteries are both vessels, they have very different functions, structural constitutions, mechanical properties, flow patterns and pathologies. In addition, blood flow pressure and velocity vary drastically between the arterial and venous systems. The consequences of these differences were demonstrated in a pilot study by Gordon et al., who deployed a similar stent graft in both the abdominal aorta and IVC of two pigs and evaluated the results after 1 month using contrast angiography and histology[33]. While the stents deployed in the arterial system demonstrated no stenosis on angiography and minimal in-stent intimal proliferation on histology, the same stents deployed in the venous system showed evidence of significant in-stent stenosis

and increased intimal hyperplasia with fibrin deposition. It is unknown whether these differences in stent patency and neointimal hyperplasia were due to blood flow, vessel characteristics, or the specific interaction between one type of device and a particular vessel.

In the literature, long-term results of venous balloon angioplasty and stenting are inconsistent. A recent systematic review found that global primary and secondary patency rates range from 32% to 98.7% and 66% to 96%, respectively[34]. Moreover, patency rates are even lower for thrombotic lesions than for nonthrombotic lesions, with inconsistent clinical improvement[35]. It is not yet known whether this variability is due to venous wall remodeling after DVT, to the stent's characteristics, or to something else.

Summary

DVT is a major healthcare issue with possible evolution towards chronic disabling PTS, especially when the iliofemoral segment is affected.

A meta-analysis of the four existing RCTs showed evidence of better results of TRS than anticoagulation alone, particularly in preventing moderate to severe PTS, with however an increased risk of major bleeding.

Endovascular devices used to treat venous occlusive diseases should be specifically developed and tested for the venous system.

2. CAPABILITY OF RESOLVING THROMBUS

As seen above, several practice guidelines from different societies of vascular surgery recommend TRS for acute ilio-femoral DVT. They are effective in recanalizing veins and preventing post-thrombotic complications; but they are also at risk of potentially severe complications, especially the increased risk of bleeding when using thrombolytic therapies with a reported range of major bleeding with CDT going from 2.2% to 3.3%[27,36].
Further practical guidelines should focus on which patients would actually benefit the most from TRS, there is indeed currently no consensus on selection criteria.

2.1. Timing of thrombus removal strategies

Optimal timing of treatment after symptoms onset is one of the unknowns; the success of venous recanalization, preservation of valve function and symptom relief may depend on the timing of treatment. What is the time threshold for a maximum of effectiveness with the minimal risks of advert events?
Clinical history and delay to symptoms onset are usually used to determine thrombus age, these are however subjective and unreliable[37]. Moreover, the beginning of thrombus presence, especially when partially occluding the vein, happens before symptoms onset.
Young thrombi are thought to be easier to mechanically retrieve and to be more responsive to thrombolysis. The threshold of 14 days has been shown to be a factor associated with better outcomes of TRS[32].
There is however no consensus on the optimal timing for efficient TRS: both thresholds of 14 and 21 days after symptoms onset have been used in RCTs[27,28,30]; the current clinical practice guidelines also do not give consensual answer: while the american guidelines indicate the threshold of 14 days, the European ones remain vague and only recommend “early” TRS[2,24].
This period of 14 days after symptoms onset is the most frequently mentioned, but seems however unprecise, since we have to rely on duration of patient complaints to estimate this period. There is currently no objective measurement to define the time threshold beyond which TRS is no longer efficient.

2.2. Thrombus age assessment

From decades, the capability of determining thrombus age has put to work many researchers.

2.2.1. Histological methods

A recent systematic review focused on the different chronological phases of thrombus evolution used for forensics purpose[38]. Several subdivisions have been proposed over time, based on the association of specific immunohistochemical markers with histological analysis; the proposed international staging reference includes three phases, with thresholds at 1 week and 2 months (Table 3).

Phase	Histological Modification
1st Phase (1–7 Days)	Flowing blood on an eroded endothelium, eliciting a platelet plug and fibrin deposition with a layered growth (Zahn's lines). No reaction between endothelium and thrombus is visible. Erythrocytes are preserved and agglomerated. Initial white blood cells pyknosis. Monocytes cells with enlarged nuclei. Calcium is observed as precipitates with von Kossa stain. The thrombus at its initiation is firmly attached to a small portion of the vessel wall and is not easily removed to leave fragments in situ. On the contrary, a coagulum maintains the usual blood composition (i.e., prevailing red cells plus leukocytes and platelets and a fine network of fibrin), is not attached to the endothelium, and can be easily removed.
2nd Phase (2–8 Weeks)	Endothelial budding and proliferative changes of the medial ring are represented by the penetration of fibroblasts. Macrophages containing hemosiderin predominate, red blood cells ghosts and fibrinous transformation. The ribbons of fibrin changing to coalescences, trapping white cells. The free surface of thrombus is covered by the endothelium. Scattered nuclear debris of white blood cells
3rd Phase (More than 2 Months)	Completely hyalinized thrombus with central sinuous cavities and more advanced recanalizing neo-formed larger vessels with fresh flowing blood. Few white cells are visible between compact, fiber-rich and cell-deficient connective tissue.

Table 3 : **Histological age determination of thromboses and embolism**

Source:Di Fazio et al. Diagnostics 2021;11 :2397 / Fineschi et al. Forensinc Science International 2009 ;186 :22-28

A more precise evolution staging describes the transformation of thrombus in 6 phases through an overall period of 12 months. This classification allows a more precise differentiation of the early stages of DVT, with the first thresholds being at 5 days, 10 days and 4 weeks (Figure 3).

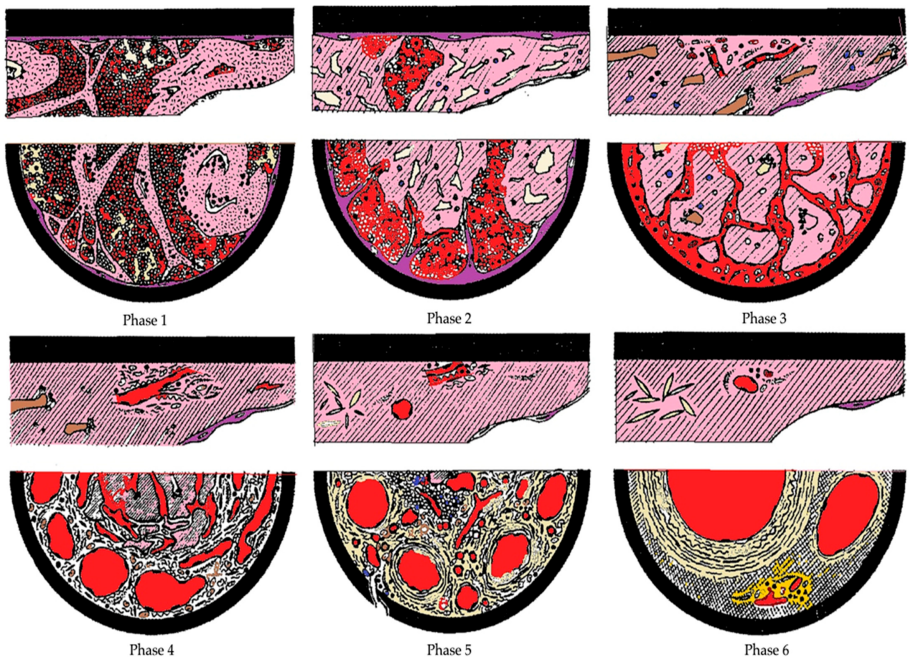

Figure 3: **Chronology of the microscopic changes related to thrombus organization**

Phase 1: Absence of reaction between endothelium and thrombus; leukocytes, platelets, and fibrin streaks are unaffected; erythrocytes agglomerated centrally and scattered peripherally.
Phase 2: At day five, penetration of endothelial buds; initial hyalinization, mainly central; pycnotic leukocytes and mononuclear cells enlarged; thrombus contraction may create fissures and cavities with erythrocytes inside.
Phase 3: By day 10, first capillaries, fibroblasts, mesenchymal cells and histiocytes with accumulations of hemosiderin; thrombus hyalinized and divided into large clumps; residual leukocyte nuclei.
Phase 4: From week four, argyrophilic fibres collagen; numerous capillaries.
Phase 5: From the eighth week to the eighth month, completely hyalinized thrombus and presence of fusiform cholesterol crystals; vascularized loose connective tissue; centrally sinuous spaces traversable by fresh blood.
Phase 6: After the sixth month, almost complete recanalization through large vessels separated by compact, fibrous connective tissue poor in cellular elements.
Source: Di Fazio et al. Diagnostics 2021;11 :2397

Immunohistochemical and immunofluorescence investigations led to a further step and allowed to establish even narrower time limits for early thrombus age determination: using a combination of the level of lymphocytic invasion and thrombus fibrosis, Mansueto et al. established a score system allowing to further subdivide early thrombus age with thresholds of 1 hour, 24 hours, 2 and 3 days[39].

2.2.2. Non-invasive imaging methods

Several non-invasive methods using various imaging modalities have shown their potential in thrombus age determination.

2.2.2.1. Duplex ultra sounds

Duplex ultrasound has been the gold standard for the diagnosis of DVT; ultrasonography related techniques have thus been widely investigated for venous thrombus aging. Elastography has rapidly been a rising method to try to chronologically classify thrombus. It is a non-invasive technique that uses deformation induced by manually compressing the transducer against the tissue of interest and measuring its displacement[40]. Such results allow to classify tissues according to their elasticity. Several pre-clinical and clinical studies found elastography and strain analysis to be efficient in differentiating acute to chronic thrombi; however, these techniques are still unable to prospectively estimate efficiency of thrombus removal or lysis[41,42].

2.2.2.2. Magnetic resonance imaging

The potential of MRI as imaging modality for DVT has been investigated for many years. Several features of the vein and thrombus have been described in a matter of determining thrombus age: In the acute phase, the vein is dilated because of luminal filling with thrombus material, the vein wall is thickened and surrounded by oedema due to the acute inflammatory response[43,44]. The appearance of signal heterogeneity within the thrombus is a possible sign of channel formation and venous recanalization in the subacute phase. The presence of structural remnants within a normal sized vein without signs of inflammation identifies an older stage of DVT. Based on this thrombus evolution, Arnoldussen et al. proposed a scoring system for MRI thrombus aging (Figure 4)[45].

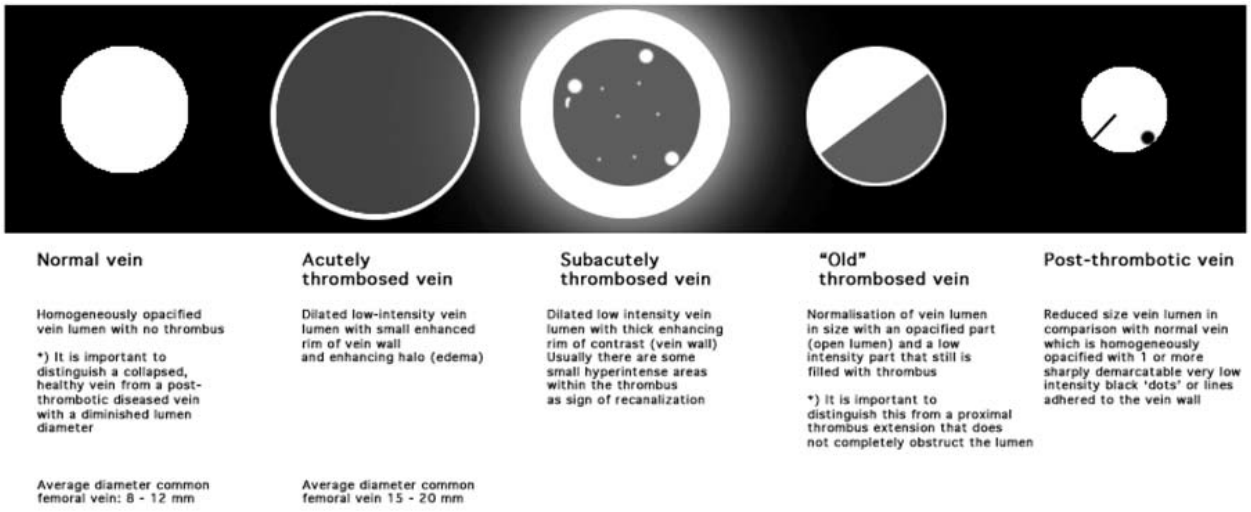

Figure 4: **Evolution of thrombus characteristics over time on MRI**

Source: Arnoldussen et al. Phlebology 2014;**29**(1 suppl):119–24

He recently showed good correlation between this MRI scoring system and procedural duration and success rate of CDT for patients with DVT, encouraging the use of MRI to enable a selection of patients who are most likely to benefit from CDT[46].

2.2.2.3. Molecular imaging

A few papers showed the capability of specific radiolabels to determine thrombus age. Technetium 99m-apticide was used to radiolabel activated platelets in patients with DVT and showed good results in determining between acute and chronic thrombi[47].

Despite many advances in imaging methods to characterize acute versus chronic stages, thrombus age is not always an informative determinant of the susceptibility to lysis. Studies in human showed that not all young venous thrombi can be lysed[48]; preclinical studies in a rabbit model also found that tissue plasminogen activator was more effective on 7-day-old thrombi than on 1 or 3-day-old thrombi[44,49].
An objective method capable of identifying thrombi susceptible to lysis is therefore needed.

2.3. Thrombus lysis

Venous thrombi resolve by a process of organization, which leads to vein recanalization.
Activation of coagulation ultimately generates thrombin, which results in thrombus formation by conversion of fibrinogen to fibrin and by platelet activation.
The process of thrombolysis, including many activators and inhibitors, will lead to the conversion of plasminogen to plasmin, the major fibrinolytic protease, which cleaves fibrin, generating soluble degradation products (Figure 5). The structure of the thrombus changes with cross-linked fibrin being gradually replaced by collagen[50,51].

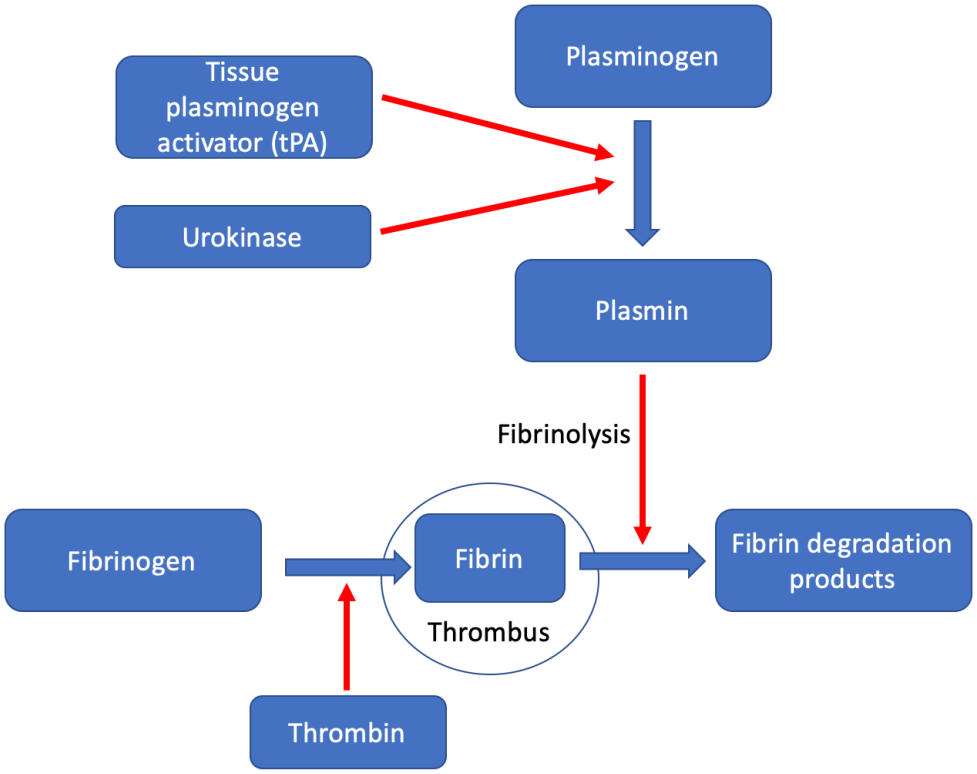

Figure 5 : **Simplified scheme of thrombus formation and lysis**

Experimental data suggest that fibrin-rich thrombi seem to be more amenable to thrombolysis, while incorporation of collagen into a fibrin clot dramatically decreases the effectiveness of fibrinolysis[52,53].

As thrombolytic therapies target fibrin within a thrombus, this molecule should represent an imaging target that could better direct lytic therapy[50]. In vivo quantification of the thrombus' fibrin content may therefore have the potential to guide therapy in terms of identifying patients suitable for thrombolysis.

2.4. Imaging assessment of the succes of thrombus lysis

Specifically targeting fibrin molecules within thrombus is possible with different imaging methods. MRI techniques have been the most promising recently.

Andia et al. showed that the use of a fibrin-specific contrast agent could accurately estimate thrombus fibrin content in a mouse model of DVT, and could thus identify amenable thrombi which are more susceptible to lysis by tissue plasminogen activator[54]. The same team published further results that highlighted specific MRI sequences (T1 mapping, magnetization transfer (MT) and diffusion weighted (DW)) as promising for the staging of thrombus composition in a mouse model of DVT, which could be translated into guiding thrombolysis efficiency[55,56].

Molecular imaging is also promising for non-invasive assessment of thrombus fibrin.
Technetium 99m-labelled rt-PA, specifically binding to fibrin, showed significant different uptake in 7-day-old thrombi versus 30-day-old thrombi[57].
A recent paper also described the use of a fibrin targeting probe using SPECT/CT in a mouse thrombosis model and showed specific binding to thrombi[58].

Summary

Optimal timing of TRS after symptoms onset is unknown. Several non-invasive imaging methods, including duplex ultrasound and MRI, have shown potential in determining thrombus age and ability to lysis. Further preclinical and clinical studies are needed to validate such imaging modalities as predictors of treatment success.

3. MECHANICAL PROPERTIES OF VEINS

Literature on vessels in both the clinical and scientific realms is heavily skewed toward arteries and greatly lacks information about veins.
Although the basic structure of arteries and veins is the same, there are huge differences in the relative constitution of their wall layers, creating vast differences in vessel mechanics. Thus, a thorough understanding of venous specific composition and material properties is required to properly treat venous disease.

3.1. Vessel Structure

Blood vessels are conduits ensuring blood transportation between the heart and the organs. They are composed of three layers that give them their unique material properties, allowing the ability to constrict and dilate as necessary during the cardiac cycle. These layers are called the intima, media, and adventitia; they variably contain vascular endothelial cells (ECs), smooth muscle cells (SMCs), collagen, and elastin (Figure 6)[59].
The innermost intima is a thin monolayer of ECs that align in the direction of blood flow. The cells are anchored to a basement membrane comprised of type IV collagen (internal elastic lamina)[60]. This thin layer of cells has little effect, if any at all, on the mechanical properties of the vessel wall. On the other side of the basement membrane is the media, which is composed of a network of elastin and collagen embedded with SMCs. The SMCs are arranged in circumferential sheets with elastin fibres running between them. The elastin forms a network of lamellae that allows stress to easily be distributed to other components of the vessel wall[61]. The elastin contributes little to the tensile strength of the wall, but is responsible for the vessel's elastic recoil. Collagen types I, III, and V are distributed throughout in dense bundles[62]. The collagen orientation appears random at low pressures, but once strained at high pressures, it quickly aligns circumferentially[63–65]. The collagen in the media exhibits extensive waviness, or crimp, which may contribute to the vessels' ability to constrict and dilate as necessary[66]. At high pressures, the collagen fibres prevent over-distention by supporting the tensile load[61].
The outer layer, the adventitia, is composed primarily of longitudinally oriented collagen type I[66]. The collagen in this layer forms thick bundles intermixed with elastin, fibroblasts, nerves, and the vasa vasorum, and it exhibits similar waviness to that in the media[66]. It is thought that this layer prevents excessive distension of the vessels and rupture at very high pressures[67].

The ability of the vessel wall to distend depends on the collagen content, and its elasticity is governed by the elastic fibers. Changes to these extracellular components can alter the mechanical abilities of the tissue. The relative ratios of collagen to elastin differ based on the location of the vessel relative to the heart, and these differences in composition affect the viscoelastic properties of the vessels[68].

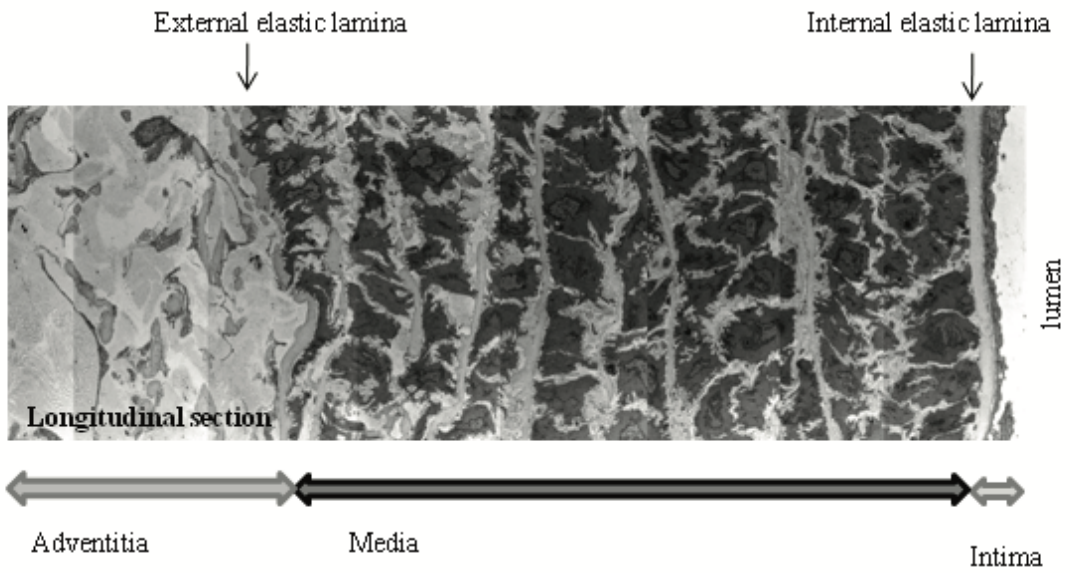

Figure 6 : **Blood vessel structure**

Source: Saitta-Rezakhaniha R. Fac Life Sci 2010;Dr. Sc.(4712):129.

3.2. Veins versus arteries

While the basic structure of both vessels is the same, the different pressures experienced by arteries and veins give rise to differences in the relative distribution of the layers (Figure 7).
Blood flow in veins is less influenced by the changing pressures of the cardiac cycle; pressures are thus typically steady at 3-20 mmHg, whereas pressures in arteries fluctuate vastly in response to pressures of the cardiac cycle (typically 80-130 mmHg).

Veins have larger diameters and larger lumens than arteries; at any given time, they hold about 2/3 of the body's blood volume[69].
In general, veins tend to have thinner, less organized walls: they have a thicker adventitia and a thinner media compared to arteries[59]. They also have higher collagen content and fewer SMCs[70].

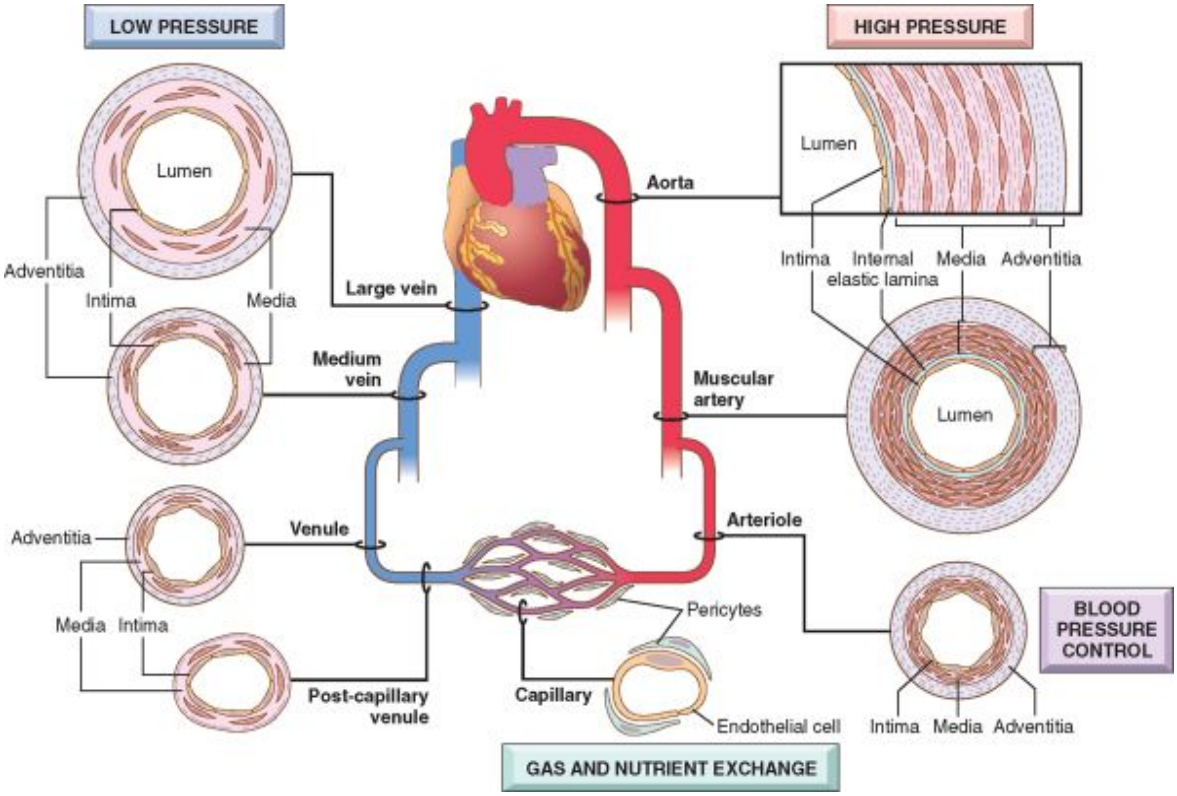

Figure 7 : Structural differences between arteries and veins

Source: Kumar V. Robbins and Cotran Pathologic Basis of Disease, 8th edition. 2010

3.3. Vessel mechanics

Vessels are constantly under multiple stresses, including shear stress along the intima induced by blood flow, longitudinal stress induced by tethering of the adventitia to other organs and tissues, and circumferential stress applied to the vessel wall by the blood pressure[61]. It follows that the exact dimensions and properties of each segment of vessel are optimized for the specific set of forces it experiences.

One of the first studies on developing vasculature conducted in 1893 concluded that in chick embryo, the diameter of the vessel lumen is determined by the volumetric flow rate, the length that a vessel is extended depends on the longitudinal stress from tethered connective tissues, and the thickness of the developing vessel wall is determined by the blood pressures it experiences[71]. This optimization of vessel properties during development serves to normalize the mechanical stresses throughout the vasculature, such that there is constant shear stress, constant longitudinal stress, and constant circumferential wall stress between varying regions of vasculature.

Adult vessels remodel when any of the governing stresses are altered. For example, if theECs sense a change in the shear stress from altered flow, signals are sent to the SMCs to remodel the extra cellular matrix, changing the composition of the vessel wall, such that the vessel diameter increases

or decreases, thereby altering the volumetric flow rate to return the shear stress to its normal constant[72,73].

Blood vessel mechanics are dominated by the behaviour of collagen and elastin, with contributions from the SMCs. As such, vessels exhibit a nonlinear stress-strain curve with two phases in which elastin fibres are responsible for the extensible behaviour at low strains and collagen and SMCs are responsible for the inextensible, stiff behaviour at high strain[74]. The physiological strain range falls somewhere between the low and high strain regions and thus allows an optimal combination of extension and contraction of the vessel throughout the cardiac cycle[61]. Since the curve is nonlinear, the local slope, or incremental elastic modulus, for a specific strain can be calculated, but a single constant, such as Young's modulus, is incorrect to report[61].
In the body, blood vessels are in constant tension, which is evidenced by the 20-50% decrease in length and diameter when a vessel is excised from the body[75].
While the ECs have little effect on the mechanical properties of the vessel wall, they are essential in sensing and transducing shear stress from blood flow[76].
The SMCs are responsible for contracting the diameter of the vessel, and excited SMCs can lead to a 20-50% decrease in diameter[77]. SMC contraction shifts the stress-strain curve to the left and thereby increases the apparent stiffness of the vessel, while SMC relaxation shifts the curve to the right, decreasing the apparent stiffness.

Modelling vessel mechanics can be complex due to the various interactions between the wall constituents.
While vein properties have not been widely characterized and modelled, a commonly accepted model for arterial wall mechanics uses a modified Maxwell model composed of both series and parallel elastic components (Figure 8). It is thought that the elastin is represented by a spring, and it is in parallel with collagen, which is represented by multiple stiffer springs of varying lengths. As described above, at low strains or pressures, the elastin bears the stress, while at higher strains or pressures, collagen fibres get recruited. SMCs are then in series with other collagen fibres, and the two of these are in parallel with the elastin and parallel collagen. The SMCs share their load with the collagen fibres with which they are in series. When not activated, the SMCs do not resist being stretched, and the mechanical properties of the relaxed wall depend mostly on elastin and parallel collagen. However, when activated, the SMCs contract, thus increasing wall stress and stiffness. The series collagen fibres vary in length, and they are recruited as SMCs become activated and contract[78].

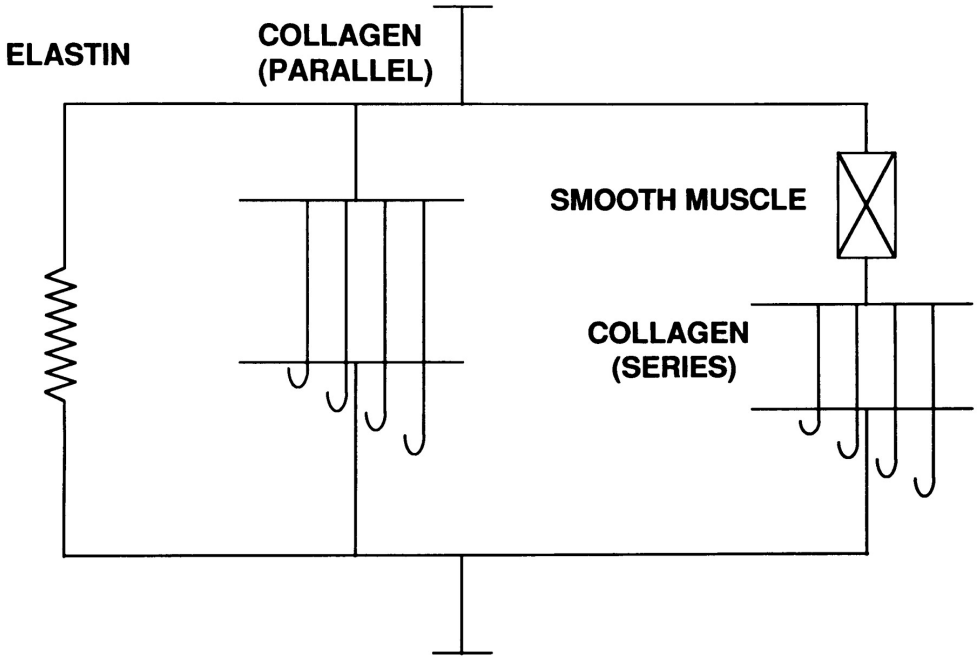

Figure 8 : Modified Maxwell model of arterial wall

Source: Bank AJ et al. Circulation 1996;94:3263

During vasodilation, SMCs are relaxed, so the collagen and elastin in parallel with the SMCs bear any stress applied to the artery wall. When SMCs are activated, and thus the vessel constricts, the SMCs and the series collagen bear any applied stress. The contraction of SMCs increases the stress felt by the wall in the circumferential direction and increases the elastic modulus of the wall[78]. According to this model, changes in blood pressure would result in strain applied to both collagen and SMCs. Applying tension to collagen stretches its flexible domains and leads to the storage of elastic energy. Some of this energy may be dissipated by fibrillar slippage[79]. SMCs are linked to collagen through integrins, so the cells would also experience any tension applied to the collagen, and fibrillary slippage could result in shearing of the cells[74].

3.4. Thrombosed vein mechanics

The processes of thrombus formation and resolution impact the composition and material properties of the venous wall.
In a murine model of IVC thrombosis, thrombus formation has been found to change the mechanical behavior of the glycosaminoglycans and proteoglycans and increase the stiffness of the collagen and elastin fibres. Ultimately, this increases the stiffness of the venous wall and reduces the vessel's distention ability in response to pressure changes[80].

Thrombus resolution also affects the mechanical properties of veins. A clinical study using duplex ultrasound as non-invasive imaging modality showed that regardless of whether or not a DVT is resolved, the venous wall increases in thickness 1.5- to 1.8-fold after 6 months compared to healthy

controls, and patients who had thrombus resolution had 1.4-fold thicker vein walls that those whose thrombus did not resolve. This thickening suggests that the cells of the vein remodel in response to thrombosis and continue this response even when the thrombus resolves, indicating that the changes in composition and material properties may be enduring[81].

Increased matrix metalloproteinase-9 has been implicated in changing the material properties of veins during DVT, and several studies have shown that thrombus resolution further increases its expression[81–83]. Matrix metalloproteinase-9 is a matrix remodeling protein, known for its ability to lyse both elastin and collagen, which plays a role in thrombus resolution but is also responsible for degrading the extracellular matrix and basement membrane of the venous wall adjacent to the thrombus, leading to fibrosis. The result is decreased wall compliance due to increased stiffness of collagen and elastin in both longitudinal and circumferential axes[82].

Venous thrombosis not only affects the composition of the adjacent vessel wall but also more distant portions of the vein, due to altered flow conditions. Using computational fluid dynamics, Wang et al. studied the effect of thrombosis on portal vein hemodynamics. In their study, blood velocity increased proportionally to the size of non-occlusive thrombus, with concomitant shear stress increase. This increase in shear stress affected a larger area on the vessel wall opposite the thrombus than it did on the wall with the thrombus, inducing vessel remodeling, thereby altering the material properties of the vessel wall[84].

Summary

While both arteries and veins have a 3-layer architecture, their precise structural composition largely varies, allowing them completely different mechanical properties and function. Few studies have looked specifically at venous properties, and those that have usually offer mathematical models for their behavior rather than actual numerical values that surgeons can use.

Even less is known on the venous wall modifications occurring during DVT and after venous recanalisation, both in terms of structural composition and mechanical properties.

Such knowledge is however needed to develop medical devices dedicated to the treatment of venous occlusive disease.

RESEARCH WORK

1. Critical review of large animal models for iliocaval DVT

1.1. Introduction

Many animal models of venous thrombosis have been described in the literature[3–5]. Most of these models used small animals and focused mainly on studying the biology behind DVT and on developing pharmaceutical approaches[6,7].
TRS as well as endovascular treatment of chronic venous obstructive diseases involve dedicated thrombectomy devices, recanalization tools, angioplasty balloons, stents and stentgrafts; there are currently unmet needs for endovascular tools specifically developed to treat venous obstructive diseases[85]. Such management needs to respond to specific pathological disease stages: how does the thrombus modify the histological content and thus the mechanical properties of the venous wall overtime? Which imaging modality can accurately detect such remodeling? Is there a non-invasive method able to predict treatment success?
Large animal models of DVT are necessary to improve our knowledge on the natural history and the optimal management of the disease, as well as to provide adequate vehicles for the development, testing and evaluation of dedicated endovascular devices.
The aim of this work was to review the existing literature on large animal models of DVT in order to select the ideal one, which should be technically simple, fast to perform, reproducible and form a consistent size of thrombosed vein with analogous characteristics to clinical human DVT.

1.2. Material and Methods

1.2.1. Search protocol

A systematic search of the literature was conducted on July 20, 2017, in Embase and on December 1st, 2019, in Medline and included all articles published from inception of the databases to the date of the search. The following terms were searched in both title and abstract: (“vein” OR “venous”) AND (“thrombus” OR “thrombosis”) AND (“animal” OR “pig” OR “swine” OR “sheep” OR “dog” OR “baboon”) NOT (“mouse” OR “mice” OR “rat” OR “rats” OR “rabbit” OR “rabbits”). Only original articles, reviews, conference papers and conference reviews published in English were considered.

1.2.2. Inclusion criteria

Articles were selected for inclusion if they described an in-vivo experimental protocol of DVT creation in a large animal model, involving the iliac vein and/or the vena cava and/or the brachiocephalic vein. Studies using mice, rats, rabbits or any other small animal species were excluded, as well as studies involving venous thrombus creation in other locations (pulmonary arteries, cerebral, retinal, portal, mesenteric, jugular or femoral veins). Experimental protocols involving arteriovenous shunts were excluded. The references of all included articles were reviewed to screen for additional inclusion.

1.2.3. Data extraction

The following information was recorded from each study where available: primary aim of the study, animal characteristics (species, strain, size, gender and number of animals used), experimental protocol (location of the induced thrombus, size of the concerned vein, use of the component of the Virchow's Triad (stasis, hypercoagulability, intimal damage)) and thrombus evaluation (means to confirm the presence, location and size of the created thrombus, acute versus chronic evaluation of the thrombus, occlusive versus non-occlusive thrombus, evidence of PE following thrombus creation, assessment of similarities to human imaging and histopathological findings).

1.2.4. Data analysis

Results are expressed in percentages and medians.

1.3. Results

1.3.1. Literature search

The initial search yielded to 803 results in Embase and 1290 results in Medline. After title and abstract review, and exclusion of duplicates, a total of 104 studies were eligible for full review. Of these, 71 articles did not meet all inclusion/exclusion criteria and were excluded. After careful review of articles references, 5 additional articles met the inclusion criteria, leading to a total of 38 papers included (Figure 9)[86–123]. All included articles were original articles, published between 1954 and 2017.

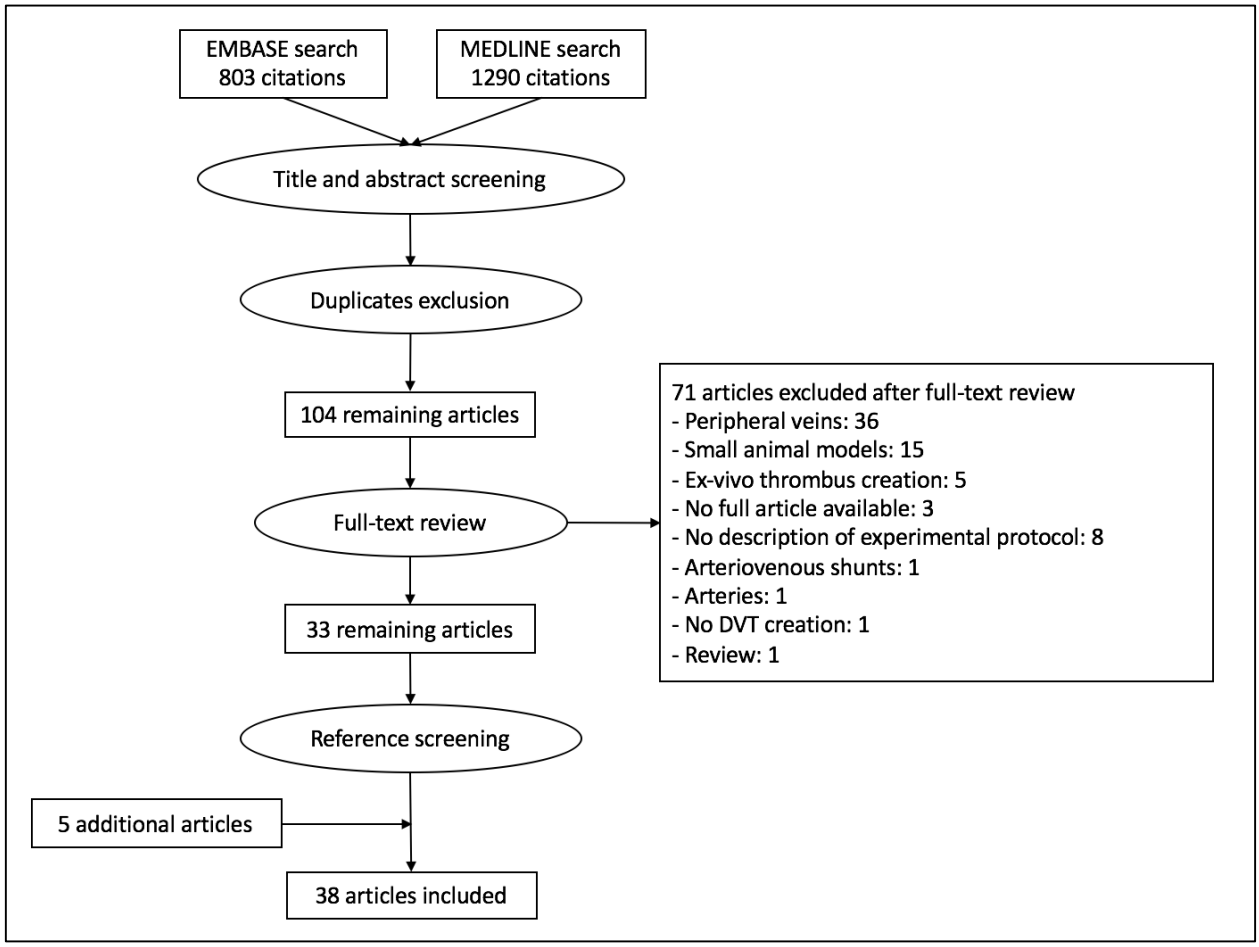

Figure 9 : Results of the literature search on large animal models of DVT

(DVT = deep venous thrombosis)
Source: Schwein A et al. Eur J Vasc Endovasc Surg. 2020 Aug;60(2):243-252.

1.3.2. Aim of the studies

The global aim of each paper was to test therapeutic drugs in 10 studies, to test therapeutic devices in 14 studies, to test surgical procedures in 2 studies, to assess imaging of DVT in 3 studies, to create an animal model of DVT in 3 studies, of PE in 1 study and to study physiopathology of DVT in 5 studies (Table 4).

Authors (reference)	Year of Publication	Aim of the paper	Animal species	Animal strain	Gender	Weight (kgs) range (R) or mean (M)	Number of animals	Location of thrombus	Baseline venous diameter (mean)
Wakefield et al. (14)	1991	DVT model	Baboon	-	M/F	5.5 (M)	10	IVC and left iliac vein	-
Wakefield et al. (15)	1993	Physiopathology assessment	Baboon	-	-	4.9 (M)	6	IVC and left iliac vein	-
Downing et al. (41)	1997	Drug testing	Baboon	-	-	4.9 (M)	12	IVC and iliac veins	-
Wakefield et al. (43)	2000	Drug testing	Baboon	-	-	6.2 (M)	12	IVC	-
Myers et al. (23)	2002	Drug testing	Baboon	Papio anubis	M	-	9	Iliac veins	-
Myers et al. (44)	2007	Drug testing	Baboon	Papio anubis	M	-	9	Iliac veins	-
Meier et al. (30)	2008	Drug testing	Baboon	Papio anubis	M	-	9	Iliac veins	-
Diaz et al. (35)	2015	Drug testing	Baboon	-	-	-	19	Iliac veins	-
Szalony et al. (25)	2003	Drug testing	Macaque	Macaca fascicularis	M	2.9 - 7.6 (R)	45	IVC	-
Meraney et al. (24)	2003	Surgical procedure testing	Beef	-	M	70 - 80 (R)	6	IVC	-
Moretz et al. (11)	1954	Physiopathology assessment	Dog	Mongrel	-	-	40	IVC	-
Anderson et al. (12)	1962	Physiopathology assessment	Dog	Mongrel	-	-	63	IVC	-
Foster et al. (38)	1971	Device testing	Dog	Mongrel	-	6.4 - 15.9 (R)	18	IVC	-
Valji et al. (13)	1987	Drug testing	Dog	Mongrel	-	16 - 26.5 (R)	12	Iliac veins	-
Gu et al. (45)	1997	Device testing	Dog	Mongrel	M/F	23 - 33 (R)	29	IVC	-
Trerotola et al. (20)	2001	Device testing	Dog	Mongrel	-	20 - 30 (R)	17	IVC	-
Trerotola et al. (21)	2001	Device testing	Dog	Mongrel	-	-	14	IVC and iliac veins	-
Besancon et al. (26)	2004	Device testing	Dog	Mixed bred	F	15.7 - 19.1 (R)	6	Left iliac vein	-
Hosaka et al. (16)	1996	DVT model	Pig	Domestic	F	21.4 (M)	18	IVC and iliac veins	-
Hosaka et al. (42)	1999	Device testing	Pig	-	F	20.2 (M)	28	IVC	-
Tacke et al. (39)	1999	Device testing	Pig	Crossbred domestic	F	30 - 40 (R)	7	Iliac veins	-
Salartash et al. (18)	2000	Drug testing	Pig	Domestic	F	25 - 30 (R)	40	IVC	-
Haage et al. (17)	2001	Device testing	Pig	Crossbred domestic	F	40 (M)	11	IVC and iliac veins	14 mm
Lin et al. (19)	2001	Device testing	Pig	Domestic	-	45 - 50 (R)	20	Iliac veins	-
Fergany et al. (22)	2002	Surgical procedure testing	Pig	Domestic	F	30 - 35 (R)	7	IVC	-
Lin et al. (46)	2003	Drug testing	Pig	Domestic	-	45 - 50 (R)	15	iliac veins	-
Geier et al. (27)	2005	DVT model	Pig	Crossbred domestic	M	32 (M)	13	IVC	-
Geier et al. (40)	2005	DVT imaging	Pig	Crossbred domestic	M	-	12	IVC	-
Lin et al. (47)	2007	Device testing	Pig	Domestic	-	55 - 65 (R)	15	iliac veins	-
Katoh et al. (28)	2007	Device testing	Pig	Domestic	-	48 - 52 (R)	12	Iliac veins	-
Katoh et al. (29)	2009	DVT imaging	Pig	Domestic	-	48 - 52 (R)	6	Iliac veins	-
Barbash et al. (31)	2011	PE model	Pig	Yorkshire	-	60 (M)	11	IVC	-
Ichiki et al. (32)	2012	DVT imaging	Pig	Crossbred	F	20.2 (M)	12	IVC	-
Schmitt et al. (33)	2013	Physiopathology assessment	Pig	Landrace	M	70 (M)	1	IVC	-
Minko et al. (34)	2014	Device testing	Pig	Domestic	-	46.5 (M)	6	Iliac veins	12 mm
Shi et al. (36)	2015	Physiopathology assessment	Pig	Hanford miniature	M/F	15 - 20 (R)	12	Left iliac vein	6.37 mm
Shi et al. (37)	2015	Device testing	Pig	Hanford miniature	M/F	16 - 20 (R)	10	IVC	9.9 mm
Weinberg et al. (48)	2017	Device testing	Pig	Domestic	-	65 - 75 (R)	12	iliac veins	-

Table 4 : Aim of studies and animal characteristics

(DVT = deep venous thrombosis, PE = pulmonary embolism, M = Male, F = Female, IVC = inferior vena cava)

Source: Schwein A et al. Eur J Vasc Endovasc Surg. 2020 Aug;60(2):243-252.

1.3.3. Animal features

Large animals used as model for DVT were pigs (20/38, 52.6%), dogs (8/38, 21.1%), monkeys (8/38 baboons, 21.1%, and 1/38 macaque, 2.6%) and 1 bovine (2.6%). Specific animal strain was mentioned in 31 studies (81.6%). Median number of animals used per study was 12, ranging from 1 to 63. Females were exclusively used in 8 studies (21.1%), males in 8 studies (21.1%), while both males and females were used in 4 studies (10.5%). The animal gender was not specified in 18 studies (47.4%). The animal's weight was below 30kgs in 15 studies (39.5%), between 30 and 50kgs in 8 studies (21.1%) and above 50kgs in 7 studies (18.4%). There was no information about animal's weight or size in 8 studies (21.1%). Animals features are summarized in Table 4.

1.3.4. Experimental protocol

DVT was induced solely in the IVC in 17 studies (44.7%), in the iliac vein in 15 studies (39.5%) and in both the IVC and iliac veins in 6 studies (15.8%).
The size of the vessel used for thrombus creation was measured on venogram in 4 studies (10.5%); mean diameters ranged from 6.37mm to 14mm. The length of the venous segment undergoing venous stasis was specified in 2 studies, ranging from 2cm to 3.5cm.

DVT was created using a totally endovascular procedure in 4 studies (10.5%), an entirely open procedure in 6 studies (15.8%) and a hybrid procedure in 28 studies (73.7%).
In regards to the use of the Virchow's Triad components for thrombus creation, all studies used venous stasis in their experimental protocol: alone in 21 studies (55.3%), in association with hypercoagulability in 13 studies (34.2%), in association with endothelial damage in 3 studies (8.3%), and in association with both hypercoagulability and endothelial damage in 1 study (2.6%).
Venous stasis was performed during less than 2 hours in 9 studies (23.7%), between 4 to 6 hours in 9 studies (23.7%), and for more than 24 hours in 20 studies (52.6%).
Balloon catheters were the most commonly used to create venous stasis in 20 studies (52.6%), followed by venous ligation in 8 (21.1%), or other means in 10 (26.3%) (coils, tapered stentgraft, bulldog clamps, net of sutures). Hypercoagulability was induced using thrombin (either human or bovine) in 12/14 studies (86%).
Foreign material was left in place after thrombus creation in 21 studies (55.3%): balloon catheters, stents, sutures, IVC filters or coils.
Experimental protocol features are summarized in Table 5.

Authors (reference)	Animal species	Surgical approach	Venous stasis	Stasis duration	Mean to induce venous stasis	Hyper-coagula-bility	Endothelial damage	Remaining foreign material	Foreign material left in place
Wakefield et al. (14)	Baboon	Hybrid	Yes	4-6h	Ligation	Yes	No	No	-
Wakefield et al. (15)	Baboon	Hybrid	Yes	4-6h	Ligation	Yes	No	No	-
Downing et al. (41)	Baboon	Hybrid	Yes	4-6h	Balloon catheter	No	No	No	-
Wakefield et al. (43)	Baboon	Hybrid	Yes	4-6h	Balloon catheter	No	No	No	-
Myers et al. (23)	Baboon	Hybrid	Yes	4-6h	Balloon catheter	No	No	No	-
Myers et al. (44)	Baboon	Hybrid	Yes	4-6h	Balloon catheter	No	No	No	-
Meier et al. (30)	Baboon	Hybrid	Yes	4-6h	Balloon catheter	No	No	No	-
Diaz et al. (35)	Baboon	Hybrid	Yes	4-6h	Balloon catheter	No	No	No	-
Szalony et al. (25)	Macaque	Hybrid	Yes	<2h	Suture net	No	No	No	-
Meraney et al. (24)	Beef	Hybrid	Yes	<2h	Balloon catheter	Yes	No	No	-
Moretz et al. (11)	Dog	Open	Yes	>24h	Ligation or clip	No	No	Yes	Suture or clip
Anderson et al. (12)	Dog	Open	Yes	>24h	Ligation	No	No	Yes	Suture
Foster et al. (38)	Dog	Hybrid	Yes	<2h	Ring device	No	No	No	-
Valji et al. (13)	Dog	Endovascular	Yes	>24h	Coil	No	No	Yes	Coil
Gu et al. (45)	Dog	Hybrid	Yes	>24h	Balloon catheter	No	No	Yes	Balloon catheter
Trerotola et al. (20)	Dog	Hybrid	Yes	>24h	Balloon catheter	No	No	Yes	Balloon catheter
Trerotola et al. (21)	Dog	Hybrid	Yes	>24h	Balloon catheter	No	No	Yes	Balloon catheter
Besancon et al. (26)	Dog	Open	Yes	>24h	Ameroid constrictor	No	No	Yes	Ameroid constrictor
Hosaka et al. (16)	Pig	Hybrid	Yes	>24h	Silicon loop or balloon catheter and coil	No	Yes	Yes	Silicon loop or balloon catheter and coil
Hosaka et al. (42)	Pig	Hybrid	Yes	>24h	Balloon catheter	No	Yes	Yes	Balloon catheter
Tacke et al. (39)	Pig	Hybrid	Yes	>24h	Balloon catheter and coil	Yes	No	Yes	Coil
Salartash et al. (18)	Pig	Hybrid	Yes	>24h	Balloon catheter	No	Yes	Yes	Balloon catheter
Haage et al. (17)	Pig	Hybrid	Yes	<2h	Balloon catheter	Yes	No	Yes	Stent
Lin et al. (19)	Pig	Hybrid	Yes	>24h	Stentgraft	No	No	Yes	Stentgraft and IVC filter
Fergany et al. (22)	Pig	Open	Yes	<2h	Bulldog clamp	Yes	No	No	-
Lin et al. (46)	Pig	Hybrid	Yes	>24h	Stentgraft	No	No	Yes	Stentgraft and IVC filter
Geier et al. (27)	Pig	Hybrid	Yes	>24h	Ligation	Yes	No	Yes	suture
Geier et al. (40)	Pig	Hybrid	Yes	>24h	Ligation	Yes	No	Yes	suture
Lin et al. (47)	Pig	Hybrid	Yes	>24h	Stentgraft	No	No	Yes	Stentgraft and IVC filter
Katoh et al. (28)	Pig	Endovascular	Yes	<2h	Balloon catheter	Yes	No	No	-
Katoh et al. (29)	Pig	Endovascular	Yes	<2h	Balloon catheter	Yes	No	No	-
Barbash et al. (31)	Pig	Endovascular	Yes	<2h	Balloon catheter	Yes	No	Yes	IVC filter
Ichiki et al. (32)	Pig	Hybrid	Yes	>24h	Balloon catheter	No	No	Yes	Balloon catheter
Schmitt et al. (33)	Pig	Open	Yes	4-6h	Ligation	Yes	Yes	No	-
Minko et al. (34)	Pig	Hybrid	Yes	<2h	Balloon catheter	Yes	No	No	-
Shi et al. (36)	Pig	Open	Yes	>24h	Ligation	No	No	Yes	Suture
Shi et al. (37)	Pig	Hybrid	Yes	>24h	Suture net	Yes	No	Yes	Suture
Weinberg et al. (48)	Pig	Hybrid	Yes	>24h	Stentgraft	No	No	Yes	Stentgraft

Table 5 : Characteristics of experimental protocols

Source: Schwein A et al. Eur J Vasc Endovasc Surg. 2020 Aug;60(2):243-252.

1.3.5. Venous thrombus evaluation

In the acute phase, 22 studies evaluated the presence of thrombus in the dedicated vessel: thrombus was absent in 1 study, and present in 21 studies. Of these 21 studies, thrombus was present in all the animals in 12 studies, and in some animals in 9 studies. In 5 studies, acute thrombus was found to be occlusive at least in one animal. Thrombus size was evaluated in 4 studies (10.5%).
Thirty-one studies (82%) involved surviving animals for the evaluation of chronic DVT. Follow-up period was very variable, from 1 day to 3.5 months.
In the chronic phase, 30 studies confirmed having thrombus in the dedicated vessel. There was no remaining thrombus in one study. In 17 studies, chronic thrombus was found to be occlusive at least in one animal.

Unexpected animal death occurred in 9 studies (23.7%) ranging from 3.2% to 37.5% of the animals. Twelve studies (31.6%) assessed the occurrence of PE following thrombus creation, either on imaging or necropsy. Six studies (50%) confirmed PE in 4.3% to 30% of their animals, causing the death of two animals. Histological examination of the thrombus was performed in 24 studies (63%), with histology being performed after clot removal or lysis in 8 of them (21%) designed for device testing. Histological comparison of experimental thrombus to human thrombus was performed in one study (2.6%)[32].
Results regarding thrombus evaluation are summarized in Table 6.

Authors (reference)	Animal species	Presence of thrombus in acute phase (# of animals)	Presence of occlusive thrombus in acute phase (# of animals)	Presence of non-occlusive thrombus in acute phase (# of animals)	Acute thombus size	Study including surviving animals	Delay	Presence of thrombus in chronic phase (# of animals)	Presence of occlusive thrombus in chronic phase (# of animals)	Presence of non-occlusive thrombus in chronic phase (# of animals)	Chronic thrombus size (length, volume or weight)	Un-expected animal death (%)	Histology
Wakefield et al. (14)	Baboon	Yes (3/10)	-	-	-	Yes	2h to 4 days	Yes (5/10)	-	-	-	Yes (20)	Yes
Wakefield et al. (15)	Baboon	Yes (6/6)	-	-	-	Yes	3-9 days	Yes (6/6)	-	-	-	No	No
Downing et al. (41)	Baboon	Yes	-	-	-	Yes	2 days - 2 months	Yes	-	-	-	No	Yes
Wakefield et al. (43)	Baboon	-	-	-	-	Yes	2-30 days	Yes	-	-	-	No	Yes
Myers et al. (23)	Baboon	Yes (8/9)	Yes (8/9)	No	-	Yes	16 days	Yes	Yes (2/9)	-	-	No	Yes
Myers et al. (44)	Baboon	Yes (6/9)	Yes (3/9)	-	-	Yes	6 days	Yes (6/9)	Yes (3/9)	Yes (3/9)	-	No	No
Meier et al. (30)	Baboon	Yes (9/9)	Yes (9/9)	No	-	Yes	6 days	Yes (9/9)	Yes (5/9)	Yes (4/9)	-	No	No
Diaz et al. (35)	Baboon	Yes	-	-	-	Yes	21 days	Yes (15/19)	-	-	-	No	Yes
Szalony et al. (25)	Macaque	-	-	-	-	No		-	-	-	3.6 - 40.7mg (range)	-	No
Meraney et al. (24)	Beef	Yes (5/6)	-	-	-	No		-	-	-	-	No	No
Moretz et al. (11)	Dog	-	-	-	-	Yes	>2weeks	Yes (10/23)	Yes	-	-	Yes (37.5)	No
Anderson et al. (12)	Dog	-	-	-	-	Yes	24h	1Yes (51/63)	-	-	-	Yes (3.2)	No
Foster et al. (38)	Dog	Yes (16/18)	Yes (1/18)	Yes (15/18)	310.8mg (mean)	No	-	-	-	-	-	No	Yes
Valji et al. (13)	Dog	-	-	-	-	Yes	2 days	Yes (12/12)	Yes (1/12)	Yes (11/12)	6.5cm (+/- 1.7) (mean +/-SD)	No	Yes
Gu et al. (45)	Dog	-	-	-	-	Yes	6-15 days	Yes (23/23)	Yes (10/23)	Yes (13/23)	-	Yes (20.7)	Yes
Trerotola et al. (20)	Dog	-	-	-	-	Yes	7 days	Yes (14/14)	-	-	31cm3 (mean)	Yes (17.6)	Yes
Trerotola et al. (21)	Dog	-	-	-	-	Yes	7 days	Yes (12/14)	-	-	-	Yes (14.3)	Yes
Besancon et al. (26)	Dog	-	-	-	-	Yes	6-98 days	Yes (6/6)	Yes (3/6)	Yes (3/6)	-	No	Yes
Hosaka et al. (16)	Pig	-	-	-	-	Yes	7 days	Yes (12/12)	Yes (10/12)	Yes (2/12)	2.94cm3 (mean)	Yes (20)	Yes
Hosaka et al. (42)	Pig	-	-	-	-	Yes	2-4days	Yes (28/28)	Yes (25/28)	Yes (3/28)	3.5ml (median)	No	No
Tacke et al. (39)	Pig	-	-	-	-	Yes	3 days	Yes (7/7)	Yes	-	6cm (mean)	No	Yes
Salartash et al. (18)	Pig	-	-	-	-	Yes	5 days	Yes (32/40)	Yes	Yes	0.069g/kg (mean)	Yes (20)	No
Haage et al. (17)	Pig	-	-	-	-	Yes	5-8 days	Yes (11/11)	Yes (10/11)	Yes (1/11)	15.2ml (mean)	No	Yes
Lin et al. (19)	Pig	Yes	-	-	-	Yes	3-14 days	Yes	-	-	-	No	Yes
Fergany et al. (22)	Pig	Yes (7/7)	-	-	-	Yes	6 weeks	No	-	-	-	No	No
Lin et al. (46)	Pig	Yes (15/15)	-	-	-	Yes	7 days	Yes	-	-	77.4 mm2	No	No
Geier et al. (27)	Pig	-	-	-	-	Yes	1-15 days	Yes (12/12)	Yes (12/12)	No	7g (mean)	Yes (7.7)	Yes
Geier et al. (40)	Pig	-	-	-	-	Yes	1-15 days	Yes (12/12)	Yes (12/12)	No	-	No	Yes
Lin et al. (47)	Pig	Yes (15/15)	-	-	-	Yes	21 days	Yes	-	-	81.57 mm2	No	No
Katoh et al. (28)	Pig	Yes (12/12)	No	Yes (12/12)	8.6cm +/- 3.6 (mean +/-SD)	No		-	-	-	-	No	No
Katoh et al. (29)	Pig	Yes (6/6)	-	-	-	No		-	-	-	-	-	No
Barbash et al. (31)	Pig	Yes (11/11)	-	-	-	Yes	7 days	Yes (11/11)	-	-	-	No	No
Ichiki et al. (32)	Pig	Yes (12/12)	-	-	-	Yes	1-14 days	Yes	-	-	-	No	Yes
Schmitt et al. (33)	Pig	Yes (1/1)	No	Yes (1/1)	-	No		-	-	-	-	-	No
Minko et al. (34)	Pig	Yes (6/6)	Yes (1.5/6)	-	92.5mm (mean)	No		-	-	-	-	No	Yes
Shi et al. (36)	Pig	No	-	-	-	Yes	14 days	Yes (3/12)	Yes (2/12)	Yes (1/12)	2.97cm3 +/-1.06 (mean +/-SD)	No	Yes
Shi et al. (37)	Pig	Yes	No	Yes	2.98cm3 +/-0.16 (mean+/-SD)	Yes	14 days	Yes (10/10)	Yes (5/10)	Yes (5/10)	5.6cm3 +/-0.95 (mean +/-SD)	No	Yes
Weinberg et al. (48)	Pig	Yes (12/12)	-	-	-	Yes	14 days	Yes (12/12)	Yes (12/12)	No	80.85 mm2 (mean)	No	No

Table 6 : Evaluation and characteristics of the created DVT

(SD = standard deviation)

Source: Schwein A et al. Eur J Vasc Endovasc Surg. 2020 Aug;60(2):243-252.

1.4. Discussion

This literature review provides a comprehensive overview of the existing large animal models of DVT involving the IVC and/or the CIVs.
Almost half of the papers chose swine models to work on; indeed, pigs present similar vascular anatomy and vessel sizes as humans. On the other hand, non-human primates present the advantage of being bipedal. In 2008, Siller-Matula et al. evaluated differences in coagulation profiles between species and found first that sheep had the clotting time most similar to humans, and second that pigs and rabbits were useful comparative models in studying fibrinolytic pathway and platelets respectively[124]. In addition, Sondeen at al compared human and porcine thromboelastograph parameters and found that swine responses were parallel to that of human blood, although pigs were hypercoagulable compared with humans[125].

One main finding from this review is the poor consensus in regard to reporting the development and results of such animal models. Important animal characteristics are often missing such as gender (47.4%), strain (18.4%) or animal size (21.1%). Moreover, 10.5% of the studies are mixing males and females without gender-based subgroup analysis, when it is now well-established that sex bias does exist[126,127].
The lack of consistency in reporting animal characteristics is critical when considering testing of medical devices. The Food and Drug Administration (FDA) recommends that there should be adequate scientific evidence in support of a model, and sees the principal goal of a reliable animal model as being its ability to embody the characteristics for which it is intended in humans, meaning the importance to standardize vessel conditions, size, tortuosity, etc…[128]
Standardization in establishing study methodology and reporting results is necessary when developing animal models, especially because strict reproducibility is essential for other teams to use such models for further research or testing. In the ARRIVE guidelines, Kilkenny et al. proposed 20 recommendations on reporting in vivo experiments; efforts should be made by authors to achieve such standardization[129].
The animal's size was an interesting characteristic to analyse. While large animal models are used to get closer to human beings, 60.6% of the animals used in current literature were less than 50kgs, and even 49.5% less than 30kgs. This is particularly true for non-human primates, with weights ranging between 2.9 and 7.6kgs. The size of the vein used to induce the thrombosis was also rarely reported, only in 10.5% of the studies, and diameters varied from 6.3mm to 14mm. These "large" animals would not be large enough to allow human-size device deployment to treat either acute or chronic venous pathologies.

Second, this review found that experimental protocols constantly use blood stasis to induce venous thrombosis, which is the component of the Virchow's Triade playing a major role regarding thrombosis in the venous circulation[130]. On the other hand, endothelial damage is rarely used in the current literature (10.5% of the studies). While endothelial injury is particularly important for thrombus formation in the arterial circulation where high flow might otherwise impede clotting by preventing platelet adhesion and washing out activated coagulation factors, in the venous circulation, endothelial injury is not compulsory for thrombus creation[130].
Means employed to induce venous stasis as well as stasis duration are very variable; endovascular venous occlusion through balloon catheters is the most used technique; it has the advantage of being easily placed and removed, through minimally invasive approach thus limiting animal harm.

Balloon catheters can also remain in-vivo during several days: the extremity can be sutured to subcutaneous tissue, allowing animal recovery while maintaining continuous venous stasis, as performed by 7 teams[88,100,111,114,119,121,123]. Unlike ligation of the iliac vein or IVC, which induce permanent loss of anatomical integrity, such endovascular technique also ensures further possibilities of therapeutics and devices testing. However, cautious has to be taken during balloon catheter positioning and inflation, avoiding excessive oversizing that could create endothelial lesions and compromise ulterior biological or histological findings.

In more than half of the studies (21/38), foreign material was left in vivo after thrombus induction. While such remaining material prolongs venous stasis and may thus improve the resulting thrombus, these materials carry drawbacks: they cause imaging artefacts (stents, coils, IVC filters), they modify venous anatomy (permanent suture or clip, ameroid constrictor) and may thus prevent the model from being used to assess therapeutics or device testing.

Efficiency results, through the evaluation of the characteristics of the created venous thrombus, is essential to evaluate a model. However, important information such as presence or absence of actual thrombus is often missing, especially its occlusive or non-occlusive character. Precisions about thrombus size are also often lacking, both in the acute and chronic phases.
Finally, histological examination of the created venous thrombus and thrombosed vein were only performed in 24 studies (63.2%), with a single one comparing experimental findings to human ones.
These results show the lack of evaluation of the created thrombus, and demonstrate the paradox of developing models to test therapeutic procedures, drugs or devices for DVT treatment, while there is no comparison tested between human and experimentally created pathologies. To our knowledge, there is to date no tissue bank on human VTE, reporting precise histology of the natural history of human DVT. Samples might be difficult to get from patients, requesting IRB approval, and sample's age is also not always precise. However, some literature does exist on histological evolution of human DVT over time; Fineschi et al. retrospectively studied histological changes of DVT and PE from human autopsies and their results can be used for comparison[131].

VTE is a multifactorial disease, involving mechanical and hemodynamic factors, coagulation and inflammation cascade, over a long-time period. Accordingly, no animal model can replicate such complex human pathology yet. To date, small animal models, especially rodents, are the most commonly used to develop and assess several aspects of thrombogenesis / thrombolysis and test novel pharmacological therapies (large availability of molecular tools, possibility of genetic manipulation, low cost). However, results from these small animal models should be interpreted with caution, in regard to discrepancies due to dosage variation regarding specimen sizes compared to human beings. In addition, these small animal models do not allow for translational studies focusing for example on imaging or interventional therapeutics. Essentially, the development of new endovascular or surgical therapeutics would benefit from a model that not only replicates the conditions encountered from a biological standpoint, but also one which allows deployment and assessment of the tools' effectiveness[128].
Previous teams did focus on analysing animal models of venous thrombosis, with a similar objective of finding one that would be suitable for the understanding of the pathology and for the development and testing of therapeutic applications. Most of the existing reviews focus on small

animal models, and the few reporting on large animal models are non-exhaustive and mainly descriptive[3–5,7,132].

We decided to exclude from our analysis studies assessing the venous thrombosis created in the femoral or jugular vein, mainly due to the lack of comparable size to clinical DVT in human beings. Likewise, we decided to exclude studies using the arteriovenous shunt model as protocol to create the thrombus, since this technique uses a synthetic surface to simulate thrombus formation (e.g., polyethylene or Dacron) in a circuit going from arterial to venous pressure, that has little relevance to most forms of pathophysiologic thrombus formation.

Large animal models of DVT are indispensable to advance our knowledge on the natural history and the optimal management of the disease. They also provide a potentially safe platform for which new devices can be tested, as mandated by the FDA. The ideal model should be technically simple, fast to perform, reproducible, form a consistent size of thrombosed vein with analogous characteristics to clinical human DVT. A minimally invasive approach should be used to be harmless as possible for the animal, we thus prone for a total endovascular protocol. Animal's size should be at least 60kg; both male and female should be tested; no foreign material has to be left in place and venous anatomy should be respected. The use of balloon catheters to induce venous stasis, associated to local infusion of coagulant drug appears to us to be the most valuable method. This model will be suitable for making correlations between histology, biomechanics and imaging features of the remodeling state, that are the corner stone to develop and test human-size therapeutic procedures and devices.

1.5. Conclusion

This systematic review shows advantages and weaknesses of the existing large animal models of DVT occurring in the iliac veins and vena cava. Given the scope of the available literature, it is clear that there should be an effort to take a step beyond proof of concept and towards model consensus. Therefore, future model development should insist on more rigor and consistency in reporting animal characteristics, as well as in evaluating the created thrombus and comparing its features to human ones.

2. Development of a large animal model of DVT

2.1. Introduction

VTE is a major healthcare issue in western countries, due to its frequency, its long-term complications and the costs generated. Unlike DVT occurring in distal veins, where BMT involving anticoagulation and elastic compression stockings is the recommended treatment, DVT occurring in iliofemoral veins or in the IVC carry higher risks of PTS, with only suboptimal results of medical management[1]. Therefore, interventional treatment may be considered: early TRS in case of acute and subacute DVT or transluminal angioplasty and stenting for PTS[2,133].
Several animal models of DVT have been described in the literature but the majority use small animals, not allowing the study of human diagnostic and therapeutic management, and focus mainly on studying the biology behind DVT and developing pharmaceutical approaches[6,7]. A recent literature review of large animal models for DVT pointed out the lack of rigor and consistency in reporting animal characteristics, as well as in evaluating the created thrombus and comparing its features to human ones[134]. Indeed, as recommended by the FDA regarding the development of medical devices, we need a model that not only replicates the conditions encountered from a biological standpoint at several time points (acute and subacute evolution of the disease), but also one which allows deployment and assessment of devices' effectiveness[128].
The aim of this work was to describe an innovative animal model of acute and subacute iliocaval DVT, similar to human disease, that should allow current human clinical imaging, management and follow-up, and which could be used for the development and evaluation of interventional management.

2.2. Material and methods

This protocol follows the ARRIVE guidelines[129,135]. Experiments were approved by the Houston Methodist Institutional Animal Care and Use Committee (IACUC) (protocol number AUP-0615-0049), in strict accordance with the Guide for the Care and Use of Laboratory Animals of the National Institutes of Health. The animals were kept in an animal care facility with ad libitum access to food and water for an acclimation period of 14 days.

2.2.1. Experimental protocol

Female domestic pigs (crossbred) were used in this study. Animal experiments were performed under general anaesthesia and all efforts were made to minimize pain. On the day of the procedure, animals were anesthetized with ketamine (11-33mg/kg) and sustained with isoflurane (1.5-5%). The animals were intubated and maintained on a mechanical respirator for the duration of the procedure.
The experiment took place in our research hybrid operating room equipped with a robotic mounted C-arm angiography system (Artis *zeego*®, VC14J, Siemens Healthcare GmbH, Germany). Under ultrasound guidance, the right internal jugular vein and bilateral common femoral veins were percutaneously accessed using micro puncture sets (Micropuncture® Access Set (reference MPIS-

501-NT-U-SST), COOK Medical, Bloomington, IN, USA). An 11 French 13cm-long sheath (Performer^{TM} Introducer (reference RCF-11.0-38-J), COOK Medical, Bloomington, IN, USA) was introduced in each femoral vein, and an 11 French 70cm-long sheath (Performer^{TM} Introducer (reference RCFW-11.0-38-70-RB), COOK Medical, Bloomington, IN, USA) was introduced through the right internal jugular vein until its extremity reached the IVC at the level of the renal veins. Two thousand units of heparin were injected intravenously after sheath placement.
Through each sheath, a 9 French 32mm diameter balloon catheter (Coda® Balloon Catheter (reference CODA-2-9.0-35-100-32), COOK Medical, Bloomington, IN, USA) was inserted and placed as follows: one balloon catheter below the lowest (right) renal vein in the IVC and one balloon catheter in each iliac vein, at the level of the ostium of the internal iliac vein (Figure 10).

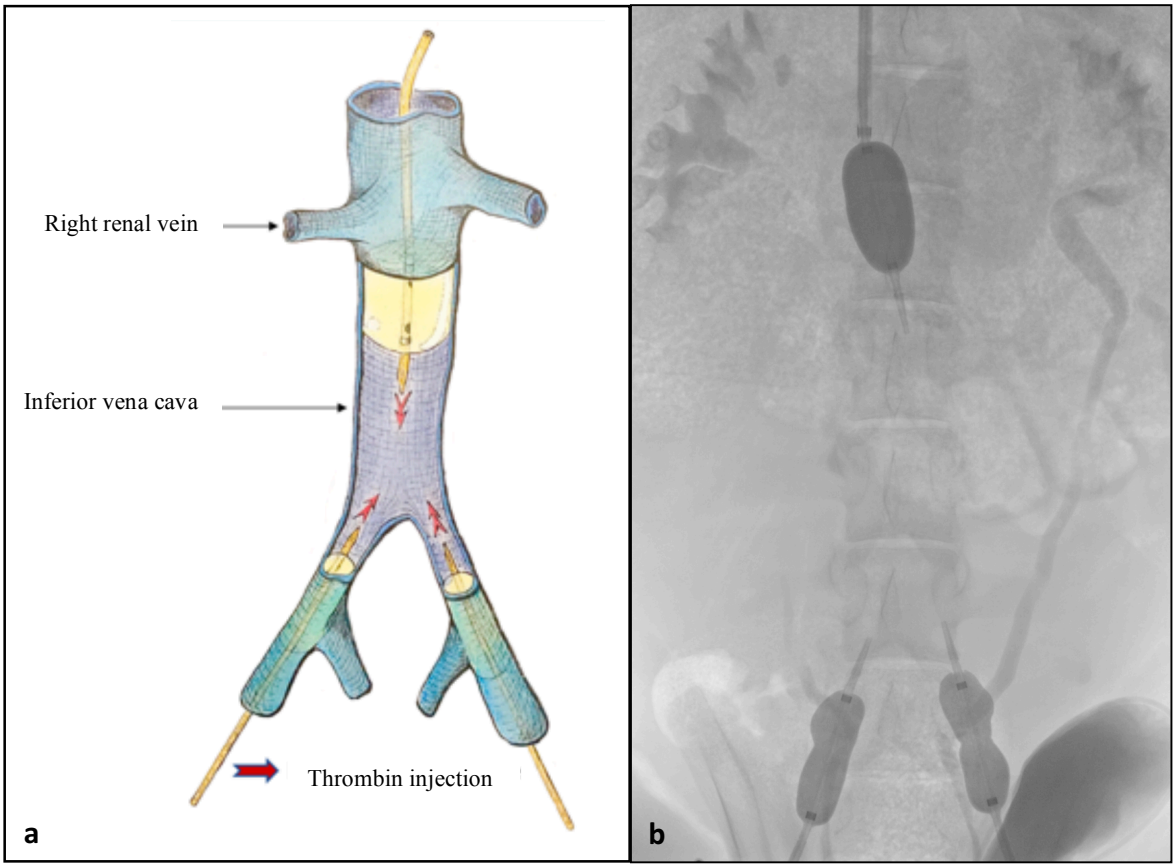

Figure 10 : Experimental protocol

Scheme (a) and digital subtraction angiography (b) showing the localization of the three balloon catheters, defining the region of thrombus creation within the infrarenal inferior vena cava and both iliac veins.
Source: Schwein et al. Eur J Vasc Endovasc Surg. 2022 Apr;63(4):623-630.

The three balloons were then inflated to occlude both left and right iliac veins and proximal IVC, creating venous stasis in the region of interest. The balloon's inflation diameter was based on each vein diameter obtained from baseline imaging to avoid oversizing and to minimize intimal damage.

Digital subtraction angiography was acquired with contrast injection through each sheath to ensure venous occlusion at all levels and verify the patency of both renal veins. Through the balloon catheter's lumen, we injected 6,000 IU of recombinant human thrombin (Evicel® Fibrin Sealant (Human), Ethicon, Bridgewater, NJ, USA) within the occluded venous segment. After 1 hour, we injected again 4,000 IU of thrombin and waited another 1.5 hour. Balloon catheters were then deflated and removed. Manual pressure was maintained on each access site for 10 minutes after material retrieval and each puncture site was closed with medical glue.
After recovery, animals were housed under veterinary care with continuous access to food and water. On postoperative day 1 and then bi-weekly, blood samples were collected through direct venous puncture under sedation and processed for haematology and coagulation. After 7, 14, 21, 28 or 35 days of follow-up (two animals for each follow-up period), animals were taken back to the research hybrid operating room. Bilateral femoral veins were accessed again percutaneously under ultrasound guidance for follow-up imaging. Animals were then euthanized and the IVC and CIV were harvested en bloc and processed for histological examination.

2.2.2. Imaging modalities

MRI, venography and contrast-enhanced cone beam computed tomography (CBCT) were performed on the day of thrombus creation, both before (baseline imaging) and after the procedure (immediate postoperative imaging), as well as on the termination day, either after 7, 14, 21, 28 or 35 days, before animal euthanasia (follow-up postoperative imaging).
Venography was performed using a single anteroposterior view after simultaneous contrast injection of iohexol (Omnipaque™, GE Healthcare, Marlborough, MA) through bilateral femoral sheaths.
CBCT imaging was performed after simultaneous contrast injection of Omnipaque™ through bilateral femoral sheaths, using a custom developed 5-second protocol (5s-DynaCT® Portrait, 0.36 microGy/frame, Siemens) with a robotic angiography system (Artis *zeego*®, VC14H, Siemens). A C-arm rotation of 200 degrees around the animal (from 60° LAO to 140° RAO) with detector in portrait mode enabled the acquisition and reconstruction of a 3D CBCT image dataset.
MRI was acquired using a 1.5 T research MRI scanner (1.5 Tesla, Aera®, Siemens Healthcare GmbH, Erlangen, Germany) with phased-array coil systems. All animals underwent magnetic resonance venography (MRV): acquisitions included equilibrium phase T1-weighted 3D gradient recalled echo sequence using volumetric interpolated breath-hold examination (T1-VIBE) with typical flip angle of 10 degrees, echo time of 2.3 ms, repetition time of 4.71 ms, in plane spatial resolution of 1.0 mm x 1.0 mm, and slice thickness of 1.0 mm. The acquisition was done approximately 10 minutes after slow bolus contrast injection (2mmol/sec) through a venous catheter in the animal's ear, followed by the same amount of saline flush. We used gadofosveset trisodium (Ablavar®) as blood pool contrast agent, at a concentration of 0.03 mmol/kg in half of the animals, then gadopentetate dimeglumine (Magnevist®) at a concentration of 0.2 ml/kg in half of the animals once the production of Ablavar® stopped.

2.2.3. Tissue post-processing

The IVC and both CIVs were removed en bloc. Each specimen was measured in vivo before harvesting and ex-vivo to assess for in-vivo stretch (Figure 11), photographed, and their ventral side was inked for orientation purposes. Cross sectional slices along the specimen were cut, stained with haematoxylin and eosin stain (H&E), MOVAT's pentachrome, Von Kossa and Carstairs stain, and prepared for histological examination performed by a veterinarian pathologist. Histological examination was performed in comparison to healthy female domestic pig's IVC and CIVs.

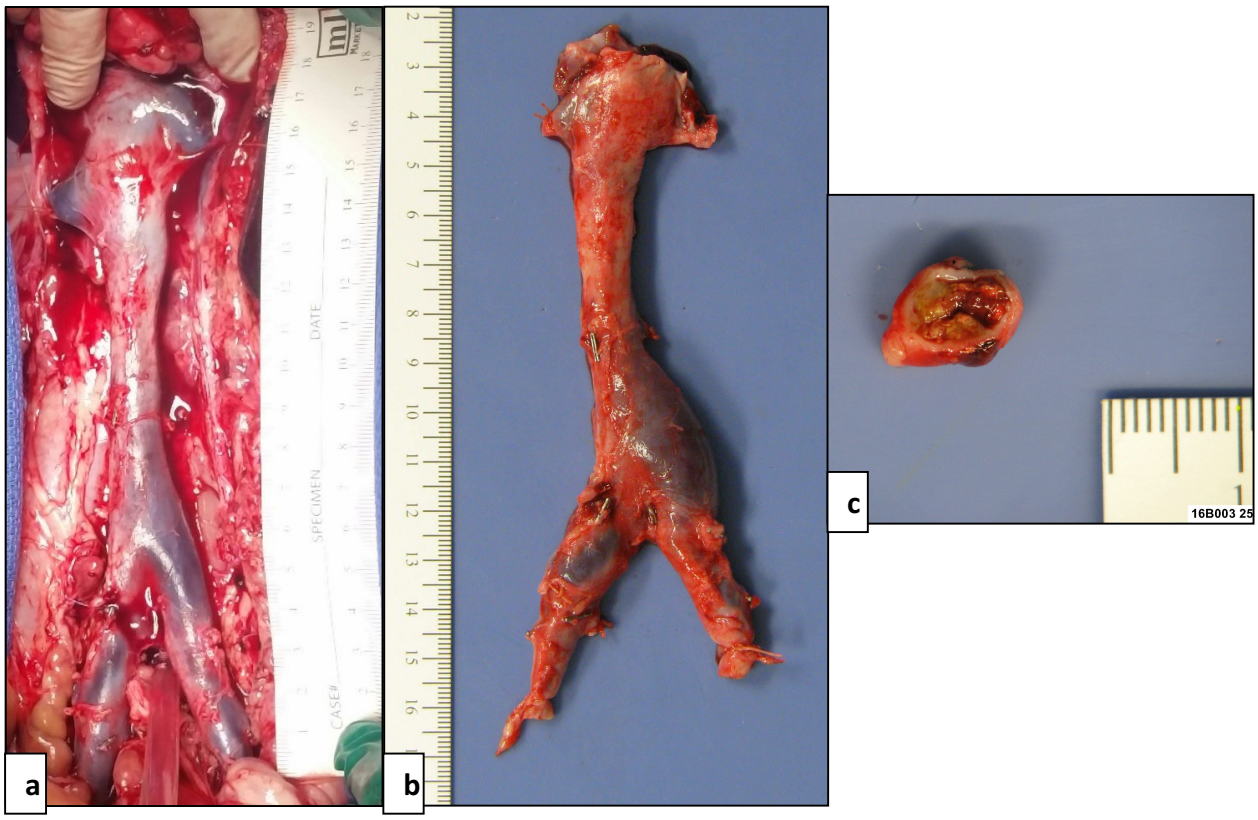

Figure 11 : Thrombosed ilio-caval segment

In vivo (a) and ex vivo (b) pictures of the 2-week old thrombosed inferior vena cava (IVC) and bilateral iliac veins. Cross-section view of the IVC, 4 cm below the right renal vein, filled with thrombus (c).

Source: Schwein et al. Eur J Vasc Endovasc Surg. 2022 Apr;63(4):623-630.

2.2.4. Studied parameters

Animal features and perioperative evolution were reported. Descriptive results are expressed in means (+/- standard deviation (SD)) and percentages. We used a paired T-test to compare pig's hemodynamics before and after IVC occlusion.
Primary endpoint of the study was the technical success of the model, defined as the creation of an occlusive acute thrombus in the region of interest and 24-hr survival of the animal. Thrombus confirmation was obtained under macroscopic examination and using imaging modalities (venogram, CBCT and MRI). Thrombus volume was computed from the morphological T1-Vibe MRI sequence using the software Osirix. Imaging, biology, macroscopic pathology and histology were used to characterize the evolution of the thrombus over time.

2.3. Results

2.3.1. Animal features and perioperative course

A total of 13 female domestic pigs (crossbred) with a mean (±SD) weight of 59.3 (±5.7) kg and a mean age of 4.2 (±0.5) months were used in the study. Baseline imaging showed the absence of previous thrombotic venous disease in all animals. The right renal vein was the lowest renal vein in all pigs. Three animals (23%) were found to have a venous fenestration at the level of the proximal IVC and/or the left CIV. Measured on T1-vibe MRI sequences, baseline mean (±SD) IVC maximal and minimal diameters as well as area were 16.4 (±1.6) mm, 8 (±2.8) mm and 1.2 (±0.2) cm^2 respectively.
No complication occurred during the procedure of thrombus creation in any of the animals. Acute endovascular occlusion of the infrarenal IVC led to a significant decrease of mean systolic arterial blood pressure (from 84.8 mmHg to 70.8 mmHg, $p<.01$) without significant change of mean heart rate (from 80.3 bpm to 78.5 bpm, $p=.35$).

2.3.2. Model efficiency

Technical success rate of the model was 92% (12/13). All animals recovered after the procedure except one that died 2 hours post-procedure; the diagnoses contributing to death determined during necropsy were right atrium and ventricle thromboembolism and gastric rupture. There was no sign of PE. Nevertheless, an occlusive thrombus was found in the infrarenal IVC and bilateral CIVs.
In all animals, on both postoperative venogram and CBCT performed immediately after balloon catheters deflation and retrieval, we observed nearly occlusive venous thrombosis in the region of interest (Figure 12a and 12b). On postoperative MRI performed 1 hour after balloon catheter removal, venous thrombosis was occlusive in all animals, and was limited to the infrarenal IVC and CIVs in all but one animal (Figure 3c), where thrombus extended to both renal veins and the suprarenal IVC up to the right atrium. This was the result of intraoperative migration of the IVC balloon upstream, while the sheath used was short and thus could not support the balloon's position. On immediate postoperative MRI, mean (±SD) total thrombus volume was 19.8 (±1.63) cm^3.

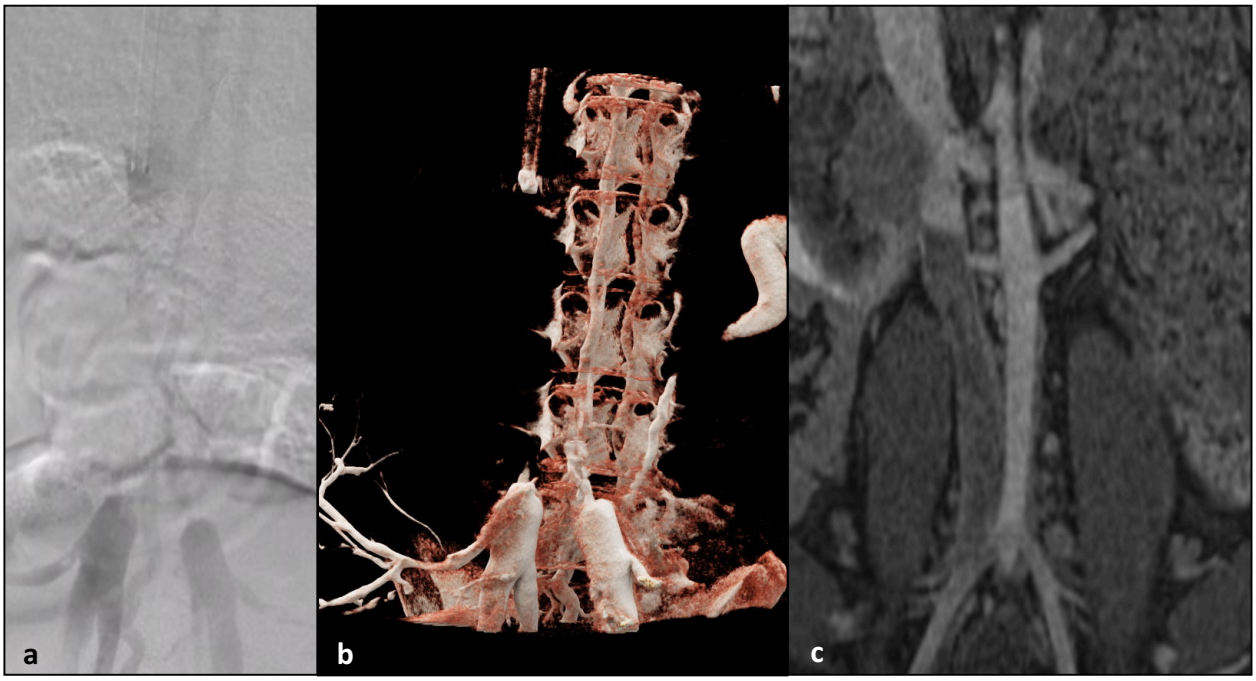

Figure 12 : **Acute postoperative imaging results**

Venogram (a) and contrast-enhanced cone-beam computed tomography (b) showing nearly occlusive thrombus in the region of interest. On magnetic resonance venography (c), the inferior vena cava thrombosis is occlusive 1 hour after balloon catheters removal.
Source: Schwein et al. Eur J Vasc Endovasc Surg. 2022 Apr;63(4):623-630.

2.3.3. Follow-up

Two additional animals unexpectedly died in the postoperative course and all underwent a necropsy performed by a veterinary pathologist. One animal died on postoperative day 1 from consumptive coagulopathy. The other animal also died on postoperative day 1 of IVC rupture. There was no sign of PE in both animals. Macroscopic pathology and histology of their harvested IVC showed occlusive thrombus.
In the 10 surviving animals, between preoperative and immediate postoperative clinical pathology results, paired t-test analysis of coagulation parameters showed a significant increase in D-dimer (from 498.9±76.8 to 2272.6±480.9 ng/mL (mean±SD), p=.006) and a significant decrease in fibrinogen (from 174.6±5.6 to 141.9±10 mg/dL (mean±SD), p=.003). Complete blood count results also showed a significant decrease in platelet count (from 392.4±25.3 to 293.2±30 K/microL (mean±SD), p<.001), in lymphocyte count (from 12.2±0.8 to 5.3±0.4 K/microL (mean±SD), p<.001), and a significant increase in neutrophil count (from 7.2±0.7 to 11.4±1.5 K/microL (mean±SD), p<.03).
Follow-up MRI showed non-occlusive thrombus at each time point (7, 14, 21, 28 and 28 days). This was confirmed at terminal necropsy: all 10 remaining animals had grossly recognizable non-occlusive thrombi.

2.3.4. Histological findings

Control healthy veins were composed of intima, media and adventitia with mostly uniform wall thickness. They occasionally contained minimal cellular infiltrates, primarily composed of mononuclear cells admixed with occasional eosinophils. The endothelial lining was intact without evidence of thrombi (Figure 13a).

One-day old thrombus (obtained from the 2 animals that unexpectedly died) consisted of erythrocytes and platelets admixed with fibrin. There was a neutrophil infiltration in both the venous wall and the thrombus (Figure 13b).

At one week, neutrophils decreased in number in the venous wall whereas eosinophils became more prominent. There was now a clear reaction between the venous wall and the thrombus, which started to be covered by endothelium. Thrombus cellularity was increased mostly with inflammatory cells with numbers of polynuclear neutrophils, as well as appearance of hemosiderin laden macrophages and eosinophils.

At two weeks, the venous wall was substantially thickened, showing degenerated muscle and containing a mixed cellular infiltrate composed of lymphocytes, eosinophils and macrophages. The elastic fibers were disrupted, and mineralization was multifocal in thrombi between accumulating mucopolysaccharide stroma. Major evolution was the appearance of collagen deposition within the thrombus (Figure 13c).

At three weeks, thrombus surface was covered by plump EC and neovascularization was characterized by cavernous structures (lined by endothelium, and containing luminal erythrocytes) on periphery of thrombi. The venous wall was asymmetrically thickened with inflammatory reaction, giant cells surrounding focal area of degeneration and mineralization. Mostly, mature thrombi contained extensive mineralization, giant cells and hemosiderin-laden macrophages (Figure 13d).

At four and five weeks, venous walls were thickened with focal areas of increased cellularity in subendothelium where hypertrophied small vessels were present. We observed mature thrombi incorporated into the venous wall. Additional features of thrombi over time included aggregates of hemosiderin laden macrophages, spindle cell proliferation in a haphazard pattern, multifocal mineralization associated with multinucleated giant cells, and an increase in extracellular matrix containing varying amounts of ground substance and increasing amounts of collagen. Collagen formation was first noted at the central core of the thrombus surrounded by mucopolysaccharides in more superficial areas, by MOVAT's Pentachrome (Figure 13e).

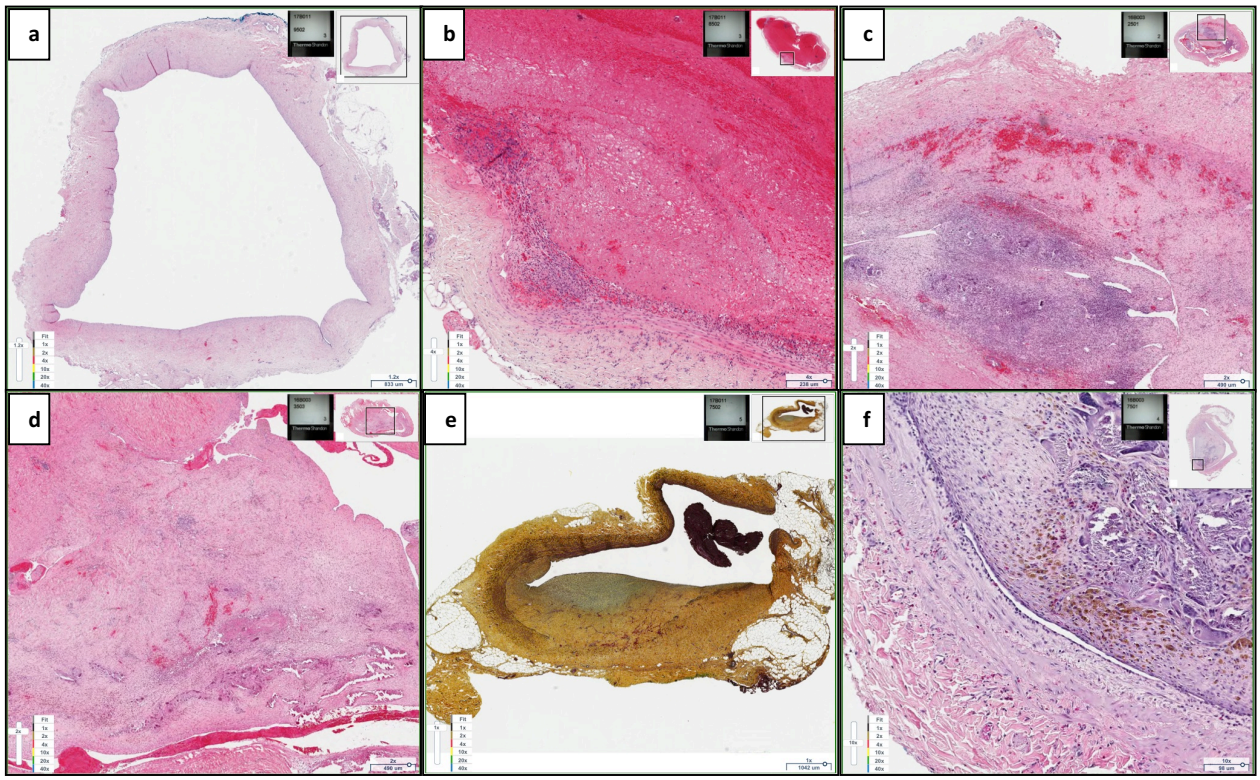

Figure 13 : Histological findings

(a) Hematoxylin and eosin (H&E) stain of a control inferior vena cava (x1.2). (b) H&E stain of a one-day old thrombus (x4) showing erythrocytes and platelets admixed with fibrin. (c) H&E stain of a 2-week old thrombus (x2) highlighting multifocal mineralization and collagen deposition. (d) H&E stain of a 3-week old thrombus (x2) showing red blood cells surrounded by a narrow layer of fibrin mixed with neutrophils and collagen of varied maturity state. (e) MOVAT's stain of a 1-month old thrombosed vein (1x) showing the disposition of collagen formation in the central core of the thrombus surrounded by mucopolysaccharides in more superficial areas. (f) H&E stain of a 1-month old thrombosed vein (x10) showing new endothelium covering the thrombus and the accumulation of hemosiderin-laden macrophages in the periphery of the thrombus.

Source: Schwein et al. Eur J Vasc Endovasc Surg. 2022 Apr;63(4):623-630.

2.4. Discussion

Herein we described a totally endovascular large animal model of acute and subacute iliocaval DVT in the pig. The protocol was reproducible in 12 animals and led to the creation of a large amount of occlusive thrombus in the immediate postoperative course. The endovascular protocol allowed a minimally invasive approach in order to ensure animal survival, limit surgical trauma and inflammation, and hence the development of a reproducible survival model.

We used large pigs since they present comparable vascular anatomy and vessel sizes as humans (mean weight of 59.3 kg and mean IVC diameter of 16 x 8 mm in our study); in addition, several studies found similarities in coagulation profiles between human and pigs[124,125]. Several animal models of DVT have been described in the literature. Most of them are small animal models, focusing on studying the biology behind DVT and on developing pharmaceutical approaches[6,7]. Even published large animal models (in pig, dog or baboon) use smaller weight animals (<50kg or even <30kg), and vessel sizes are either not specified or inadequate for interventional treatment modalities[94,109,119,136].

We developed a model combining venous stasis and hypercoagulability through human recombinant thrombin injection, limiting artificial intimal damages. We were particularly cautious during endovascular balloon inflation, limiting over-dilation by respecting initial venous diameter. While endothelial injury is particularly important for thrombus formation in the arterial circulation where high flow might otherwise impede clotting by preventing platelet adhesion and washing out activated coagulation factors, in the venous circulation, endothelial injury is not compulsory for thrombus creation but stasis plays a major role[130]. Venous intimal damage has been used by some previous large animal models to induce venous thrombosis, but appears to us as a limitation, creating non-physiological lesions that could compromise the natural evolution of the thrombus or modify histological examination[101,111,119,121].

One particular advantage of the described model is the respect of the anatomical integrity of the venous system. Many described large animal models are performing IVC or iliac ligation, or are leaving foreign material (stents, coils) within the vein to induce extended stasis, modifying physiological flow conditions, creating artefacts on imaging, and precluding the model to be used for development or testing of interventional therapeutics[86,94,108,136,93,98,107,120,122].

Histological examination of the thrombi produced in our model showed on day 1 a mixed thrombus rich in red blood cells and platelets caught in a fibrin mesh. Thrombus organization starts at one week with increased cellularity mostly with inflammatory cells with numbers of polynuclear neutrophils, as well as appearance of hemosiderin laden macrophages and eosinophils. Collagen deposition appears on week 2 and neo-vascularization on week 3. Mature thrombi contained extensive mineralization, giant cells and hemosiderin-laden macrophages.
When compared to histological changes of experimental IVC thrombus in mice, it seems like the remodeling process happens slower in the pig: whereas hemosiderin-laden macrophages, neo-vessels and collagen were appearing in the thrombus within the first week in mice (precisely 3, 5 and 7 days respectively), they were respectively appearing after 7, 21 and 14 days in our pig model[137].

Retrospective histological study of DVT and PE from human autopsies found that thrombi were mainly composed of fibrin, erythrocytes and platelets between 1 and 7 days; hemosiderin-laden macrophages and endothelium covering the thrombus appeared after 1 week[131]. It appears that our findings are in concert with these results; pigs may thus better resemble humans in term of timing of DVT evolution and fit better for translational research.

Considering the suboptimal results of BMT alone for DVT occurring in iliofemoral veins and in the IVC, interventional treatment may be considered: early TRS in case of acute and subacute DVT or transluminal angioplasty and stenting for post-thrombotic fibrosis[1,2,133]. The wider scope of this model gathers two main objectives regarding therapeutic management of DVT in human, i.e. translation to vascular surgery.
First, we will have the possibility to assess the efficacy of early TRS depending on thrombus age. Indeed, recanalization methods fail to achieve their goal if the thrombus is too adherent to the vessel wall or if the remodeling process is too advanced. Since the age of the thrombus is clearly defined in our model, we will be able to both study non-invasive imaging methods, i.e. MRI, to date the thrombus, and investigate the results of several venous recanalization techniques.

Second, this model makes it possible to design and test new generations of endovascular venous devices: thrombectomy devices, recanalization tools, angioplasty balloons and stents or stentgrafts. While there is an extensive number of endovascular devices designed and studied for arterial pathologies, there are currently only very few endovascular tools specifically developed and tested to treat either acute and subacute DVT, or post-thrombotic fibrosis.
Because of a paucity of purpose-built venous devices, many teams have to use stents or stentgrafts initially designed for arterial pathologies, despite universal recognition that arteries and veins have different structures and behavior.[85]

The use of female pigs only in this study is a main limitation. While it is more and more known that gender may have an impact on results, we would ideally need to repeat our experiments in male pigs. Secondly, PE was not investigated, we are thus not able to evaluate embolization of the created thrombus. Two animals died at day one (consumptive coagulopathy and IVC rupture); these deaths occurred among the first animals of our study, investigators might thus be aware of a certain learning curve with this model. The protocol finally still needs to be experimented in other labs to demonstrate its reproducibility.

2.5. Conclusion

We are proposing a minimally invasive endovascular model of acute and subacute iliocaval DVT, which is effective in 60kg-animals, as well as being safe and reproducible. It is important to note that the model respects the integrity of the vascular system and does not leave foreign material, avoiding artificial lesions and imaging artefacts. Further use of this model will focus on assessing non-invasive imaging modalities to determine thrombus age, as well as developing and testing dedicated devices for venous pathologies.

3. APPLICATIONS OF THE PORCINE MODEL OF ILIOCAVAL DVT

3.1. Non-invasive characterization of DVT using MRI (on-going work)

3.1.1. Introduction

As above-mentioned, MRI has been a very promising imaging modality in first the assessment of thrombus age, but also especially in analysing its fibrin content. The association of multiple specific sequences might lead to further characterization of thrombus over time, thus guiding the success of thrombolytic therapies[54–56].
However, most of the current published studies are preclinical work focusing on small animals.

Texture analysis is also an innovating method of increasing the information obtained from medical imaging, using computational methods applied on radiological images obtained from routine practice.
It uses a wide range of techniques modelling spatial distributions of pixel grey levels in order to characterize underlying tissue structure and intra-lesional heterogeneity[138].
Its applications are increasingly used in a wide range of studies in different body regions: semi-automatic segmentation of the hippocampus and corpus callosum, diagnosis of skeletal muscle dystrophy or differentiation between various obstructive lung diseases[139–141].
More recent studies on the vascular system supported the use of texture analysis in estimating red blood cell counts and iron content of acute ischemic stroke clots, or in differentiating neoplasic from bland thrombi in portal vein thrombosis[142,143].

The aim of our work was to extensively use MRI capabilities to characterize experimental iliocaval DVT and its evolution over time, focusing on morphometrics, image texture, and analysis of fibrin content.

3.1.2. Material and methods

Experiments were done in strict accordance with the Guide for the Care and Use of Laboratory Animals of the National Institute of Health (NIH) and approved by our IACUC (protocol number AUP-0615-0049).

3.1.2.1. Experimental protocol

The exact same protocol as above-described in section “2. Development of the model” was used to create acute and subacute iliocaval DVT.

3.1.2.2. Imaging modalities

All animals underwent MRV using a 1.5 T research MRI scanner (1.5 Tesla, Aera®, Siemens Healthcare GmbH, Erlangen, Germany) with phased-array coil systems.
Each animal underwent three imaging sessions:

- MRI_1 was performed on the day of thrombus creation, before the procedure,
- MRI_2 was performed immediately after the creation of iliocaval DVT, on the acute phase,
- MRI_3 was considered as follow-up imaging, either after 7, 14, 21, 28 or 35 days, before animal euthanasia.

The following sequences were acquired:

- First Pass Angiography done with time-resolved Magnetic Resonance Angiography with repetition time (TR) of 2.61ms, TE of 0.94ms, slice thickness of 1.40mm, base resolution 320, phase resolution of 100% and voxel size of 1.4x1.4x1.4mm.

- Equilibrium phase T1-weighted 3D gradient recalled echo sequence using volumetric interpolated breath-hold examination (T1-VIBE) with typical flip angle of 10 degrees, echo time of 2.3 ms, repetition time of 4.71 ms, in plane spatial resolution of 1.0 mm x 1.0 mm, and slice thickness of 1.0 mm.

- The acquisition was done 10 minutes after slow bolus contrast injection (2mmol/sec) through a venous catheter in the animal's ear, followed by the same amount of saline flush. We used gadofosveset trisodium (Ablavar®) as blood pool contrast agent, at a concentration of 0.03 mmol/kg in half of the animals, then gadopentetate dimeglumine (Magnevist®) at a concentration of 0.2 ml/kg in half of the animals once the production of Ablavar® stopped.

After contacting the team from the King's College of London (Dr. Prakash Saha) that already published on MRI assessment of thrombus' content[54–56], we utilized their MRI protocol, adapted on human use, and acquired the following sequences:

- T1 mapping (2D-MOLLI) with typical flip angle of 35 degrees, echo time of 1.6 ms, repetition time of 3.3 ms, in plane spatial resolution of 2.0 mm x 2.0 mm and slice thickness of 6.0 mm.
- MT (3D-GRE) T1-weighted spoiled 3D gradient-echo images were acquired with an on-resonance MT prepulse with typical flip angle of 18 degrees, echo time of 2.2 ms, repetition time of 69 ms, in plane spatial resolution of 2.0 mm x 2.0 mm and slice thickness of 6.0 mm.
- Two-dimensional DW spin-echo images (2D-SE) were acquired with typical flip angle of 90 degrees, echo time of 82 ms, repetition time of 1780 ms, in plane spatial resolution of 2.0 mm x 2.0 mm and slice thickness of 10.0 mm. The apparent diffusion coefficient was calculated from 4 b values of 0, 333, 667, and 1000 mm2/s.

3.1.2.3. Image analysis

3.1.2.3.1. Volume and morphometric assessment

Working with the Software Osirix (OsiriX Foundation, Geneva, Switzerland), we used the T1-VIBE sequences to manually segment the contours of the native iliocaval segment and of the created venous thrombus; the software then automatically computed the preoperative venous volume and postoperative thrombus volume on immediate and follow-up periods.

We then defined 4 levels of interest for each animal: 2 locations in the infrarenal IVC (IVC1 and IVC2) and one for each common right and left iliac vein.
Using the software ImageJ (NIH, Bethesda, Maryland, USA), we will again manually segment the contours of the thrombus and the vein on each of the four levels of interest and extract the following parameters:

- Diameter (mm)
- Area (mm^2)
- Perimeter (mm)
- Mean, minimum (Min) and maximum (Max) grey value within each segmentation.
- Skewness, which appreciates the symmetry of the distribution. A symmetric distribution has a result equal to 0, a distribution asymmetric to the left has a result strictly lower than 0, and a result strictly higher than 0 reflects an asymmetry to the right.

This analysis will be performed on MRI_2 and MRI_3 of each animal. All measurements will be performed twice, so that an intraclass correlation coefficient could validate the reproducibility of the measures.

3.1.2.3.2. Texture analysis

Texture features of segmented MRIs will be analysed by the method of grey level co-occurrence matrix. The following variables described by Haralick et al. were studied[144–146]:

- Contrast reflecting the sharpness of images and the 217 depth of texture grooves. Contrast is a measure of intensity or grey level variations between the reference pixel and its neighbour. Texture grooves are associated with high contrast and better visual sharpness; on the contrary, low contrast leads to shallow grooves and blurred images. Higher number of pixels with high difference in grayscale is associated with higher values of contrast.
- Correlation reflects the consistency of image texture. It shows the linear dependency of grey level values in the co-occurrence matrix.
- Energy, the square sum of each matrix element, reflects the grayscale distribution homogeneity of images and texture crudeness. It measures the local uniformity of the grey levels.
- Homogeneity reflects the homogeneity of image textures and scaled the local changes of image texture. High values of homogeneity denote the absence of intra-regional changes and locally homogenous distribution in image textures.

Our analysis will finally include the measurement of the mean T1 relaxation times for each of the MRI images.

3.1.2.3.3. Assessment of fibrin content

We will reproduce the method described by Phinikaridou et al. comparing MRI analysis to histological findings[55]. Briefly, regions of interest encompassing the thrombus will be manually segmented using the software Osirix (OsiriX Foundation, Geneva, Switzerland) and then copied to MT and to DW images in order to generate MT ratio maps, showing the protein content or density of the thrombus per centimeter, and to calculate the apparent diffusion coefficient on similar region of interest.

Thrombus cross-sectional area (mm^2) will be measured on Martius scarlet blue–stained sections by computerized planimetry (ImageJ, NIH, Bethesda, MD). Using computer-assisted color image analysis (Color Threshold plug-in, ImageJ), we will quantify the collagen and fibrin area on Martius scarlet blue–stained sections. These measurements will serve to calculate the total histological protein content of the thrombus. For registration of the in vivo MRIs and histological sections, the distances from the renal and iliac bifurcations will be used as internal landmarks.

3.1.2.4. Statistical analysis

Data are shown as means (± SD) for continuous variables or as percentages for dichotomous variables, unless otherwise mentioned. A p-value of < 0.05 was considered significant.
The statistical data analysis was done with the non-parametric Wilcoxon signed-rank test after pairing the imaging results of MRI_2 and MRI_3 for each pig, allowing a comparison of the same pig in the acute phase and after a predefined follow-up period.
A Student's t-test and a Kruskal-Wallis test were used to compared the volumetric reconstructions between the different MRIs.
To appreciate the degree of correlation and agreement between measurements, the parameters were delineated twice in order to get an intraclass correlation coefficient that is calculated by mean squares obtained through analysis of variance.
This statistical analysis was conducted with Stata 248 statistical software (Stata/IC 15.1 for Mac, College Station, TX, USA).

3.1.3. Preliminary results

3.1.3.1. Population

This work will carry out with 20 female pigs including 17 domestic pigs (USDA class A, Oak Hill Genetics, Ewing, IL) with a mean weight of 57.15 ± 7.48 kg and 3 Yucatan pigs (USDA class A, S & S Farms, Ramona, CA) with a mean weight of 51.86 ± 1.83 kg.

3.1.3.2. Volume analysis

On acute postoperative MRI_2, total thrombus volume created was 17.05 ± 6.382 cm^3:

- 9.601 ± 4.709 cm^3 contained in the infrarenal IVC, 56.31 ± 19.89% of total volume;
- 4.312 ± 3.354 cm3 in the right CIV, 25.29 ± 17.31% of total volume;
- 3.138 ± 2.281 cm3 in the left CIV, 18.40 ± 11.19% of total volume.

The comparison of thrombus volume in-between animals showed no statistically significant difference.

3.1.4. Discussion

Current guidelines on the management of acute iliofemoral DVT mostly depend on the delay from symptoms onset: this threshold of 14 days will orientate treatment between BMT and early TRS. This paradigm of therapeutic management appears to be based on several assumptions, which seems quite irrelevant: the fact that symptoms of DVT start at the beginning of the DVT process; the fact that the evolution of DVT is a linear process over time. Thus, the determination of a precise non-invasive diagnostic method of DVT dating and/or DVT content characterization seems determining.

This ongoing work presents our very preliminary results of MRI characterization of iliocaval DVT in a swine model at different time points after DVT creation. Results are so far too limited to allow for further analysis or discussion, but expectations are multiple.
While the capabilities of MRI to accurately analyze thrombus content in a mouse model of DVT has been shown, similar work on a large animal model of DVT has not been performed and gathers challenges, especially regarding the much larger regions of interest to cover, meaning longer acquisition periods and decreased resolution. A first objective of our work is thus to confirm the feasibility of the described MRI acquisitions on a large animal.
Using our porcine model of DVT with known thrombus creation date and defined follow-up imaging periods, the second aim of this work is to draw a precise MRI profile of the evolution of DVT, assessing morphometric and textural changes occurring over time.

Finally, the comparison of a specific association of acquisitions (MT and DW sequences) with histological findings should ultimately allow the validation of MRI as a non-invasive imaging method to assess structural content of DVT over time.

3.1.5. Conclusion

While MRI has lately become a cornerstone in non-invasive cardiac functional explorations, complementing clinical findings and echocardiographic results, its use in the field of vascular disease, and especially in obstructive venous disease is currently very limited.
Its excellent spatial and tissue resolution, the possibility of dynamic acquisitions and finally the capabilities of qualitative and quantitative structural assessment should open the door for future patient-specific management based on its objective and non-invasive findings.

3.2. Mechanical properties of veins in a porcine model of DVT

3.2.1. Introduction

DVT alters the mechanics, hemodynamics, and cell biology of the afflicted vein over the course of the disease. The last ESVS clinical practice guidelines on acute venous thrombosis recommend early TRS for DVT occurring in the iliofemoral vein, with, if necessary, additional venous stenting[2]. Similarly, the last ESVS clinical practice guidelines on CVD recommend endovascular treatment for venous outflow obstructions for patients with severe PTS[23].

The endovascular devices designed for these procedures, however, are often optimized for the treatment of arterial pathologies, despite the well-studied compositional, structural, and functional differences between arteries and veins[74,147]. While there is a clear need for venous-specific endovascular devices[85], their development is constrained by a limited understanding of venous mechanics. Because balloons, stents, and stent grafts apply forces on the adjacent venous wall, the material properties of veins in healthy and diseased conditions are essential design criteria for these devices.

Over the past several decades, researchers have investigated venous mechanics and how they change in DVT, often employing small animal models to do so[6]. While these studies provide the only reported changes to material properties of the venous wall during DVT, their clinical application is limited due to disparities in size and complexity of the vascular systems. One study assessed the elasticity of thrombus in a pig model using ultrasound elastography, but did not analyse changes in the venous wall properties[108].
There is an unmet need to better understand how DVT alters the mechanics of the veins over time in order to best develop treatment tools specific to these diseased veins.

In the present study, our aim was first to characterize the material properties of healthy veins to serve as baseline values and to contribute to a general understanding of venous mechanics, and second to conduct mechanical analysis of the venous wall of a porcine model of central DVT. Based on previous studies in rat models of thrombosis[80,82,148], we hypothesized that the stiffness of the venous walls in our large animal model would increase over time.

3.2.2. Material and methods

Experiments were done in strict accordance with the Guide for the Care and Use of Laboratory Animals of the NIH and approved by our IACUC (protocol number AUP-0615-0049).

3.2.2.1. Experimental protocol

For the characterization of healthy veins, we analysed material from female domestic pigs (crossbred) used for studies unrelated to the cardiovascular system.

For the characterization of thrombosed veins, the exact same protocol as above-described in section "2. Development of the model" was used to create acute and subacute iliocaval DVT (Figure 14A).

3.2.2.2. Sample preparation

After animal euthanasia, both for healthy and diseased animals (at 1, 2, 3, 4 or 5 weeks after DVT creation), the infrarenal IVC and the two CIVs were dissected en bloc. The suprahepatic IVC was dissected out as a separate segment to serve as a non-thrombosed distal control region. The anterior wall of the vein was marked with blue dye (Figure 14B).

The segment was then cut into smaller sections approximately 2 cm long for each of the following anatomical regions: suprahepatic IVC, infrarenal IVC 1 (IVC1), infrarenal IVC 2 (IVC2), right iliac and left iliac veins (Figure 14C). Tissue samples were stored in phosphate buffered saline (PBS) at 4°C until testing, for a maximum of five days. Each segment was then cut along the lateral edge to open the vessel. Longitudinal and circumferential strips were cut from the anterior and posterior walls. In instances where there was interesting presentation of thrombus along the lateral wall, strips were taken from this region as well. If the tissue section was too small to acquire both longitudinal and circumferential strips, priority was given to longitudinal strips (Figure 14D).

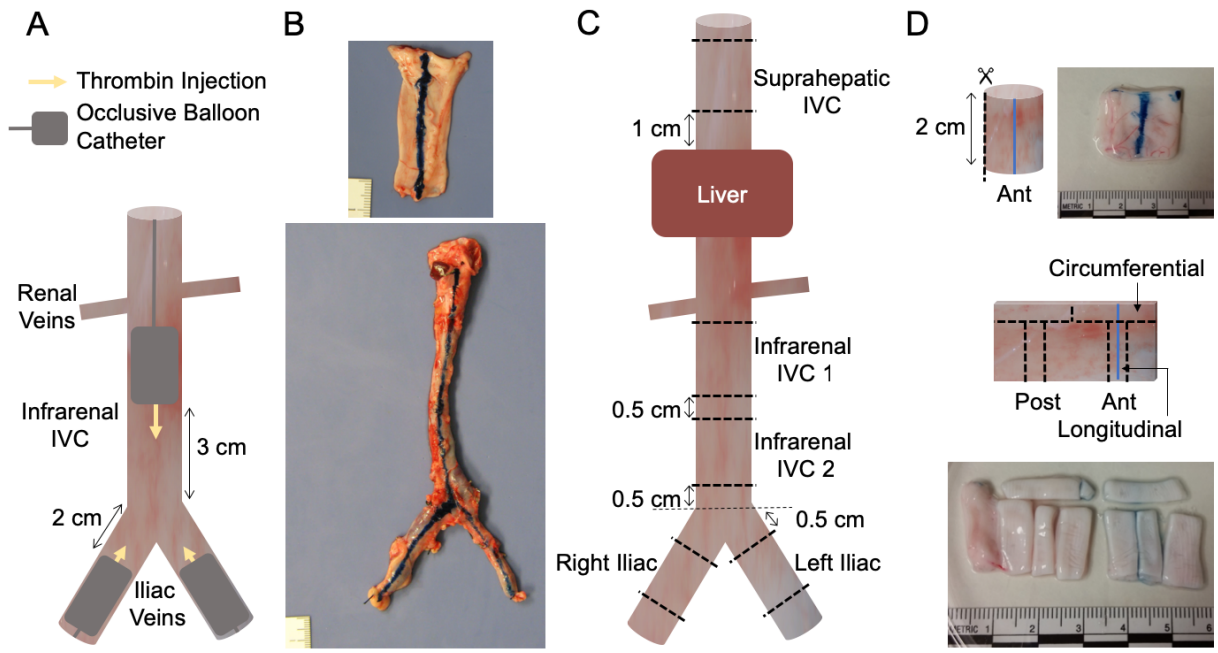

Figure 14 : Samples preparation for mechanical testing

(A) Experimental protocol of creation of iliocaval DVT (B) Suprahepatic IVC, infrarenal IVC and bilateral iliac veins harvesting and dying of their anterior face. (C) Sections were cut from multiple venous segments. (D) Tissue sections were cut along the lateral wall; then longitudinal and circumferential strips were cut from the anterior and posterior walls for uniaxial tensile testing

3.2.2.3. Thrombosis progression classification

Photographs of tissue sections acquired during sample preparation were reviewed to classify the level of thrombus present in each sample into one of four classifications (Figure 15):

- None, or no thrombus present
- Unattached, or thrombus present but completely separable from the venous wall
- Major Incorporation, or large continuous segment of fibrotic thrombus incorporated into and spanning majority of venous wall
- Minor Incorporation, or small pieces of fibrotic thrombus incorporated into the venous wall.

To calculate the proportion of samples in each classification at each location for each time point, the number of samples in each classification was divided by the total number of samples for each specific location and time point, excluding healthy and suprahepatic samples.

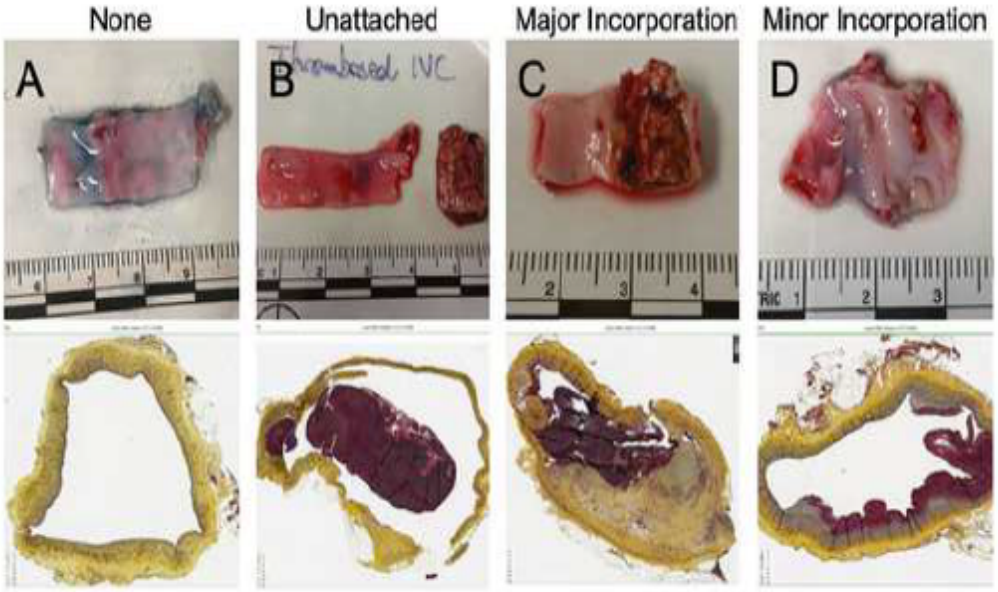

Figure 15 : Thrombus classifications

Thrombus classification by gross evaluations as described in the text above mentioned (A-D). MOVAT staining in the middle row images stains collagen yellow, proteoglycans and glycosaminoglycans blue, elastin black, and fibrin and smooth muscle cells red.

3.2.2.4. Uniaxial tensile testing

To obtain accurate sample width and thickness dimensions, each sample was photographed in multiple orientations, along with a metal piece of known dimensions, using a Leica MZ6 stereomicroscope (Wetzlar, Germany) prior to loading in the mechanical tester. The width and thicknesses were measured using ImageJ software (NIH; Bethesda, MD).

Tissue strips were glued to balsa wood on both ends to prevent slippage from the grips during testing.

The tissue was then loaded into the EnduraTEC ELF 3220 (TA Instruments; Eden Prairie, MN) uniaxial tension tester, and the gauge length was measured as the length at which loading could be first detected. Tissues were preconditioned with 20 cycles of 3 mm displacement before being stretched to failure at a strain rate of 1 mm/second. The tissues were kept hydrated in a bath of PBS at 37°C for the duration of the test. Samples that failed prior to the stretch to failure step or that slipped from the tester grips were excluded.

The tissue widths and gauge lengths were used to convert raw load and displacement data to tension-strain curves, as previously described[149]. The maximum slope of the bilinear curve that spanned at least 4% strain was used to calculate the stiffness. The maximum tension achieved prior to failure was considered the failure strength.

3.2.2.5. Statistical analysis

For all analyses (other than for thickness), samples were separated into longitudinal and circumferential groups, and analysis was performed on each orientation independently. The circumferential group had no samples for some animals at the 2 week timepoint, as well as for both iliac vein locations, so these samples were excluded from the circumferential analysis. Multifactorial analysis of variance (ANOVA) with post hoc Tukey's multiple comparisons test was performed using R Studio (R Studio; Boston, MA). Results were considered significant at $p < 0.05$. Data are reported as mean (± SD). Unless otherwise stated, the two-way ANOVA did not find significance for the interaction terms.

3.2.3. Results

3.2.3.1. Anterior versus posterior

A three-way ANOVA showed no significant overall differences in longitudinal stiffness ($p=0.1340$) or in thickness ($p=0.1010$) between anterior and posterior walls and did not show a difference at each location, except in one instance. Therefore, the remaining analyses do not consider the wall side as a factor, and include the lateral wall sections of interest.

3.2.3.2. Presence of visible thrombus

Thrombus was often visible in the venous segments after dissection (Figure 16). At 1 week, most samples had unattached thrombus (73%). Weeks 2 and 3 had the most samples with major incorporation of thrombus into the venous wall, 27% and 22% respectively. At weeks 4 and 5, more samples had minor incorporation (4 weeks: 11%; 5 weeks: 13%) compared to major incorporation (4 weeks: 7%; 5 weeks: 9%). The left iliac had more samples with no thrombus present (50%), while the right iliac had the most samples with major incorporation of thrombus (26%). The trends of IVC1 and IVC2 closely matched over time.

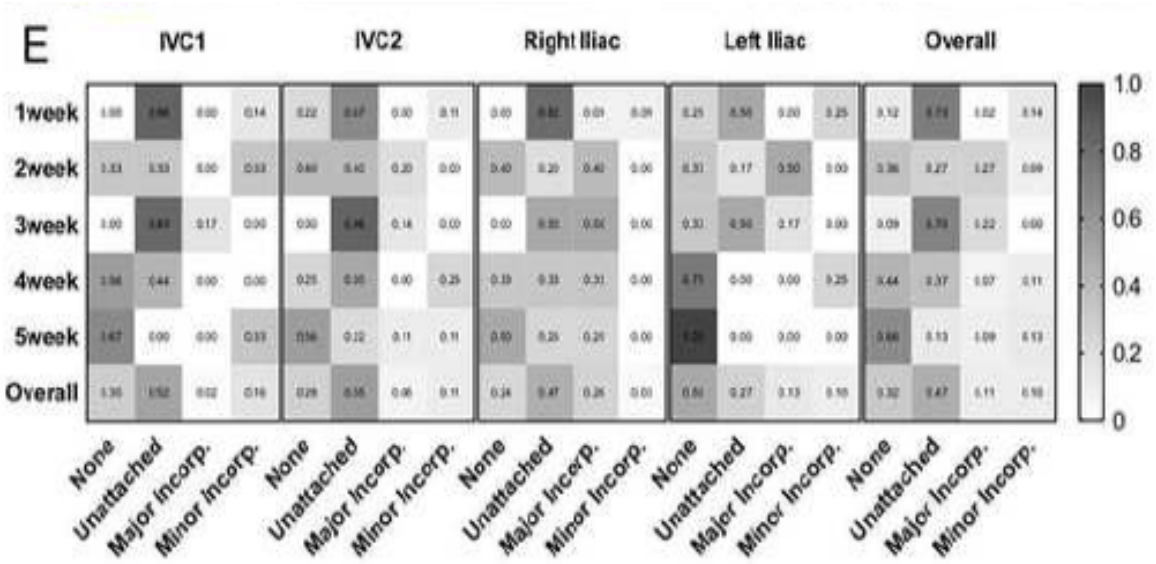

Figure 16 : Presence of visible thrombus

The proportion of samples that fell into each category for each location and timepoint. (IVC = inferior vena cava)

3.2.3.3. Thickness of vessel wall

In healthy veins, the wall thickness of the suprahepatic IVC was greater than that of the other segments (each: $p<0.0001$; Figure 17A). There were no significant differences in thickness between the other venous segments.

The wall thickness was greater in the DVT veins than for healthy veins, when considered overall ($p= 0.0005$; Figure 17C) and specifically at 2 and 3 weeks (each: $p<0.0001$; Figure 17D). Moreover, the venous wall at 2 weeks was thicker than that of all other time points (1 week, 4 week: $p<0.0001$; 5 week: $p=0.0024$). The vessel wall at 3 weeks was also thicker than that of the 1-week ($p<0.0001$) and 4-week ($p=0.0184$) time points. Unlike the healthy veins, the DVT veins showed no differences in thickness between locations (Figure 17E). Over time, the thicknesses of the IVC2 and the left iliac changed significantly. The thickness of IVC2 at 2 and 3 weeks was greater than that of both healthy (2 weeks: $p=0.0311$; 3 weeks: $p=0.0050$) and 1 week (2 weeks: $p=0.0280$; 3 weeks: $p=0.0052$) tissue (Figure 17F). The thickness of the left iliac at 2 weeks was greater than that of healthy ($p<0.0001$) and all other time points (1 week: $p=0.0002$; 4 weeks: $p=0.0237$; 5 weeks: $p=0.0034$), except 3 weeks.

When analysing the samples according to the thrombus classification, the thickness of the major incorporation group was greater than the remaining three classifications (each $p<0.0001$; Figure 17B). Therefore, the comparison of thickness between groups was repeated after censoring all samples classified as major incorporation to assess the effects of thrombosis on vessel wall thickness independent of these extreme samples. Even after this censoring, the DVT veins were thicker than those of healthy pigs ($p= 0.0003$; Figure 17G). Additionally, the thickness of the venous wall at 2, 3, and 5 weeks was significantly increased compared to healthy (2 week, 3 week: $p<0.0001$; 5 week: $p=0.0003$) and 1 week (2 week, 3 week: $p<0.0001$; 5 week: 0.0005; Figure 17H). At the 4 week timepoint, IVC2 ($p=0.0268$) and right iliac ($p=0.0025$) were thinner than

IVC1. This censoring also revealed differences between anatomical locations (Figure 17I). The suprahepatic IVC was thicker than IVC2 ($p<0.0001$), right iliac ($p=0.0011$), and left iliac ($p<0.0001$). IVC1 was thicker than IVC2 ($p=0.0016$) and left iliac ($p=0.0013$). IVC1 increased in thickness compared to healthy at 2 weeks ($p=0.0222$), 4 weeks ($p=0.0003$), and 5 weeks ($p=0.0413$), and it was thicker at 4 weeks than at 1 week ($p=0.0060$; Figure 17J).

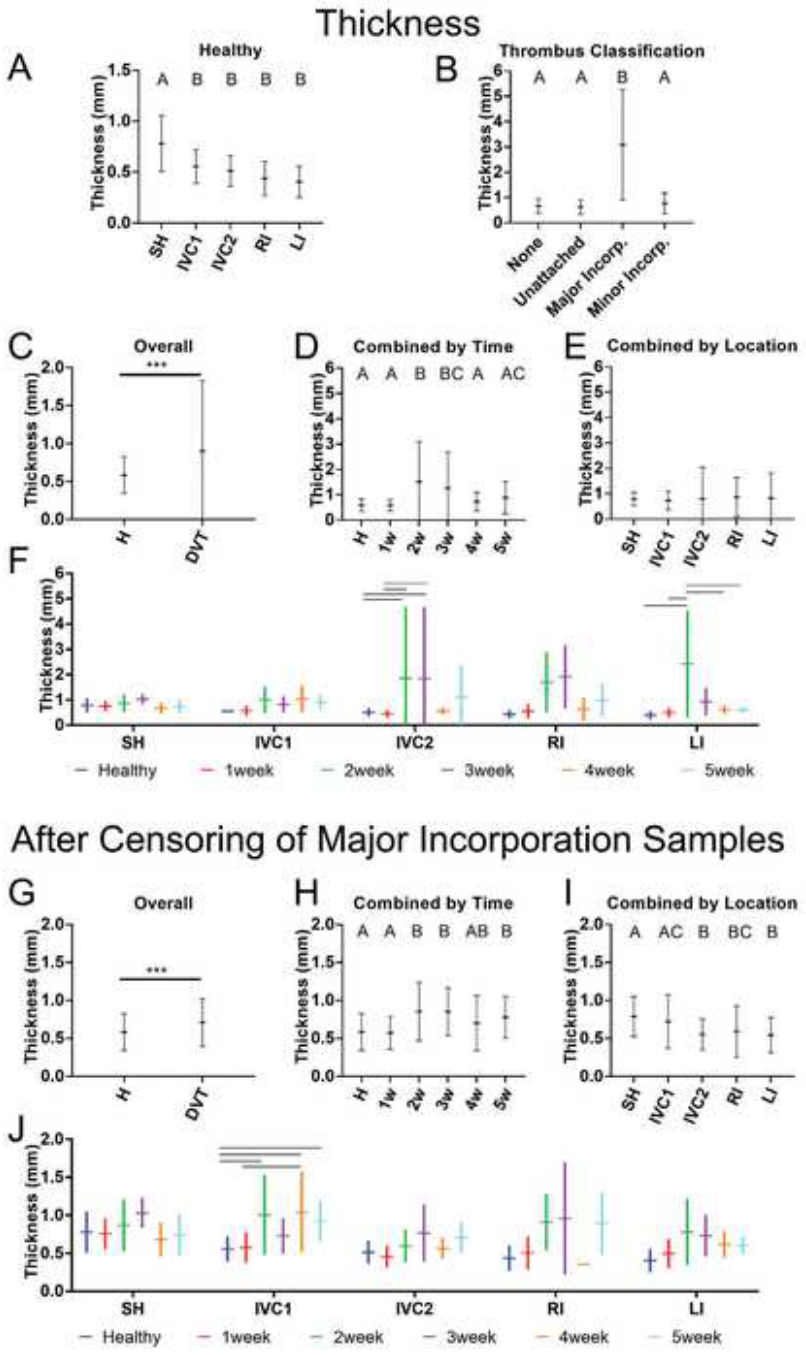

Figure 17 : Thickness of the venous wall

In healthy veins, SH was significantly thicker than other anatomical regions (A). Samples classified as major incorporation were significantly thicker than those in other classifications (B). The venous wall in the DVT model was thicker overall than that in healthy pigs (C). The thickness was greatest at 2 and 3 weeks in the DVT model (D). Thickness did not differ between anatomical locations (E). IVC2 and LI displayed significant differences between time points (F). After censoring the major incorporation samples, the venous wall of the DVT model remained thicker overall than that in healthy pigs (G). After censoring, thickness increased at time points 2 weeks and later compared to healthy and 1 week (H). Censoring revealed differences between anatomical locations that were not present previously (I). IVC1 thickness was different between time points (J). Groups that do not share a letter are significantly different from one another. ***= $p<0.001$. A bar indicates significant difference between the groups at the two endpoints. (H = healthy; DVT = deep vein thrombosis model; w = weeks; SH = suprahepatic inferior vena cava; IVC1 = infrarenal inferior vena cava 1; IVC2 = infrarenal inferior vena cava 2; RI = right iliac vein; LI = left iliac vein).

3.2.3.4. Mechanical behaviour of healthy veins

The longitudinal stiffness (IVC1: $p=.0014$; IVC2: $p<0.0001$) and failure strength (each $p<0.0001$) of suprahepatic IVC was lower than that of both infrarenal IVCs but not that of the iliac veins (Figure 18A, B). The left iliac was less stiff longitudinally than IVC2 ($p=0.0051$) and had a lower longitudinal failure strength than IVC1 ($p=0.0008$) and IVC2 ($p=0.0007$).
In the circumferential direction, suprahepatic IVC showed the reverse trend in that it was stiffer (IVC1: $p=0.0007$; IVC2: $p=0.0002$) and stronger (IVC1: $p=0.0103$; IVC2: $p=0.0076$) than the infrarenal IVCs (Figure 18C, D). When comparing circumferential to longitudinal orientations, suprahepatic IVC (stiffness: $p<0.0001$; strength: $p=0.0088$) and IVC2 (stiffness: $p=0.0027$; strength: $p=0.0006$) showed anisotropy for both stiffness (Figure 18E) and failure strength (Figure 18F), whereas IVC1 was only different for failure strength ($p=0.0009$). However, the suprahepatic and infrarenal IVCs were anisotropic in opposite ways with suprahepatic IVC stiffer circumferentially and the IVCs stiffer longitudinally.

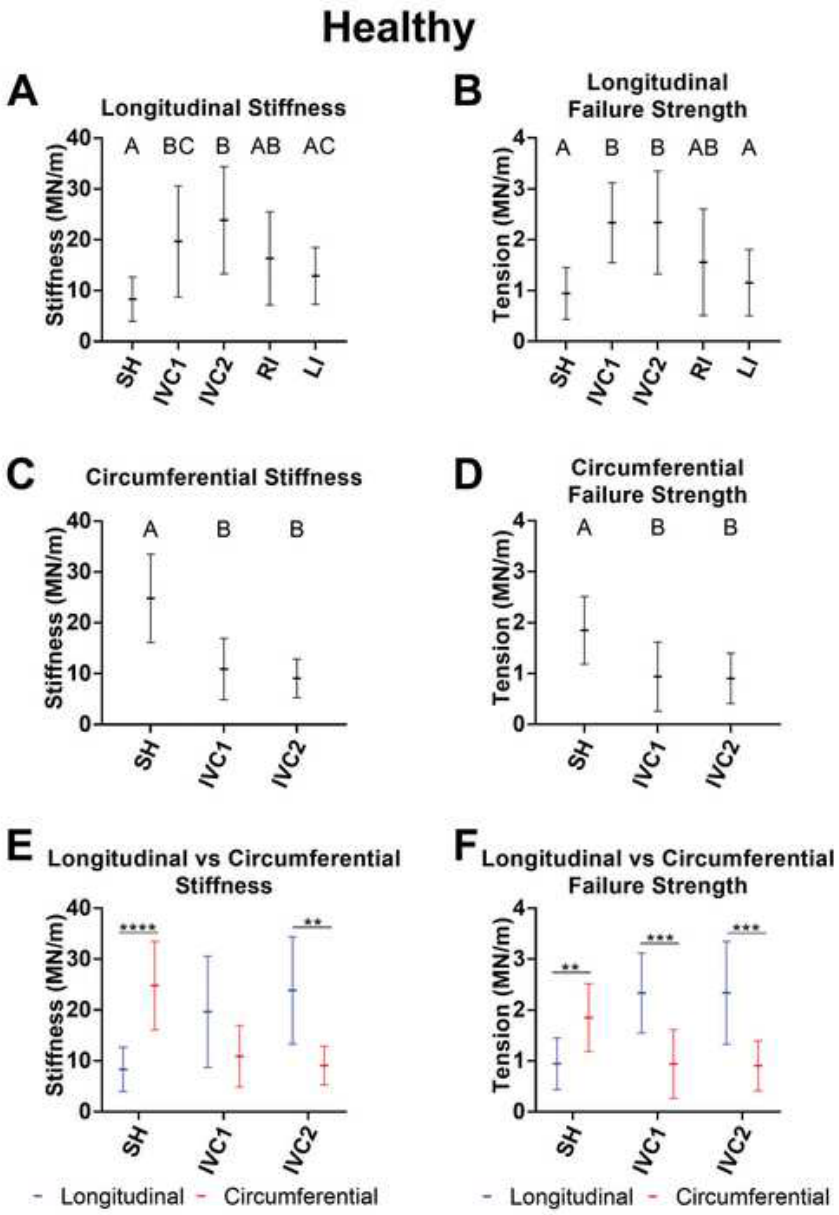

Figure 18 : Mechanical properties of healthy veins

The stiffness and failure strength of SH was lower in the longitudinal direction (A,B) and higher in the circumferential direction (C,D) than IVC1 and IVC2. SH and IVC2 displayed anisotropy in stiffness (E). SH, IVC1, and IVC2 displayed anisotropy in failure strength (F). Groups that do not share a letter are significantly different from one another. (** = $p<0.01$; *** = $p<0.001$; **** = $p<0.0001$. SH = suprahepatic inferior vena cava; IVC1 = infrarenal inferior vena cava 1; IVC2 = infrarenal inferior vena cava 2; RI = right iliac vein; LI = left iliac vein).

3.2.3.5. Longitudinal material behaviour

Overall, the longitudinal stiffness of the venous wall in the thrombosis models was greater than that of healthy pigs (p=0.0277; Figure 19A). Over time, the longitudinal stiffness displayed an increasing trend, becoming stiffer than healthy at 4 weeks (p=0.0154) and with a nearly significant increase at 5 weeks (p=0.1092; Figure 19B). The suprahepatic IVC was the least stiff (IVC1, IVC2: p<0.0001; right iliac: p=0.0049; left iliac: p=0.0010), while IVC1 (right iliac: p=0.0095; left iliac: p=0.0184) and IVC2 (right iliac, left iliac: p<0.0001) were the stiffest (Figure 19C). There were no differences between the IVC1 and IVC2, nor between the two iliac veins.
There were no significant differences in failure strength between the healthy and DVT veins overall or over time (data not shown). However, IVC1 and IVC2 were both stronger than suprahepatic, right iliac, and left iliac (each: p<0.0001).

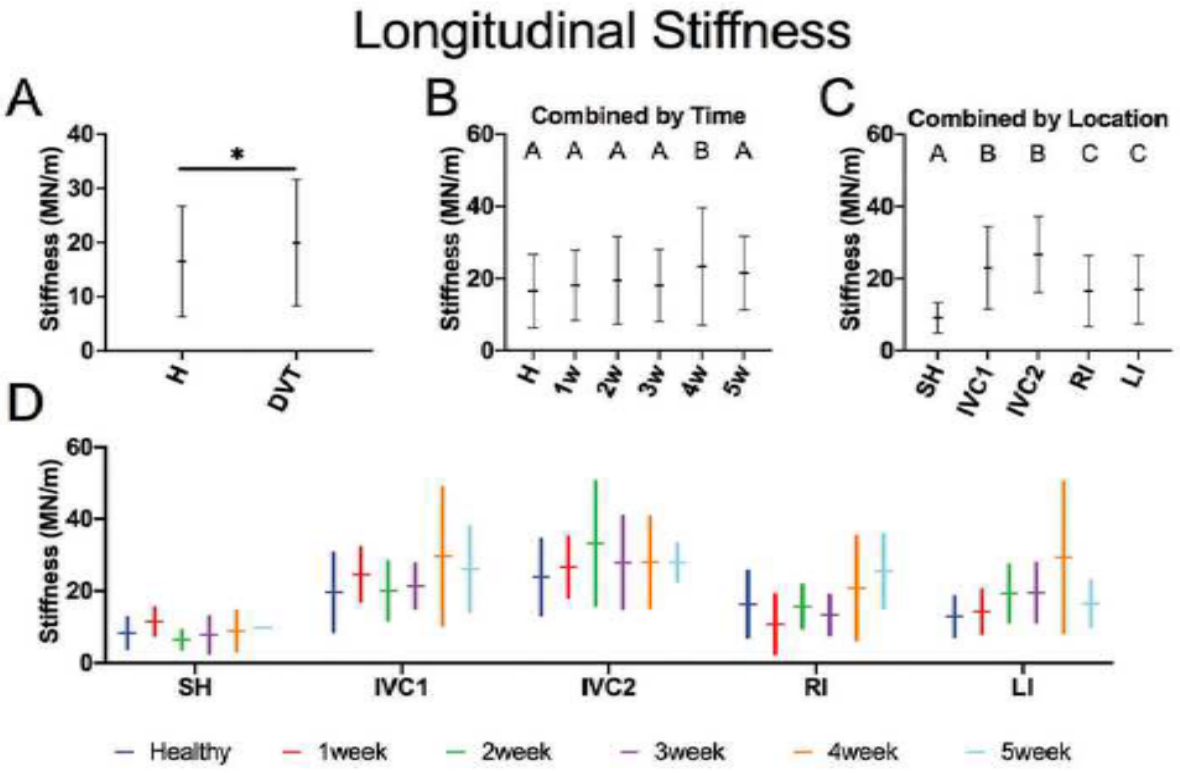

Figure 19 : Longitudinal stiffness in the DVT model

The DVT venous wall was stiffer overall than in healthy pigs (A). The stiffness had an increasing trend over time (B). SH was the least stiff, and IVC1 and IVC2 were the stiffest of the anatomical regions (C). There were no significant changes in stiffness for the individual locations (D). In B and C, groups that do not share a letter are significantly different from one another. (*= p<0.05. H = healthy; DVT = deep vein thrombosis model; w = weeks; SH = suprahepatic inferior vena cava; IVC1 = infrarenal inferior vena cava 1; IVC2 = infrarenal inferior vena cava 2; RI = right iliac vein; LI = left iliac vein).

3.2.3.6. Circumferential material behaviour

There were no significant differences in circumferential stiffness (Figure 20A) or failure strength (data not shown) detected over time. However, the suprahepatic IVC was stiffer (Figure 20B, C) and stronger than IVC1 and IVC2 (each: $p<0.0001$).

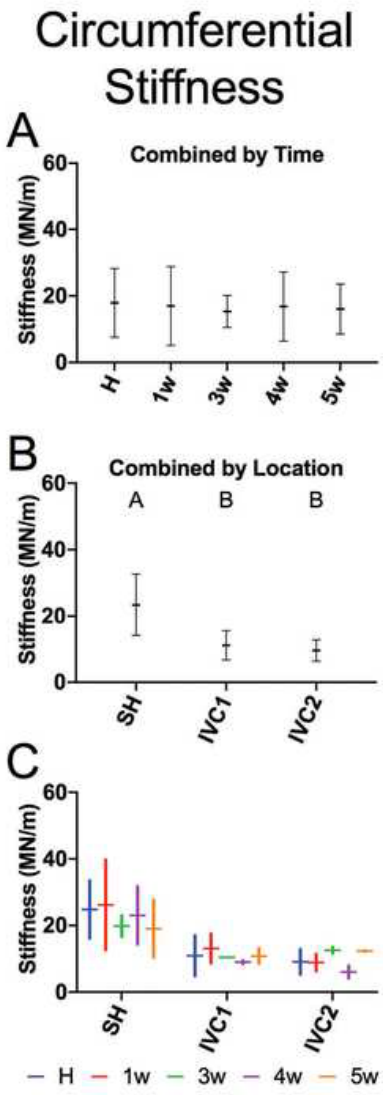

Figure 20 : Circumferential stiffness of the venous wall in the DVT model

No significant differences were detected over time (A). SH was stiffer than IVC1 and IVC2 (B). No significant differences were found between time points for each location (C). Groups that do not share a letter are significantly different from one another. (H = healthy; w = weeks; SH = suprahepatic inferior vena cava; IVC1 = infrarenal inferior vena cava 1; IVC2 = infrarenal inferior vena cava 2).

3.2.3.7. Material behaviour based on thrombus classification

When the venous samples were classified according to the presence of thrombus, there were no significant differences detected in longitudinal stiffness or failure strength between groups (data not shown). However, the unattached ($p=0.0801$) and minor incorporation ($p=0.0817$) groups trended toward being stiffer than the none group. There were not enough samples in each group to perform a similar analysis for circumferential samples.

3.2.4. Discussion

This work describes the first analysis of altered material properties in a clinically relevant porcine model of DVT with comparison to healthy venous tissue. This model demonstrated the progression of thrombosis observed clinically, with fibrotic transformation and vessel wall incorporation, and resolution,[69] which further underscores the significance of our findings. Our study revealed differences in thickness, stiffness, and failure strength between anatomical sites in healthy and diseased pigs. Additionally, we found the venous wall becomes thicker and stiffer longitudinally over the course of DVT. These results provide valuable information for the design of endovascular devices specific to the central venous system.

Our analysis of healthy tissue showed region-specific differences in material properties and significant anisotropy in the venous wall. Within the IVC, stiffness increased longitudinally and decreased circumferentially with distance from the heart. The suprahepatic IVC, which is located proximal to the heart compared to the infrarenal IVC and iliac veins, is thicker than the more distal locations, a pattern also reported in the canine superior vena cava.[68] The canine superior vena cava study, however, found that circumferential stiffness increased over a 5 cm distance from the right heart.[68] Here, both the suprahepatic IVC and the IVC regions showed a pronounced anisotropy, but in an opposite manner. The suprahepatic IVC region was stiffer in the circumferential direction than in the longitudinal direction, which has previously been reported in the thoracic IVC[147]. The reversal of this pattern for the infrarenal IVC may reflect the differences in the mechanical loading environment between the anatomical locations. The suprahepatic IVC is intrathoracic and is thus exposed to negative pressure during inhalation, which would increase the blood load in the suprahepatic IVC, while the abdominal location of the infrarenal IVC is exposed to positive pressure during this process. Together, these data illuminate the regional inhomogeneity within the venous system.

The venous wall thickness increased in the DVT model compared to healthy, changes that were evident regardless of whether or not the incorporated thrombus was considered. In the initial data analysis, it was noted that the wall thickness was much greater at 2 and 3 weeks, which were the time points with the most major incorporation samples. Because it was not possible to measure the thickness of the venous wall without including the thrombus in these samples, we censored the data from the major incorporation samples. This removal of 5% of the samples decreased the overall mean thickness by 21% while decreasing the SD by 66%, enabling detection of smaller differences in the remaining samples. The censored analysis still shows thickening of the veins at 2 and later, indicative of progression from acute stage thrombosis to chronic stage thrombosis. Increased thickness of the venous wall over the course of thrombosis progression, even after

resolution, has been noted both clinically[81,150] and in rat models[6]. The censored analysis also showed similar anatomic variation in thickness to that observed in healthy veins, suggesting that despite increases in thickness, the overall physiological patterns between regions are maintained.

The venous wall was stiffer in the DVT model than in healthy pigs. The increase in longitudinal stiffness over the progression of thrombosis was expected due to reports of fibrosis of the thrombus, stiffening of fibres embedded in the venous wall, and activation of matrix remodeling enzymes such as Matrix Metalloproteinase-9[80–82]. Increased stiffness in DVT has also been reported in murine models[80,82,148] and is consistent with reports of decreased venous compliance during the disease.[151] It should be noted that the stiffness and failure strength in this study were obtained by normalizing to the width of the test tissue instead of the cross-sectional area, since the thrombus-driven thickening was though not to contribute to the load-bearing capacity of the venous wall. Nonetheless, this stiffening should be considered in the development of venous endovascular devices for the treatment of DVT. Interestingly, the relationships between locations in the DVT model for stiffness and failure strength (e.g., suprahepatic IVC < iliac veins < IVC1 and IVC2 for longitudinal parameters) closely mirrored those in healthy veins. In addition, IVC1 and IVC2 displayed similar trends in thrombus classification proportions, despite their different roles in the initiation of the DVT model, and also did not differ in their material properties over time. This similarity suggests that the effects of thrombin may spread to immediately neighbouring regions. In contrast, the left and right iliac veins in the DVT model had similar longitudinal material behaviour, but very different presentations of thrombus. The effect of thrombosis on venous wall remodeling may depend more on the biological response to thrombosis, such as inflammation and hypoxia, than on the direct presence of thrombus.

Additionally, the relatively stable mechanics of the suprahepatic IVC over time suggests that DVT does not affect the venous wall mechanics of distant regions. Overall, the similarities in the relationships between locations in the DVT model and in healthy tissue suggest a uniformity in the tissues' responses to thrombosis.

Although this characterization of porcine venous material behaviour in health and DVT is novel, there are notable limitations to the study. First, the presentation of DVT in this porcine model mimicked the clinical condition, but the results may not be fully generalizable to humans. Additionally, there were only small number of pigs at each time point as this was a pilot evaluation of the DVT model[152]. The use of different commercial suppliers for the DVT and healthy pigs likely contributed to greater pig-to-pig variation than normal. Furthermore, the thin, floppy nature of veins in their planar state[153] made it difficult to measure the width and thickness, so the tissue was gently pulled taut until all folding was removed and the tissue laid flat. Lastly, the ex vivo tensile testing methods required sacrificing animals at each time point. Non-invasive methods, such as ultrasound elastography,[154] would enable the measurement of DVT-driven changes to the venous wall mechanics in the same animal at multiple time points.

3.2.5. Future work

3.2.5.1. Creation of a spatial deformation map

While uniaxial mechanical testing provided valuable information about the viscoelastic properties of several regions of the IVC and iliac veins, as described in our preliminary data, it is not able to fully characterize properties of the whole vessel.
A future work will consist in using digital image correlation (DIC) of the pressurized thrombosed venous segment to map the strain of each region and assess heterogeneity of the entire segment.

The thrombosed infrarenal IVC and bilateral iliac veins will be measured in-vivo, harvested en bloc and again measured ex-vivo to assess physiological longitudinal stretch. Every collateral vein will be sutured to prevent leakage. In a warm room (37°C), the venous segment will be attached to the pressure head, anterior wall facing up. The entire vessel segment will be kept planar and maintained at the same height to ensure equal pressure along the entire vessel. The pressure sensor will be connected to the analog input channel of the DIC system (Figure 21).

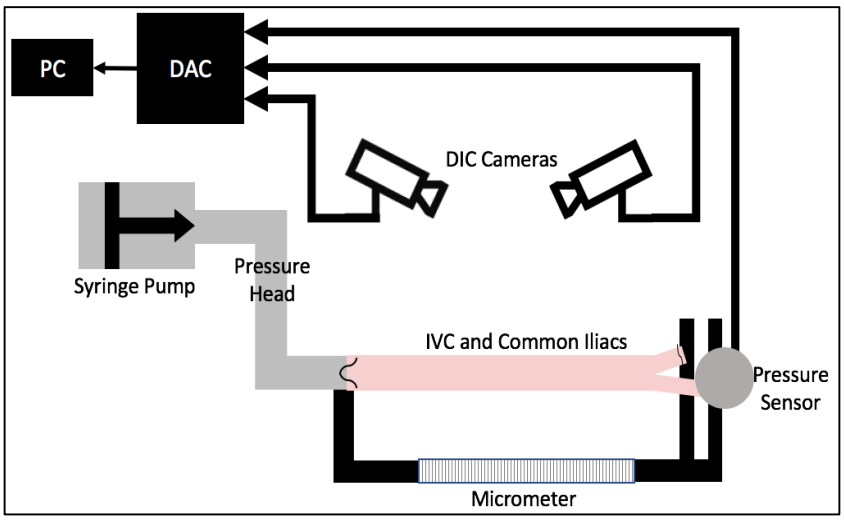

Figure 21: Pressurized system for creating of 3D strain map of thrombosed venous tissue

We will set up the micrometer to stretch the vessel segment to its *in situ* length. This will ensure that physiological longitudinal strains are properly sensed by the tissue. The venous segment will be speckled with enamel spray paint to create a speckle pattern for tracking deformation with the DIC system. A paint speckle pattern has been shown to have a nonsignificant effect on soft tissue mechanics[155]. The vein will then be filled with PBS to maintain its three-dimensional structure. We will use a syringe pump to incrementally pump PBS into the vessel segment, allowing time after pumping for all the fluid to stabilize in order to avoid any pressure differences along the length of the vessel caused by active flow. At each pressure increment, the DIC system will track deformation of the speckle pattern and will compute strains by assessing deformation of each point (Figure 22). It will also record pressure as measured by the analog pressure sensor. We will repeat

the process for pressure increments up to 20 mmHg, then rotate the vein to get a similar spatial deformation map of the posterior wall.
This pressurized DIC system will produce a heat map of deformation values for the anterior and posterior walls along the length of the venous segment for each pressure increment. This will allow us to correlate deformation with specific pressures and assess the heterogeneity of deformation in the vessel wall following thrombosis.

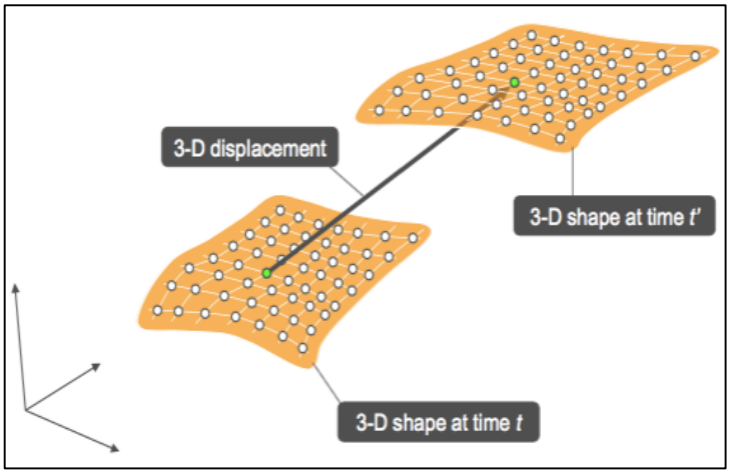

Figure 22 : Deformation tracking via digital image correlation

3.2.5.2. Characterization of the thrombus and venous wall elastic properties

We have seen that a thrombus undergoes fibrotic transformation after several days in a vessel and eventually begins to incorporate into the vessel wall. However, it has not been studied how the fibrotic transformation affects the elastic properties of the thrombus and the venous wall, or how different compositional components of the thrombus vary in their properties. The goal of this step is to characterize the radial elastic properties of the venous wall, incorporated thrombus, and detached thrombus using bio-indentation.

Following completion of the spatial strain map, we will remove the venous segment from the platform and cut 2mm-thick segments along the IVC and bilateral iliac veins. An Anton Parr Bio-indentor will be used to perform indentation on each segment along the radial length of the vessel wall using the flat head tip (100 μm diameter), starting at the adventitia and moving toward the intima and into incorporated thrombus with multiple points in a straight line to assess changing properties of vessel wall. The Anton Parr software will calculate indentation modulus from the unloading curve of each point, which will allow us to assess how stiffness changes through the layers and into the thrombus.

3.2.5.3. Characterization of the bulk properties of the thrombus

We aim to assess how the bulk viscoelastic properties of the venous thrombus change over time by performing rheology on the thrombus. Rheology will allow us to characterize the relationship between stress and deformation of the thrombus.
To do this, we will place the thrombus from each thrombosis model porcine vein segment on a parallel plate of a TA Instruments Rheometer. We will drip several drops of mineral oil on each sample to coat the exterior and maintain hydration of the thrombus. The rheometer will perform amplitude sweeps with varying amplitudes of shear on each thrombus sample, while the frequency remains constant. The storage and loss modulus are plotted as a function of the deformation. The resulting graph will provide information about the rigidity, viscosity, and viscoelastic characteristics of the thrombus.

3.2.5.4. Comparison of mechanical properties to histological findings

In addition to bio-indentation and rheometer study, 5mm-thick sections at several levels of the venous sample will be fixed in formalin and embedded in paraffin. Blocks will be further sectioned and stained using H&E to observe general tissue morphology, MOVAT to assess tissue layer composition, and Picrosirius red to visualize collagen alignment. Tissue slides will be quantitatively analyzed using the Aperio image analysis software.
We hypothesize to demonstrate significant correlation between histological content (mainly elastin and collagen) and mechanical findings of the thrombosed vein.

3.2.6. Conclusion

In conclusion, this porcine model of DVT induced gradual increases in the thickness and longitudinal stiffness of the venous wall, even after thrombus resolution (Figure 23). Despite these pathological alterations, the thrombosed veins showed the same location-based patterns of material behaviour and thickness found in healthy veins. Together, these findings broaden our understanding of venous mechanics and provide guidance for designing venous-specific endovascular devices to treat DVT.

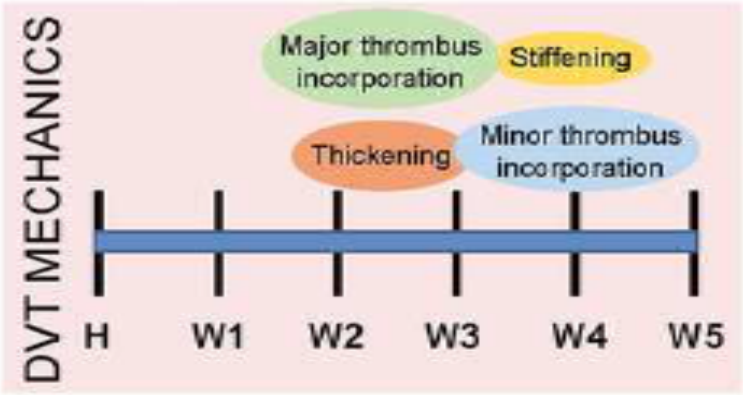

Figure 23 : Summary of our mechanical findings

GENERAL CONCLUSION

Although DVT is a major healthcare issue in western countries, many unknown persists regarding its natural history and optimal management.
In this work, we developed a minimally invasive totally endovascular model of acute and subacute iliocaval DVT, which is effective in 60kg-animals, as well as being safe and reproducible.
We paid particular attention to the respect of the ARRIVE Guidelines on reporting in vivo experiments in a matter of standardization and reproducibility by other teams.
It is important to note that the model respects the integrity of the vascular system and does not leave foreign material, avoiding artificial lesions and imaging artefacts.

We performed exhaustive imaging modalities both in the preoperative period, immediate postoperative period and after 1 to 5 weeks of follow up, gathering fluoroscopy, CBCT and MRI images. The obtained data still need further analysis; our hypothesis is that results should emphasize the use of specific MRI sequences as non-invasive imaging modality to assess the structural content of the thrombosed vein and could thus guide optimal management of acute iliofemoral DVT.

Analysis of the mechanical properties of the thrombosed vein showed that DVT induced gradual increase in the thickness and longitudinal stiffness of the venous wall, even after thrombus resolution. Despite these pathological alterations, the thrombosed veins showed the same location-based patterns of material behaviour and thickness found in healthy veins. Further characterization of the thrombus, of the elastic properties of the venous wall, as well as the establishment of a spatial deformation map will broaden our understanding of venous mechanics and provide guidance for designing venous-specific endovascular devices to treat venous obstructive diseases.

Our large animal model of DVT will finally serve as a valuable support for device testing and surgeon training in a field that has for long been the forgotten side of vascular surgery.

REFERENCES

1 Kahn SR, Shapiro S, Wells PS, Rodger MA, Kovacs MJ, Anderson DR, et al. Compression stockings to prevent post-thrombotic syndrome: A randomised placebo-controlled trial. *Lancet* 2014;**383**(9920):880–8. Doi: 10.1016/S0140-6736(13)61902-9.

2 Kakkos SK, Gohel M, Baekgaard N, Bauersachs R, Bellmunt-Montoya S, Black SA, et al. Editor's Choice – European Society for Vascular Surgery (ESVS) 2021 Clinical Practice Guidelines on the Management of Venous Thrombosis. *Eur J Vasc Endovasc Surg* 2021;**61**(1):9–82. Doi: 10.1016/j.ejvs.2020.09.023.

3 Albadawi H, Witting AA, Pershad Y, Wallace A, Fleck AR, Hoang P, et al. Animal models of venous thrombosis. *Cardiovasc Diagn Ther* 2017;**7**(Suppl 3):197–206. Doi: 10.21037/cdt.2017.08.10.

4 Grover SP, Evans CE, Patel AS, Modarai B, Saha P, Smith A. Assessment of Venous Thrombosis in Animal Models. *Arterioscler Thromb Vasc Biol* 2016;**36**(2):245–52. Doi: 10.1161/ATVBAHA.115.306255.

5 Jagadeeswaran P, Cooley BC, Gross PL, Mackman N. Animal Models of Thrombosis From Zebrafish to Nonhuman Primates. *Circ Res* 2016;**118**:1363–80. Doi: 10.1161/CIRCRESAHA.115.306823.

6 Diaz J a., Obi AT, Myers DD, Wrobleski SK, Henke PK, MacKman N, et al. Critical review of mouse models of venous thrombosis. *Arterioscler Thromb Vasc Biol* 2012;**32**(3):556–62. Doi: 10.1161/ATVBAHA.111.244608.

7 Levi M, Dörffler-Melly J, Johnson GJ, Drouet L, Badimon L. Usefulness and limitations of animal models of venous thrombosis. *Thromb Haemost* 2001;**86**:1331–3.

8 Vedantham S, Sista AK, Klein SJ, Nayak L, Razavi MK, Kalva SP, et al. Quality improvement guidelines for the treatment of lower-extremity deep vein thrombosis with use of endovascular thrombus removal. *J Vasc Interv Radiol* 2014;**25**(9):1317–25. Doi: 10.1016/j.jvir.2014.04.019.

9 De Maeseneer MGR, Bochanen N, Van Rooijen G, Neglén P. Analysis of 1,338 Patients with Acute Lower Limb Deep Venous Thrombosis (DVT) Supports the Inadequacy of the Term "proximal DVT." *Eur J Vasc Endovasc Surg* 2016;**51**(3):415–20. Doi: 10.1016/j.ejvs.2015.11.001.

10 Heit JA, Spencer FA, White RH. The epidemiology of venous thromboembolism. *J Thromb Thrombolysis* 2016;**41**(1):3–14. Doi: 10.1007/s11239-015-1311-6.

11 Barco S, Woersching AL, Spyropoulos AC, Piovella F, Mahan CE. European Union-28: An annualised cost-of-illness model for venous thromboembolism. *Thromb Haemost* 2016;**115**(4):800–8. Doi: 10.1160/TH15-08-0670.

12 Lee B, Nicolaides A, Myers K, Meissner M, Kalodiki E. Venous hemodynamic changes in lower limb venous disease: the UIP consensus according to scientific evidence. *Int Angiol* 2016;**35**(3):236–352.

13 Partsch H. Therapy of deep vein thrombosis with low molecular weight heparin, compression and walking exercises. *An Cir Card y Cir Vasc* 2001;**7**(4):322–4.

14 Prandoni P, Lensing A, Prins M, Frulla M, Marchiori A, Bernardi E, et al. Below-Knee Elastic Compression Stockings To Prevent the Post-Thrombotic Syndrome. *Ann Intern Med* 2004;**141**:249–56.

15 Kahn SR, Shrier I, Julian JA, Ducruet T, Arsenault L, Miron MJ, et al. Determinants and time course of the postthrombotic syndrome after acute deep venous thrombosis. *Ann Intern Med* 2008;**149**(10):698–707. Doi: 10.7326/0003-4819-149-10-200811180-00004.
16 Prandoni P, Anthonie WA, Lensing AW, Cogo A, Cuppini S, Villalta S, et al. The long-term clinical course of acute deep vein thrombosis. *Ann Intern Med* 1996;**125**(1):1–7.
17 Saarinen J, Kallio T, Lehto M, Hiltunen S, Sisto T. The occurrence of the post-thrombotic changes after an acute deep venous thrombosis. A prospective two-year follow-up study. *J Cardiovasc Surg* n.d.;**41**(3):441–6.
18 Lurie F, Passman M, Meisner M, Dalsing M, Masuda E, Welch H, et al. The 2020 update of the CEAP classification system and reporting standards. *J Vasc Surg Venous Lymphat Disord* 2020;**8**(3):342–52. Doi: 10.1016/j.jvsv.2019.12.075.
19 Kahn SR, Comerota AJ, Cushman M, Evans NS, Ginsberg JS, Goldenberg NA, et al. The postthrombotic syndrome: Evidence-based prevention, diagnosis, and treatment strategies: A scientific statement from the American heart association. *Circulation* 2014;**130**(18):1636–61. Doi: 10.1161/CIR.0000000000000130.
20 Kahn SR. Measurement properties of the Villalta scale to define and classify the severity of the post-thrombotic syndrome. *J Thromb Haemost* 2009;**7**(5):884–8. Doi: 10.1111/j.1538-7836.2009.03339.x.
21 Villalta S, Bagatella P, Piccioli A, Lensing A, Prins M, Prandoni P. Assessment of validity and reproducibility of a clinical scale for the post-thrombotic syndrome (abstract). *Haemostasis* 1994;**24**:158a.
22 Kahn SR, Partsch H, Vedantham S, Prandoni P, Kearon C. Definition of post-thrombotic syndrome of the leg for use in clinical investigations: A recommendation for standardization. *J Thromb Haemost* 2009;**7**(5):879–83. Doi: 10.1111/j.1538-7836.2009.03294.x.
23 De Maeseneer MG, Kakkos SK, Aherne T, Baekgaard N, Black S, Blomgren L, et al. Editor's Choice – European Society for Vascular Surgery (ESVS) 2022 Clinical Practice Guidelines on the Management of Chronic Venous Disease of the Lower Limbs. *Eur J Vasc Endovasc Surg* 2022;**63**(2):184–267. Doi: 10.1016/j.ejvs.2021.12.024.
24 Meissner MH, Gloviczki P, Comerota AJ, Dalsing MC, Eklof BG, Gillespie DL, et al. Early thrombus removal strategies for acute deep venous thrombosis: Clinical Practice Guidelines of the Society for Vascular Surgery and the American Venous Forum. *J Vasc Surg* 2012;**55**:1449–62. Doi: 10.1016/j.jvs.2011.12.081.
25 Ortel TL, Neumann I, Ageno W, Beyth R, Clark NP, Cuker A, et al. American society of hematology 2020 guidelines for management of venous thromboembolism: Treatment of deep vein thrombosis and pulmonary embolism. *Blood Adv* 2020;**4**(19):4693–738. Doi: 10.1182/bloodadvances.2020001830.
26 Tran HA, Gibbs H, Merriman E, Curnow JL, Young L, Bennett A, et al. New guidelines from the Thrombosis and Haemostasis Society of Australia and New Zealand for the diagnosis and management of venous thromboembolism. *Med J Aust* 2019;**210**(5):227–35. Doi: 10.5694/mja2.50004.
27 Enden T, Haig Y, Kløw NE, Slagsvold CE, Sandvik L, Ghanima W, et al. Long-term outcome after additional catheter-directed thrombolysis versus standard treatment for acute iliofemoral deep vein thrombosis (the CaVenT study): A randomised controlled trial. *Lancet* 2012;**379**(9810):31–8. Doi: 10.1016/S0140-6736(11)61753-4.
28 Notten P, ten Cate-Hoek AJ, Arnoldussen CWKP, Strijkers RHW, de Smet AAEA, Tick

LW, et al. Ultrasound-accelerated catheter-directed thrombolysis versus anticoagulation for the prevention of post-thrombotic syndrome (CAVA): a single-blind, multicentre, randomised trial. *Lancet Haematol* 2020;**7**(1):e40–9. Doi: 10.1016/S2352-3026(19)30209-1.

29 Sharifi M, Bay C, Mehdipour M, Sharifi J. Thrombus obliteration by rapid percutaneous endovenous intervention in deep venous occlusion (TORPEDO) trial: Midterm results. *J Endovasc Ther* 2012;**19**(2):273–80. Doi: 10.1583/11-3674MR.1.

30 Vedantham S, Goldhaber SZ, Julian JA, Kahn SR, Jaff MR, Cohen DJ, et al. Pharmacomechanical Catheter-Directed Thrombolysis for Deep-Vein Thrombosis. *N Engl J Med* 2017;**377**(23):2240–52. Doi: 10.1056/nejmoa1615066.

31 Haig Y, Enden T, Grøtta O, Kløw NE, Slagsvold CE, Ghanima W, et al. Post-thrombotic syndrome after catheter-directed thrombolysis for deep vein thrombosis (CaVenT): 5-year follow-up results of an open-label, randomised controlled trial. *Lancet Haematol* 2016;**3**(2):e64–71. Doi: 10.1016/S2352-3026(15)00248-3.

32 Foegh P, Jensen LP, Klitfod L, Broholm R, Bækgaard N. Editor's Choice – Factors Associated with Long-Term Outcome in 191 Patients with Ilio-Femoral DVT Treated With Catheter-Directed Thrombolysis. *Eur J Vasc Endovasc Surg* 2017;**53**(3):419–24. Doi: 10.1016/j.ejvs.2016.12.023.

33 Gordon BM, Fishbein MC, Levi DS. Polytetrafluoroethylene-covered stents in the venous and arterial system: angiographic and pathologic findings in a swine model. *Cardiovasc Pathol* 2008;**17**:206–11. Doi: 10.1016/j.carpath.2007.09.001.

34 Seager MJ, Busuttil A, Dharmarajah B, Davies AH. Editor's Choice - A Systematic Review of Endovenous Stenting in Chronic Venous Disease Secondary to Iliac Vein Obstruction. *Eur J Vasc Endovasc Surg* 2016;**51**(1):100–20. Doi: 10.1016/j.ejvs.2015.09.002.

35 Razavi MK, Jaff MR, Miller LE. Safety and Effectiveness of Stent Placement for Iliofemoral Venous Outflow Obstruction: Systematic Review and Meta-Analysis. *Circ Cardiovasc Interv* 2015;**8**(10). Doi: 10.1161/CIRCINTERVENTIONS.115.002772.

36 Bækgaard N, Klitfod L, Broholm R. Safety and efficacy of catheter-directed thrombolysis. *Phlebology* 2012;**27**:149–54.

37 Patterson BO, Hinchliffe R, Loftus IM, Thompson MM, Holt PJE. Indications for catheter-directed thrombolysis in the management of acute proximal deep venous thrombosis. *Arterioscler Thromb Vasc Biol* 2010;**30**(4):669–74. Doi: 10.1161/ATVBAHA.109.200766.

38 Di Fazio N, Delogu G, Ciallella C, Padovano M, Spadazzi F, Frati P, et al. State-of-art in the age determination of venous thromboembolism: A systematic review. *Diagnostics* 2021;**11**(12). Doi: 10.3390/diagnostics11122397.

39 Mansueto G, Costa D, Capasso E, Varavallo F, Brunitto G, Caserta R, et al. The dating of thrombus organization in cases of pulmonary embolism: An autopsy study. *BMC Cardiovasc Disord* 2019;**19**(1):1–8. Doi: 10.1186/s12872-019-1219-8.

40 Varghese T. Quasi-Static Ultrasound Elastography. *Ultrasound Clin* 2009;**4**(3):323–38. Doi: 10.1016/j.cult.2009.10.009.

41 Dharmarajah B, Sounderajah V, Rowland S, Leen E, Davies A. Aging techniques for deep vein thrombosis: a systematic review. *Phlebology* 2015;**30**(2):77–84. Doi: 10.1177/0268355514528691.

42 Hoang P, Wallace A, Sugi M, Fleck A, Pershad Y, Dahiya N, et al. Elastography

techniques in the evaluation of deep vein thrombosis. *Cardiovasc Diagn Ther* 2017;**7**(Suppl 3):S238–45. Doi: 10.21037/cdt.2017.10.04.
43 Parellada AJ, Morrison WB, Reiter SB, Carrino JA, Glickman PL, Kloss LA, et al. Unsuspected lower extremity deep venous thrombosis simulating musculoskeletal pathology. *Skeletal Radiol* 2006;**35**(9):659–64. Doi: 10.1007/s00256-006-0128-y.
44 Froelich. " Bull ' s-eye " sign on gadolinium-enhanced magnetic resonance venography determines thrombus presence and age : A preliminary study n.d.:809–16.
45 Arnoldussen C, Strijkers R, Lambregts D, Lahaye M, de Graaf R, Wittens C. Feasibility of identifying deep vein thrombosis characteristics with contrast enhanced MR-Venography. *Phlebology* 2014;**29**(1 suppl):119–24. Doi: 10.1177/0268355514529697.
46 Arnoldussen CWKP, Notten P, Brans R, Vroegindeweij D, Tick LW, van de Poel MHW, et al. Clinical impact of assessing thrombus age using magnetic resonance venography prior to catheter-directed thrombolysis. *Eur Radiol* 2022:4555–64. Doi: 10.1007/s00330-022-08599-5.
47 Bates SM, Lister-James J, Julian JA, Taillefer R, Moyer BR, Ginsberg JS. Imaging characteristics of a novel technetium Tc 99m-labeled platelet glycoprotein IIb/IIIa receptor antagonist in patients with acute deep vein thrombosis or a history of deep vein thrombosis. *Arch Intern Med* 2003;**163**(4):452–6. Doi: 10.1001/archinte.163.4.452.
48 Mewissen M, Seabrook G, Meisnner M, Cynamon J, Labropoulos N, Haughton S. Catheter-directed thrombolysis for lower extremity deep venous thrombosis: report of a national multicenter registry. *Radiology* 1999;**211**(1):39–49.
49 Collen D, Stassen JM, Verstraete M. Thrombolysis with human extrinsic (tissue-type) plasminogen activator in rabbits with experimental jugular vein thrombosis. Effect of molecular form and dose of activator, age of the thrombus, and route of administration. *J Clin Invest* 1983;**71**(2):368–76. Doi: 10.1172/JCI110778.
50 Wakefield TW, Myers DD, Henke PK. Mechanisms of venous thrombosis and resolution. *Arterioscler Thromb Vasc Biol* 2008;**28**(3):387–91. Doi: 10.1161/ATVBAHA.108.162289.
51 Saha P, Humphries J, Modarai B, Mattock K, Waltham M, Evans CE, et al. Leukocytes and the natural history of deep vein thrombosis: Current concepts and future directions. *Arterioscler Thromb Vasc Biol* 2011;**31**(3):506–12. Doi: 10.1161/ATVBAHA.110.213405.
52 Cesarman-Maus G, Hajjar KA. Molecular mechanisms of fibrinolysis. *Br J Haematol* 2005;**129**(3):307–21. Doi: 10.1111/j.1365-2141.2005.05444.x.
53 Mirshahi M, Soria J, Lu H, Soria C, Samama M, Caen J. Defective thrombolysis due to collagen incorporation in fibrin clots. *Thromb Res* 1988;**8**:73–80.
54 Andia ME, Saha P, Jenkins J, Modarai B, Wiethoff AJ, Phinikaridou A, et al. Fibrin-targeted magnetic resonance imaging allows in vivo quantification of thrombus fibrin content and identifies thrombi amenable for thrombolysis. *Arterioscler Thromb Vasc Biol* 2014;**34**(6):1193–8. Doi: 10.1161/ATVBAHA.113.302931.
55 Phinikaridou A, Andia ME, Saha P, Modarai B, Smith A, Botnar RM. In Vivo Magnetization Transfer and Diffusion-Weighted Magnetic Resonance Imaging Detects Thrombus Composition in a Mouse Model of Deep Vein Thrombosis 2013;**6**(3):433–40. Doi: 10.1161/CIRCIMAGING.112.000077.
56 Saha P, Andia ME, Modarai B, Blume U, Humphries J, Patel AS, et al. Magnetic resonance T1 relaxation time of venous thrombus is determined by iron processing and

predicts susceptibility to lysis. *Circulation* 2013;**128**(7):729–36. Doi: 10.1161/CIRCULATIONAHA.113.001371.
57 Brighton T, Janssen J, Butler SP. Aging of acute deep vein thrombosis measured by radiolabeled 99mTc-rt-PA. *J Nucl Med* 2007;**48**(6):873–8. Doi: 10.2967/jnumed.106.039396.
58 Dickhout A, Van de Vijver P, Bitsch N, van Hoof SJ, Thomassen SLGD, Massberg S, et al. Molecular Detection of Venous Thrombosis in Mouse Models Using SPECT/CT. *Biomolecules* 2022;**12**(6):829. Doi: 10.3390/biom12060829.
59 Boron WF, Boulpaep EL. Medical physiology : a cellular and molecular approach. 2nd ed. Philadelphia, PA: Saunders/Elsevier; 2009.
60 Jacob MP. Extracellular matrix remodeling and matrix metalloproteinases in the vascular wall during aging and in pathological conditions. *Biomed Pharmacother* 2003;**57**(5–6):195–202. Doi: 10.1016/S0753-3322(03)00065-9.
61 Wagenseil JE, Mecham RP. Vascular Extracellular Matrix and Arterial Mechanics. *Physiol Rev* 2009;**89**(3):957–89. Doi: 10.1152/physrev.00041.2008.Vascular.
62 Clark JM, Glagov S. Transmural Organization of the Arterial Media The Lamellar Unit Revisited 1977. Doi: 10.1161/01.ATV.5.1.19.
63 Dobrin PB. Mechanical properties of arterises. *Physiol Rev* 1978;**58**(2).
64 Roach MR, Burton AC. The reason for the shape of the distensibility curves of arteries. *Can J Biochem Physiol* 1957;**35**(8):681–90.
65 Wolinsky H, Glagov S. Structural Basis for the Static Mechanical Properties of the Aortic Media. *Circ Res* 1964;**14**(5):400–13. Doi: 10.1161/01.RES.14.5.400.
66 Vesely J, Horny L, Chlup H, Zitny R. Collagen Orientation and Waviness within the Vein Wall. *Comput Plast Xi Fundam Appl* 2011:720–8.
67 Saitta-Rezakhaniha R, Stergiopulos N. Biomechanics of Vascular Wall: the Role of Structural Organization of Elastin and Collagen. *Fac Life Sci* 2010;**Dr. Sc.**(4712):129. Doi: 10.5075/epfl-thesis-4712.
68 Minten J, Verheyen A, Cornelissen F, Rombauts W, Dequeker J, De Geest H. Correlation between mechanical properties and wall composition of the canine superior vena cava. *Arch Int Physiol Biochim* 1986;**94**:349–62.
69 Kumar V, Abbas A, Fausto N, Aster JC. Robbins and Cotran Pathologic Basis of Disease 8th edition. Philadelphia, PA; 2010.
70 Marieb EN. Human Anatomy & Physiology. San Francisco: Pearson Benjamin Cummings; 2007.
71 Clark ER. Studies on the growth of blood-vessels in the tail of the frog larva?by observation and experiment on the living animal. *Am J Anat* 1918;**23**(1):37–88. Doi: 10.1002/aja.1000230103.
72 Diamond SL, Sharefkin JB, Dieffenbach C, Frasier-Scott K, McIntire L V., Eskin SG. Tissue plasminogen activator messenger RNA levels increase in cultured human endothelial cells exposed to laminar shear stress. *J Cell Physiol* 1990;**143**(2):364–71. Doi: 10.1002/jcp.1041430222.
73 Olesen S-P, Claphamt D, Davies P. Haemodynamic shear stress activates a K+ current in vascular endothelial cells. *Nature* 1988;**331**(6152):168–70. Doi: 10.1038/331168a0.
74 Silver FH, Snowhill PB, Foran DJ. Mechanical behavior of vessel wall: A comparative study of aorta, vena cava, and carotid artery. *Ann Biomed Eng* 2003;**31**(7):793–803. Doi: 10.1114/1.1581287.

75 Patel DJ, Janicki JS, Carew TE. Static anisotropic elastic properties of the aorta in living dogs. *Circ Res* 1969;**25**(6):765–79.
76 Davies PF. Flow-mediated endothelial mechanotransduction. *Physiol Rev* 1995;**75**(3):519–60.
77 Dobrin PB, Rovick a a. Influence of vascular smooth muscle on contractile mechanics and elasticity of arteries. *Am J Physiol* 1969;**217**(6):1644–51.
78 Bank AJ, Wang HY, Holte JE, Mullen K, Shammas R, Kubo SH. Contribution of collagen, elastin, and smooth muscle to in vivo human brachial artery wall stress and elastic modulus. *Circulation* 1996;**94**:3263–70. Doi: 10.1161/01.CIR.94.12.3263.
79 Silver FH, Horvath I, Foran DJ. Viscoelasticity of the vessel wall: the role of collagen and elastic fibers. *Crit Rev Biomed Eng* 2001;**29**(3):279–301.
80 McGilvray KC, Sarkar R, Nguyen K, Puttlitz CM. A biomechanical analysis of venous tissue in its normal and post-phlebitic conditions. *J Biomech* 2010;**43**(15):2941–7. Doi: 10.1016/j.jbiomech.2010.07.012.
81 Deatrick KB, Elfline M, Baker N, Luke CE, Susan B, Stabler C, et al. Post Thrombotic Vein Wall Remodeling. *J Vasc Surg* 2011;**53**(1):139–46. Doi: 10.1016/j.immuni.2010.12.017.Two-stage.
82 Nguyen KP, McGilvray KC, Puttlitz CM, Mukhopadhyay S, Chabasse C, Sarkar R. Matrix Metalloproteinase 9 (MMP-9) Regulates Vein Wall Biomechanics in Murine Thrombus Resolution. *PLoS One* 2015;**10**(9):e0139145. Doi: 10.1371/journal.pone.0139145.
83 Dewyer N a, Sood V, Lynch EM, Luke CE, Jr GRU, Wakefield TW, et al. Decreases Vein Wall Stiffness During Venous 2007;**142**(2):357–63.
84 Wang X, Li G, Chen B, Pu Y, Nie P, Li X, et al. Numerical Simulation of Hemodynamics in Portal Vein With Thrombosis By Computational Fluid Dynamics. *J Mech Med Biol* 2014;**14**(06):1440006. Doi: 10.1142/S0219519414400065.
85 Schwein A, Georg Y, Lejay A, Nicolini P, Hartung O, Contassot D, et al. Endovascular Treatment for Venous Diseases : Where are the Venous Stents ? *Methodist Debakey Cardiovasc J* 2018;**14**(3):208–13.
86 Moretz WH, Naisbitt PF, Stevenson GP. Experimental studies on temporary occlusion of the inferior vena cava. *Surgery* 1954;**36**(3):384–98.
87 Anderson MC, Shields TW. An evaluation of factors which influence the incidence and extent of venous thrombosis. *Surgery* 1962;**51**:347–50.
88 Trerotola SO, Mclennan G, Eclavea AC, Salis A, Davidson D, Dreesen RG, et al. Mechanical Thrombolysis of Venous Thrombosis in an Animal Model with Use of Temporary Caval Filtration. *J Vasc Interv Radiol* 2001;**12**:1075–85.
89 Fergany AMRF, Gill IS, Schweizer DK, Kaouk JH, Fettouh HAEL, Cherullo EE, et al. Laparoscopic radical nephrectomy with level II vena caval thrombectomy: survival porcine study. *J Urol* 2002;**168**:2629–31. Doi: 10.1097/01.ju.0000034999.02786.9a.
90 Myers D, Wrobleski S, Londy F, Fex B, Hawley A, Schaub R, et al. New and Effective Treatment of Experimentally Induced Venous Thrombosis with Anti-inflammatory rPSGL-Ig. *Thromb Haemost* 2002;**87**:374–82.
91 Meraney AM, Gill IS, Ch M, Desai MM, Harasaki H, Ph D, et al. Second Prize Laparoscopic Inferior Vena Cava and Right Atrial Thrombectomy Utilizing Deep Hypothermic Circulatory Arrest. *J Endourol* 2003;**17**(5):275–82.
92 Szalony JA, Suleymanov OD, Salyers AK, Panzer-knodle SG, Blom JD, Lachance RM, et

al. Administration of a small molecule tissue factor / Factor VIIa inhibitor in a non-human primate thrombosis model of venous thrombosis : effects on thrombus formation and bleeding time. *Thromb Res* 2003;**112**:167–74. Doi: 10.1016/j.thromres.2003.10.017.
93 Besancon MF, Kyles AE, Griffey S, Gregory C. Evaluation of the Characteristics of Venous Occlusion After Placement of an Ameroid Constrictor in Dogs. *Vet Surg* 2004;**33**:597–605. Doi: 10.1111/j.1532-950X.2004.04082.x.
94 Geier B, Muth-Werthmann D, Barbera L, Bolle I, Militzer K, Philippou S, et al. Laparoscopic ligation of the infrarenal vena cava in combination with transfemoral thrombin infusion: a new animal model of chronic deep venous thrombosis. *Eur J Vasc Endovasc Surg* 2005;**29**:542–8.
95 Katoh M, Haage P, Spuentrup E, Gunther RW, Tacke J. A Porcine Deep Vein Thrombosis Model for Magnetic Resonance-Guided Monitoring of Different Thrombectomy Procedures. *Invest Radiol* 2007;**42**:727–31.
96 Katoh M, Haage P, Wiethoff AJ, Gunther RW, Bucker A, Tacke J, et al. Molecular Magnetic Resonance Imaging of Deep Vein Thrombosis Using a Fibrin-Targeted Contrast Agent A Feasibility Study. *Invest Radiol* 2009;**44**:146–50.
97 Meier TR, Myers DD, Wrobleski SK, Zajkowski PJ, Hawley AE, Bedard PW, et al. Prophylactic P-selectin inhibition with PSI-421 promotes resolution of venous thrombosis without anticoagulation. *Thromb Haemost* 2008;**99**:343–51. Doi: 10.1160/TH07-10-0608.
98 Valji K, Bookstein J. Fibrinolysis with intrathrombic injection of urokinase and tissue-type plasminogen activator. Results in a new model of subacute venous thrombosis. *Invest Radiol* 1987;**22**(1):23–7.
99 Barbash IM, Schenke WH, Halabi M, Ratnayaka K, Faranesh AZ, Kocaturk O, et al. Experimental model of large pulmonary embolism employing controlled release of subacute caval thrombus in swine. *J Vasc Interv Radiol* 2011;**22**(10):1471–7. Doi: 10.1016/j.jvir.2011.06.011.
100 Ichiki M, Sakai Y, Nango M, Nakamura K, Matsui H, Cho H, et al. Experimental venous thrombi: MRI characteristics with histopathological correlation. *Br J Radiol* 2012;**85**:331–8.
101 Schmitt C, Montagnon E, Henni AH, Qi S, Cloutier G. Shear Wave Induced Resonance Elastography of Venous Thrombi : A Proof-of-Concept. *IEEE Trans Med Imaging* 2013;**32**(3):565–77.
102 Minko P, Bucker A, Laschke M, Menger M, Bohle R, Katoh M. Mechanical Thrombectomy of Iliac Vein Thrombosis in a Pig Model Using the Rotarex and Aspirex Catheters. *Cardiovasc Intervent Radiol* 2014;**37**(1):211–7. Doi: 10.1007/s00270-013-0661-8.
103 Diaz JA, Wrobleski SK, Alvarado CM, Hawley AE, Doornbos NK, Lester PA, et al. P-Selectin Inhibition Therapeutically Promotes Thrombus Resolution and Prevents Vein Wall Fibrosis Better Than Enoxaparin and an Inhibitor to von Willebrand Factor. *Arterioscler Thromb Vasc Biol* 2015;**35**(4):829–37. Doi: 10.1161/ATVBAHA.114.304457.
104 Shi W-Y, Hu L-Y, Wu S, Liu C-J, Gu J-P. Two swine models of iliac vein occlusion: Which form most contributes to venous thrombosis? *Thromb Res* 2015;**135**:1172–8. Doi: 10.1016/j.thromres.2015.03.006.
105 Shi W, Wu S, Hu L, Liu C, Gu J. Swine Model of Thrombotic Caval Occlusion Created by Autologous Thrombus Injection with Assistance of Intra-caval Net Knitting. *Sci Rep*

2015;**5**:1–9. Doi: 10.1038/srep18546.
106 Foster ED, Dobell AR. Evaluation of rigid prosthetic rings as in vivo intravascular thrombogenic models. *J Surg Res* 1971;**11**:550–8.
107 Tacke J, Vorwerk D, Bücker A, Klosterhalfen B, Grosskortenhaus S, Hunter DW, et al. Experimental Treatment of Early Chronic Iliac Vein Thrombosis with a Modified Hydrodynamic Thrombectomy Catheter : Preliminary Animal Experience. *J Vasc Interv Radiol* 1999;**10**:57–63.
108 Geier B, Barbera L, Muth-Werthmann D, Siebers S, Ermert H, Philippou S, et al. Ultrasound elastography for the age determination of venous thrombi. *Thromb Haemost* 2005;**93**:368–74.
109 Wakefield TW, Wrobleski SK, Sarpa MS, Taylor FB, Esmon CT, Cheng A, et al. Deep venous thrombosis in the baboon : An experimental model. *J Vasc Surg* 1991;**14**:588–98.
110 Downing L, Wakefield TW, Strieter RM, Prince MR, Londy FJ, Fowlkes J, et al. Anti-P-selectin antibody decreases inflammation and thrombus formation in venous thrombosis. *J Vasc Surg* 1997;**25**:816–28.
111 Hosaka J, Roy S, Kuroki K, Xian Z, Kvernebo K, Enge I, et al. Placement of a Spring Filter during Interventional Treatment of deep Venous Thrombosis to Reduce the Risk of Pulmonary Embolism. *Acta Radiol* 1999;**40**(5):545–51.
112 Wakefield TW, Strieter RM, Schaub R, Myers DD, Prince MR, Wrobleski SK, et al. Venous thrombosis prophylaxis by inflammatory inhibition without anticoagulation therapy. *J Vasc Surg* 2000;**31**:309–24.
113 Myers DD, Wrobleski SK, Longo C, Bedard PW, Kaila N, Shaw G, et al. Resolution of venous thrombosis using a novel oral small-molecule inhibitor of P-selectin (PSI-697) without anticoagulation. *Thromb Haemost* 2007;**97**:400–7.
114 Gu X, Sharafuddin M, Titus J, Urness M, Cervera-Ceballos J, Ruth J, et al. Acute and delayed outcomes of mechanical thrombectomy with use of the steerable Amplatz thrombectomy device in a model of subacute inferior vena cava thrombosis. *J Vasc Interv Radiol* 1997;**8**(6):947–56.
115 Lin PH, Johnson CK, Pullium JK, Bush RL, Conklin BS, Chen C, et al. L-Arginine improves endothelial vasoreactivity and reduces thrombogenicity after thrombolysis in experimental deep venous thrombosis. *J Vasc Surg* 2003;**38**(6):1396–403. Doi: 10.1016/S0741-5214(03)00952-2.
116 Lin PH, Okada T, Steinberg JL, Zhou W, El Sayed HF, Rawat A, et al. Rheolytic pharmacomechanical thrombectomy in experimental chronic deep vein thrombosis: Effect of L-arginine on thrombogenicity and endothelial vasomotor function. *World J Surg* 2007;**31**(4):664–75. Doi: 10.1007/s00268-007-0733-5.
117 Weinberg RJ, Okada T, Chen A, Kim W, Chen C, Lin PH. Comparison of ASPIRE Mechanical Thrombectomy Versus AngioJet Thrombectomy System in a Porcine Iliac Vein Thrombosis Model. *Ann Vasc Surg* 2017;**42**:254–62. Doi: 10.1016/j.avsg.2016.12.014.
118 Wakefield TW, Greenfield LJ, Rolfe MW, DeLucia A, Strieter RM, Abrams G, et al. Inflammatory and procoagulant mediator interactions in an experimental baboon model of venous thrombosis. *Thromb Haemost* 1993;**69**(2):164–72.
119 Hosaka J, Roy S, Kvernebo K, Enge I, Laerum F. Induced thrombosis in the pig inferior vena cava: a model of deep venous thrombosis. *J Vasc Interv Radiol* 1996;**7**:395–400.
120 Haage P, Tacke J, Bovelander J, Wildberger JE, Klosterhalfen B, Vorwerk D, et al.

Prototype percutaneous thrombolytic device: preclinical testing in subacute inferior vena caval thrombosis in a pig model. *Radiology* 2001;**220**:135–41. Doi: 10.1148/radiology.220.1.r01jl28135.
121 Salartash K, Lepore M, Gonze MD, Leone-Bay A, Baughman R, Sternbergh WC, et al. Treatment of experimentally induced caval thrombosis with oral low molecular weight heparin and delivery agent in a porcine model of deep venous thrombosis. *Ann Surg* 2000;**231**(6):789–94. Doi: 10.1097/00000658-200006000-00002.
122 Lin PH, Chen C, Surowiec SM, Conklin B, Bush RL, Lumsden AB. Evaluation of thrombolysis in a porcine model of chronic deep venous thrombosis: An endovascular model. *J Vasc Surg* 2001;**33**:621–7. Doi: 10.1067/mva.2001.109773.
123 Trerotola SO, Mclennan G, Davidson D, Lane KA, Ambrosius WT, Lazzaro C, et al. Preclinical In Vivo Testing of the Arrow- Trerotola Percutaneous Thrombolytic Device for Venous Thrombosis. *J Vasc Interv Radiol* 2001;**12**:95–103.
124 Siller-Matula JM, Plasenzotti R, Spiel A, Quehenberger P, Jilma B. Interspecies differences in coagulation profile. *Thromb Haemost* 2008;**100**:397–404. Doi: 10.1160/TH08-02-0103.
125 Sondeen JL, De Guzman R, Amy Polykratis I, Dale Prince M, Hernandez O, Cap AP, et al. Comparison between human and porcine thromboelastograph parameters in response to ex-vivo changes to platelets, plasma, and red blood cells. *Blood Coagul Fibrinolysis* 2013;**24**:818–29. Doi: 10.1097/MBC.0b013e3283646600.
126 Klein SL, Schiebinger L, Stefanick ML, Cahill L. Opinion : Sex inclusion in basic research drives discovery 2015;**112**(17):10–1. Doi: 10.1073/pnas.1502843112.
127 Yoon DY, Mansukhani NA, Stubbs VC. Sex bias exists in basic science and translational surgical research. *Surgery* 2012;**156**(3):508–16. Doi: 10.1016/j.surg.2014.07.001.
128 Center for Devices and Radiological Health. Guidance for Industry and FDA Staff General Considerations for Animal Studies for Cardiovascular Devices. 2010.
129 Kilkenny C, Browne W, Cuthill IC, Emerson M, Altman DG. Animal research: Reporting in vivo experiments: The ARRIVE Guidelines. *Br J Pharmacol* 2010;**160**:1577–9. Doi: 10.1038/jcbfm.2010.220.
130 Mackman N, Tilley RE, Key NS. Role of the extrinsic pathway of blood coagulation in hemostasis and thrombosis. *Arterioscler Thromb Vasc Biol* 2007;**27**(8):1687–93. Doi: 10.1161/ATVBAHA.107.141911.
131 Fineschi V, Turillazzi E, Neri M, Pomara C, Riezzo I. Histological age determination of venous thrombosis: A neglected forensic task in fatal pulmonary thrombo-embolism. *Forensic Sci Int* 2009;**186**:22–8. Doi: 10.1016/j.forsciint.2009.01.006.
132 Owens III AP, Mackman N. Tissue factor and thrombosis : The clot starts here. *Thromb Haemost* 2010;**104**:432–9. Doi: 10.1160/TH09-11-0771.
133 Wittens C, Davies AH, Bækgaard N, Broholm R, Cavezzi A, Chastanet S, et al. Editor's choice - Management of chronic venous disease: Clinical practice guidelines of the European Society for Vascular Surgery (ESVS). *Eur J Vasc Endovasc Surg* 2015;**49**(6):678–737. Doi: 10.1016/j.ejvs.2015.02.007.
134 Schwein A, Magnus L, Chakfe N, Bismuth J. Critical review of large animal models for central deep venous thrombosis. *Eur J Vasc Endovasc Surg* 2020;**60**:243–52.
135 Percie du Sert N, Hurst V, Ahluwalia A, Alam S, Avey MT, Baker M, et al. The ARRIVE guidelines 2019: updated guidelines for reporting animal research. 2019;**July 15**.
136 Shi W, Hu L, Wu S, Liu C, Gu J. Two swine models of iliac vein occlusion : Which form

most contributes to venous thrombosis ? *Thromb Res* 2015;**135**:1172–8. Doi: 10.1016/j.thromres.2015.03.006.
137 Nosaka M, Ishida Y, Kimura A, Kondo T. Time-dependent organic changes of intravenous thrombi in stasis-induced deep vein thrombosis model and its application to thrombus age determination. *Forensic Sci Int* 2010;**195**:143–7. Doi: 10.1016/j.forsciint.2009.12.008.
138 Castellano G, Bonilha L, Li LM, Cendes F. Texture analysis of medical images. *Clin Radiol* 2004;**59**(12):1061–9. Doi: 10.1016/j.crad.2004.07.008.
139 Herlidou S, Rolland Y, Bansard JY, Le Rumeur E, De Certaines JD. Comparison of automated and visual texture analysis in MRI: Characterization of normal and diseased skeletal muscle. *Magn Reson Imaging* 1999;**17**(9):1393–7. Doi: 10.1016/S0730-725X(99)00066-1.
140 Pérez de Alejo R, Ruiz-Cabello J, Cortijo M, Rodriguez I, Echave I, Regadera J, et al. Computer-assisted enhanced volumetric segmentation magnetic resonance imaging data using a mixture of artificial neural networks. *Magn Reson Imaging* 2003;**21**(8):901–12. Doi: 10.1016/S0730-725X(03)00193-0.
141 Chabat F, Yang GZ, Hansell DM. Obstructive lung diseases: Texture classification for differentiation at CT. *Radiology* 2003;**228**(3):871–7. Doi: 10.1148/radiol.2283020505.
142 Canellas R, Mehrkhani F, Patino M, Kambadakone A, Sahani D. Characterization of portal vein thrombosis (neoplastic versus bland) on CT images using software-based texture analysis and thrombus density (hounsfeld units). *Am J Roentgenol* 2016;**207**(5):W81–7. Doi: 10.2214/AJR.15.15928.
143 Bretzner M, Lopes R, McCarthy R, Corseaux D, Auger F, Gunning G, et al. Texture parameters of R2* maps are correlated with iron concentration and red blood cells count in clot analogs: A 7-T micro-MRI study. *J Neuroradiol* 2020;**47**(4):306–11. Doi: 10.1016/j.neurad.2019.10.004.
144 Haralick RM, Dinstein I, Shanmugam K. Textural Features for Image Classification. *IEEE Trans Syst Man Cybern* 1973;**SMC-3**(6):610–21. Doi: 10.1109/TSMC.1973.4309314.
145 Zhao Q, Shi CZ, Luo LP. Role of the texture features of images in the diagnosis of solitary pulmonary nodules in different sizes. *Chinese J Cancer Res* 2014;**26**(4):451–8. Doi: 10.3978/j.issn.1000-9604.2014.08.07.
146 Zayed N, Elnemr HA. Statistical Analysis of Haralick Texture Features to Discriminate Lung Abnormalities. *Int J Biomed Imaging* 2015;**2015**. Doi: 10.1155/2015/267807.
147 Mattson JM, Zhang Y. Structural and Functional Differences Between Porcine Aorta and Vena Cava. *J Biomech Eng* 2017;**139**(7):0710071. Doi: 10.1115/1.4036261.
148 Vekilov DP, Grande-allen KJ, Ph D. Mechanical Properties of Diseased Veins 2018;**14**(3):1–6.
149 Puperi DS. Biomimetic heterogeneous scaffolds for a layered tissue engineered heart valve. 2016.
150 Chandrashekar A, Garry J, Sikalas N, Gasparis A, Labropoulos N. Heterogeneity in Post-Thrombotic Vein Wall Remodeling. *J Vasc Surg Venous Lymphat Disord* 2017;**5**(1):145. Doi: 10.1016/j.jvsv.2016.10.011.
151 Neglén P, Raju S. Compliance of the normal and post-thrombotic calf. *J Cardiovasc Surg (Torino)* 1995;**36**(3):225–31.
152 Schwein A, Magnus L, Markovits J, Chinnadurai P, Autry K, Jenkins L, et al. A new porcine model of acute and chronic central venous thrombosis mimicking human

pathology. *Eur J Vasc Endovasc Surg* n.d.
153 Desch GW, Weizs??cker HW. A model for passive elastic properties of rat vena cava. *J Biomech* 2007;**40**(14):3130–45. Doi: 10.1016/j.jbiomech.2007.03.028.
154 Mumoli N, Mastroiacovo D, Giorgi-Pierfranceschi M, Pesavento R, Mochi M, Cei M, et al. Ultrasound elastography is useful to distinguish acute and chronic deep vein thrombosis. *J Thromb Haemost* 2018;**16**(12):2482–91. Doi: 10.1111/jth.14297.
155 Lionello G, Sirieix C, Baleani M. An effective procedure to create a speckle pattern on biological soft tissue for digital image correlation measurements. *J Mech Behav Biomed Mater* 2014;**39**:1–8. Doi: 10.1016/j.jmbbm.2014.07.007.

Résumé long

Mise au point et applications d'un modèle porcin de thrombose veineuse profonde

1. INTRODUCTION

La maladie thromboembolique veineuse (MTEV) est un problème majeur de santé publique dans les pays occidentaux. Alors que le traitement médical optimal associant anticoagulation et compression veineuse est le traitement recommandé en cas de thrombose veineuse profonde (TVP) dans le territoire fémoro-poplité et jambier, ses résultats restent médiocres en particulier sur le syndrome post-thrombotique (SPT) lorsque la TVP survient dans la veine fémorale commune, les veines iliaques ou dans la veine cave inférieure (VCI)[1]. Par conséquent, les dernières recommandations de la Société Européenne de Chirurgie Vasculaire (ESVS) préconisent une prise en charge interventionnelle par technique d'ablation du thrombus (TAT) en cas de TVP ilio-fémorale aiguë symptomatique[2].

Les TAT utilisent des agents thrombolytiques et/ou une thrombectomie mécanique. Le délai idéal de prise en charge après l'apparition des symptômes de TVP n'est pas clair. Une méthode objective et non invasive capable d'identifier l'âge du thrombus et sa susceptibilité à être lysé est nécessaire et devrait aider à définir quels groupes de patients bénéficieront le plus des TAT.
De plus, les propriétés mécaniques de la paroi veineuse sont peu étudiées, et leurs modifications après TVP le sont encore moins. De telles connaissances sont cependant nécessaires à la conception de dispositifs endovasculaires spécifiques pour le traitement de l'obstruction veineuse persistante après TAT ou chez les patients atteints de SPT sévère.

Les modèles de TVP chez le grand animal sont indispensables pour faire progresser nos connaissances sur l'histoire naturelle et la prise en charge optimale de cette maladie, ainsi que pour le développement et l'évaluation de dispositifs endovasculaires dédiés.

Dans ce contexte, nos objectifs étaient les suivants :

1. Réaliser une revue de la littérature existante sur les modèles de TVP chez le grand animal en vue de sélectionner un protocole idéal.
2. Développer un protocole de TVP ilio-cave aiguë et subaiguë chez le grand animal.
3. Utiliser le modèle animal pour :
    a. Etudier les méthodes non invasives de caractérisation du thrombus, notamment via l'imagerie par résonance magnétique (IRM).
    b. Etudier les modifications des propriétés mécaniques de la paroi veineuse après TVP.

Nous présenterons nos travaux de recherche après avoir rappelé des notions importantes pour la compréhension de notre problématique.

2. RAPPELS

2.1. Thrombose veineuse profonde

La TVP se définit par la présence de thrombus dans une veine profonde, prédominant au niveau du membre inférieur. Considérée comme une maladie bénigne le plus souvent, son évolution peut cependant se compliquer d'embolie pulmonaire (EP) ou de SPT.
La TVP est classée en phase aiguë, subaiguë et chronique en fonction du délai par rapport à l'apparition des symptômes, soit respectivement de 0 à 14 jours, de 14 à 28 jours et plus de 28 jours. D'un point de vue anatomique, elle est divisée en TVP distale quand elle concerne une veine jambière, en TVP fémoro-poplité lorsqu'elle concerne la veine fémorale, fémorale profonde ou poplité, et en TVP ilio-fémorale lorsqu'elle concerne la veine fémorale commune et/ou iliaque[3].

Avec un taux d'incidence annuelle de 104 à 183 pour 100000 personnes, similaire à celui de l'accident vasculaire cérébral, la MTEV est un problème majeur de santé publique. A elle seule, la TVP symptomatique du membre inférieur a une incidence annuelle de 45 à 117 pour 100000 personnes[4]. L'âge moyen d'apparition est de 62 ans, sans prédominance de genre. Elle touche le côté gauche dans 57% des cas, et le segment ilio-fémoral dans 38% des cas[3].

La thrombose aiguë va générer des modifications hémodynamiques (augmentation de la pression veineuse) et l'activation d'un important état inflammatoire, qui expliquent l'apparition des symptômes : œdème et douleur[5]. Le niveau anatomique et l'extension de la thrombose vont influencer la sévérité des anomalies hémodynamiques et donc des symptômes.
La lyse spontanée du thrombus commence dès les premiers jours et peut aboutir à une recanalisation veineuse après plusieurs semaines ou mois. Le taux de recanalisation varie selon la localisation de la TVP : 80% au niveau jambier contre seulement 20% au niveau iliaque[2]. En cas d'absence de recanalisation ou de recanalisation incomplète, l'obstruction veineuse chronique ainsi que l'atteinte des valves et l'apparition de reflux peuvent entrainer un SPT.

Le SPT est une complication à long terme de la TVP qui touche entre 20 à 50% des patients dans les 2 ans suivants l'évènement aigu[6–9]. La présentation clinique peut se traduire par tous les stades de la classification CEAP (Tableau 1) et résulte de l'association de reflux valvulaire et d'un syndrome obstructif chronique. Il a été montré que la localisation ilio-fémorale de la TVP est un des facteurs de risque d'apparition et de sévérité du SPT[10]. Il a également été montré que le traitement médical optimal n'était pas suffisant dans la prévention et le traitement du SPT[1].

L'ablation du thrombus à la phase aiguë a pour but d'éviter l'obstruction veineuse chronique et les lésions valvulaires responsables de reflux au long cours, l'objectif final étant la prévention du SPT.
Les TAT incluent la thrombectomie chirurgicale, la thrombolyse dirigée par cathéter, la thrombolyse pharmacomécanique, la thrombectomie mécanique et utilisent également des techniques d'angioplastie et stenting complémentaires.
Une méta-analyse a montré l'avantage des TAT par thrombolyse dirigée par cathéter ou pharmacomécanique par rapport à l'anticoagulation curative seule concernant la prévention des SPT ($p=0.05$), avec cependant un risque accru de saignement majeur ($RR = 5.68$, $p = 0.02$)[2]. (Figure 1 et 2).

2.2. Efficacité des techniques d'ablation du thrombus

Les sociétés européennes et américaines de chirurgie vasculaire recommandent l'utilisation des TAT à la phase aiguë après TVP dans le but de prévenir le SPT[2,11].
Le délai idéal de prise en charge par TAT n'est cependant pas connu ; aujourd'hui on ne sait pas quels sont les patients qui bénéficieront d'un succès maximal d'une TAT avec un minimum de risque de complications.
Les TVP récentes sont souvent considérées comme étant plus susceptibles de répondre à la fibrinolyse que les plus anciennes ; la limite de 14 jours après l'apparition des symptômes a été avancée comme facteur de risque de meilleur résultat après TAT[12]. Cette durée de 14 jours semble cependant arbitraire et ne fait pas l'unanimité au sein des sociétés savantes.

La détermination de l'âge d'un thrombus a été la source de nombreux travaux de recherche. Plusieurs méthodes d'imagerie non-invasive ont été proposées : l'écho-doppler est la méthode de première intention dans le diagnostic de TVP et a donc été largement étudié dans le but de dater le thrombus, notamment par l'intermédiaire de l'élastographie, sans pour autant être capable d'estimer la probabilité de lyse du caillot[13,14].

L'IRM possède une excellente résolution tissulaire et a été utilisée depuis 2014 pour proposer une datation de la TVP selon l'hétérogénéité du signal (Figure 4)[15].
De manière plus précise que l'âge du thrombus, il semblerait que ce soit sa composition en fibrine qui conditionne sa capacité à être lysé. Une méthode non-invasive permettant de quantifier la teneur en fibrine d'une TVP permettrait ainsi de guider le succès des TAT par thrombolyse.
Une étude menée sur un modèle de TVP chez la souris a montré que l'association des résultats de séquences spécifiques d'IRM était capable d'analyser la composition d'un thrombus et d'anticiper le succès d'une prise en charge par thrombolyse[16,17].

2.3. Propriétés mécaniques de la paroi veineuse

Les publications scientifiques, tant en recherche clinique qu'en recherche fondamentale, concernant la pathologie vasculaire sont nettement en faveur de l'étude des artères par rapport aux veines.
Bien que la structure de base des deux vaisseaux soit similaire en 3 couches, il existe de grandes différences dans la constitution de leur paroi, leur conférant des propriétés mécaniques et des fonctions très distinctes.
Les veines ont un diamètre et une lumière plus large que les artères ; elle possèdent également une capacité de dilatation plus importante, leur permettant de stocker en permanence les 2/3 du volume sanguin corporel[18]. Leur paroi est globalement plus fine et moins organisée, l'adventice est plus épaisse et la media plus fine que celle des artères[19]. Elles sont enfin constituées de plus de collagène et de moins de cellules musculaires lisses que la paroi artérielle[20].

Les propriétés mécaniques des vaisseaux sont conditionnées principalement par le comportement du collagène, de l'élastine et des cellules musculaires lisses présents dans leur paroi. La modélisation de leur comportement mécanique est complexe et dépend de l'interaction de ses différents constituants en réponse à différents stimuli. Les vaisseaux présentent une courbe contrainte-déformation non linéaire avec deux phases dans lesquelles les fibres d'élastine sont responsables du comportement extensible à de faibles contraintes, alors que le collagène et les cellules musculaires lisses sont responsables du comportement inextensible et rigide à des contraintes élevées[21].

La formation d'une TVP va modifier la composition et les propriétés mécaniques de la paroi veineuse. Ces modifications ont été étudiées dans un modèle murin de TVP et a montré une augmentation de la rigidité de la paroi veineuse ainsi qu'une diminution de sa capacité à répondre aux changements de pression sanguine[22]. La résolution du thrombus au cours du temps ne va pas permettre de reverser ces modifications ; au contraire, une étude clinique par échodoppler a montré que la paroi veineuse continue à s'épaissir même après reperméabilisation veineuse[23].
Enfin, la TVP pourrait non seulement modifier les propriétés mécaniques de la paroi veineuse en regard du thrombus, mais également de la paroi veineuse plus à distance[24].

3. TRAVAIL DE RECHERCHE

3.1. Revue de la littérature des modèles de thrombose veineuse profonde ilio-cave chez le grand animal

3.1.1. Introduction

Un modèle de TVP ilio-cave chez le grand animal est indispensable dans le but d'améliorer la compréhension de la pathologie veineuse occlusive et de développer, tester et évaluer de nouveaux outils diagnostiques et thérapeutiques.
Le but de ce travail était de réaliser une revue de la littérature existante concernant les modèles de TVP chez le grand animal et d'analyser les avantages et inconvénients de chacun, dans le but de sélectionner le plus pertinent pour notre projet de recherche.

3.1.2. Matériel et méthodes

Nous avons mené une recherche documentaire systématique dans les bases de données PubMed et Embase. Les articles décrivant un protocole expérimental in vivo de TVP chez le grand animal impliquant la veine iliaque et/ou la veine cave et/ou la veine brachiocéphalique ont été inclus. L'objectif principal de chaque étude, les caractéristiques des animaux, les protocoles expérimentaux et l'évaluation du thrombus ont été analysés.

3.1.3. Résultats

Trente-huit articles décrivant plus de 30 protocoles expérimentaux différents ont été inclus. Les animaux utilisés étaient des cochons (53 %), chiens (21 %), singes (24 %) et bovins (3 %). Le nombre médian d'animaux par étude était de 12. Les informations concernant le genre des animaux, la race et le poids manquaient dans 18 études (47 %), sept études (18 %) et huit études (21 %) respectivement (Tableau 4).
La TVP était toujours induite par stase veineuse, soit seule (55%), soit associée à un phénomène d'hypercoagulabilité (37%) ou de lésion endothéliale (10%) (Tableau 5). Les dimensions de la veine utilisée pour la création de la TVP ont été rapportées dans quatre études (10 %). Le protocole expérimental a conduit à une mort animale inattendue dans 9 études (24%), allant de 3 % à 37 % des animaux.
La présence ou l'absence de thrombus créé a été rapporté dans 22 études (58 %) en phase aiguë et dans 31 études en phase chronique (82 %) ; le caractère occlusif de la TVP a été rapporté respectivement dans 5 et 17 études. Un examen histologique a été réalisé dans 24 études (63 %) dont une seule l'a comparé avec le thrombus humain (Tableau 6).

3.1.4. Conclusion

Cette revue a montré les avantages et les faiblesses des modèles existants de TVP chez le grand animal. Les protocoles futurs devront rapporter de manière plus systématique et rigoureuse les caractéristiques des animaux, l'évaluation du thrombus créé et sa comparaison au thrombus humain en vue de dépasser la simple preuve de concept et de tendre vers un modèle consensuel.

3.2. Développement d'un modèle porcin de thrombose veineuse ilio-cave

3.2.1. Introduction

Plusieurs protocoles expérimentaux de TVP chez le grand animal ont été rapportés dans la littérature mais comportent de nombreuses lacunes autant dans la conception que dans la manière de rapporter les résultats. Le but de ce travail était de développer un modèle de TVP ilio-cave chez le grand animal, qui permette le développement et l'évaluation de nouveaux outils diagnostiques et thérapeutiques.

3.2.2. Matériel et méthodes

Le protocole expérimental consistait en une approche totalement endovasculaire. Par ponction percutanée des veines fémorales bilatérales et de la veine jugulaire droite, trois ballons d'angioplastie ont été positionnés et inflatés dans la VCI sous-rénale et les veines iliaques communes bilatérales dans le but d'induire une stase veineuse ilio-cave (Figure 10). L'injection de 10 000 UI de thrombine recombinante humaine dans la région d'intérêt a ensuite crée un état d'hypercoagulabilité. Après 2,5 heures de stase, les ballons d'angioplastie ont été déflatés, tout le matériel a été retiré et les animaux ont été réveillés et surveillés en animalerie par l'équipe vétérinaire.
Après un délai de 7, 14, 21, 28 ou 35 jours, les animaux ont été euthanasiés ; la portion ilio-cave thrombosée a été prélevée en bloc, sectionnée et préparée pour analyse histologique (Figure 11). Une imagerie multimodale par phlébographie, tomodensitométrie et IRM a été réalisée chez chaque animal avant et après création de la TVP ainsi qu'avant leur euthanasie (Figure 12).

3.2.3. Résultats

Treize cochons domestiques femelles d'un poids moyen de 59,3 kilogrammes ont été utilisés. Les dimensions maximales moyennes de la VCI étaient de 16,4 mm pour le diamètre et de 1,2 cm^2 pour la surface. Le succès technique de la procédure a été de 92,3% avec 12 animaux présentant une thrombose veineuse occlusive dans la région d'intérêt sur l'IRM postopératoire immédiate ; le volume moyen de thrombus créé était de 19,8 cm^3. Les résultats d'analyse biologique ont montré une consommation plaquettaire, une augmentation des D-dimères et une réponse inflammatoire aiguë en postopératoire. L'examen histologique a mis en évidence un thrombus riche en érythrocytes, en fibrine et en plaquettes

à 1 jour, avec une infiltration progressive de cellules inflammatoires à partir du 7ème jour. Un dépôt de collagène est apparu à la 2ème semaine et une néo-vascularisation à la 3ème semaine postopératoire (Figure 13).

3.2.4. Conclusion

Nous proposons un modèle endovasculaire mini-invasif de TVP ilio-cave aiguë et subaiguë, efficace chez un animal de 60 kg, sûr et reproductible. Il est important de noter que le modèle respecte l'intégrité du système vasculaire et ne laisse pas en place de matériel étranger, évitant ainsi des lésions artificielles et les artefacts d'imagerie.

3.3. Utilisation du modèle porcin de thrombose veineuse ilio-cave

3.3.1. Caractérisation non invasive de la TVP en IRM

3.3.1.1. Introduction

Plusieurs études menées sur le petit animal ont montré les capacités de l'IRM à établir l'âge d'un thrombus et à analyser son contenu en fibrine, permettant ainsi d'anticiper le succès d'une prise en charge par fibrinolyse. L'analyse de la texture des résultats d'IRM par modélisation de la distribution spatiale des niveaux de gris a également été utilisée dans le but de caractériser les contenus tissulaires. L'objectif de notre travail était d'analyser les résultats d'IRM pré et postopératoire en vue de caractériser la TVP ilio-cave expérimentale et son évolution dans le temps, en se concentrant sur la morphométrie, la texture de l'image et l'analyse du contenu en fibrine.

3.3.1.2. Matériel et méthodes

Pour chaque animal, une IRM a été réalisée avant création du thrombus, en postopératoire immédiat, ainsi qu'avant euthanasie après un délai de 7, 14, 21, 28 ou 35 jours. Chaque examen comprenait une séquence d'angiographie dynamique 3D à haute résolution, une séquence statique 3D à l'équilibre (T1-VIBE), et les séquences spécifiques utilisées par l'équipe du King's College à Londres pour l'analyse de la constitution en fibrine (diffusion, transfert de magnétisme, carte pondérée en T1).
Nous avons manuellement segmenté les contours de la région d'intérêt sur le logiciel ImageJ (ImageJ, NIH, Bethesda, MD) pour en obtenir le diamètre, la surface, le périmètre, le niveau de gris minimal, maximal et moyen, la symétrie de leur distribution et la texture.
Une segmentation similaire sera ensuite effectuée sur le logiciel Osirix (OsiriX Foundation, Geneva, Switzerland) à partir des séquences en diffusion et transfert de magnétisme dans le but de générer une cartographie de la teneur en protéine de la région d'intérêt. Cette cartographie sera comparée aux

résultats d'analyse histologique après coloration au bleu de Martius Scarlet dans le but de valider la méthode.

3.3.1.3. Résultats préliminaires

Pour un total de 20 animaux étudiés, le volume total moyen de thrombus créé était de 17.05 cm^3 réparti en 56.3% dans la VCI, 25.3% dans la veine iliaque droite et 18.4% dans la veine iliaque gauche.

3.3.1.4. Conclusion

Nos prochains résultats devraient permettre d'évaluer l'utilisation de l'IRM comme méthode non-invasive d'analyse de la composition du thrombus dans un modèle de TVP chez le grand animal, ce qui, à terme, pourrait conduire à guider la prise en charge thérapeutique de la TVP.

3.3.2. Etudes des propriétés mécaniques des veines thrombosées

3.3.2.1. Introduction

Il existe très peu d'études dans la littérature analysant les propriétés mécaniques de la paroi veineuse saine et après TVP, or ces informations sont essentielles au développement de dispositifs thérapeutiques endovasculaires dédiés à la prise en charge thérapeutique de cette pathologie.
Dans ce travail, notre objectif était double : premièrement, il s'agissait de caractériser les propriétés mécaniques de la paroi veineuse saine chez le grand animal, et secondairement, d'étudier ses modifications au cours du temps après TVP.

3.3.2.2. Matériel et méthodes

Les portions ilio-caves saines et thrombosées explantées ont été sectionnées en région sus-hépatique, infra-rénale, iliaque droite et iliaque gauche. Chaque segment veineux a ensuite été divisé en bandes longitudinales et circonférentielles, antérieures et postérieures. Leur épaisseur a été mesurée en stéréo-microscopie puis chaque bande a été testée en traction uni-axiale selon le protocole suivant : pré-conditionnement par 20 cycles de 3 mm de déplacement puis traction jusqu'à rupture. Nous avons converti les données obtenues en courbes de tension-déformation pour calculer la rigidité de chaque spécimen. La tension maximale atteinte avant la rupture était considérée comme la résistance à la rupture.

3.3.2.3. Résultats

Aucune différence en termes d'épaisseur ni de rigidité n'a été retrouvée entre la paroi antérieure et postérieure des échantillons.
De manière générale, la paroi veineuse thrombosée est significativement plus épaisse que la paroi veineuse saine (p=0.0005), et notamment à 2 et 3 semaine après création de la TVP, quelle que soit la localisation (sus-hépatique, infra-rénale ou iliaque). La rigidité longitudinale de la paroi veineuse est également significativement augmentée après TVP (p=0.0277) quelle que soit la localisation. Il n'y avait par contre pas de différence significative entre la paroi veineuse thrombosée et saine concernant la tension de rupture.

3.3.2.4. Conclusions

La création d'une TVP ilio-cave induit des augmentations progressives de l'épaisseur et de la rigidité longitudinale de la paroi veineuse, même après résolution du thrombus. Ensemble, ces résultats élargissent notre compréhension de la mécanique veineuse et fournissent des conseils pour la conception de dispositifs endovasculaires veineux spécifiques dans la prise en charge de la maladie occlusive veineuse.

4. CONCLUSIONS GÉNÉRALES

Bien que la TVP soit un problème de santé majeur, de nombreuses inconnues persistent quant à son histoire naturelle et sa prise en charge diagnostique et thérapeutique.
Dans ce travail, nous avons développé un modèle totalement endovasculaire mini-invasif de TVP ilio-cave aiguë et subaiguë, qui est efficace chez les animaux de 60 kg et qui respecte l'intégrité du système vasculaire. Nous avons porté une attention particulière au respect des recommandations ARRIVE dans un souci de standardisation et de reproductibilité par les autres équipes.

Les données obtenues par l'imagerie multimodale nécessitent encore une analyse plus approfondie ; notre hypothèse est que les résultats devraient mettre l'accent sur l'utilisation de séquences IRM spécifiques comme modalité d'imagerie non invasive pour évaluer le contenu structurel de la TVP et pourraient ainsi guider la prise en charge de la TVP ilio-fémorale aiguë par thrombolyse.

L'analyse des propriétés mécaniques de la veine thrombosée a montré que la TVP induisait une augmentation progressive de l'épaisseur et de la rigidité longitudinale de la paroi veineuse, même après résolution du thrombus. Une caractérisation plus poussée du thrombus, des propriétés élastiques de la paroi veineuse, ainsi que l'établissement d'une carte de déformation spatiale élargiront notre compréhension de la mécanique veineuse et fourniront des orientations pour la conception de dispositifs endovasculaires veineux spécifiques pour traiter les maladies veineuses obstructives.

Notre modèle de TVP chez le grand animal servira enfin de support précieux pour le développement et l'évaluation de matériel endoveineux dédié et pour la formation des chirurgiens dans un domaine qui a longtemps été le côté oublié de la chirurgie vasculaire.

5. BIBLIOGRAPHIE

1 Kahn SR, Shapiro S, Wells PS, Rodger MA, Kovacs MJ, Anderson DR, et al. Compression stockings to prevent post-thrombotic syndrome: A randomised placebo-controlled trial. *Lancet* 2014;**383**(9920):880–8. Doi: 10.1016/S0140-6736(13)61902-9.

2 Kakkos SK, Gohel M, Baekgaard N, Bauersachs R, Bellmunt-Montoya S, Black SA, et al. Editor's Choice – European Society for Vascular Surgery (ESVS) 2021 Clinical Practice Guidelines on the Management of Venous Thrombosis. *Eur J Vasc Endovasc Surg* 2021;**61**(1):9–82. Doi: 10.1016/j.ejvs.2020.09.023.

3 De Maeseneer MGR, Bochanen N, Van Rooijen G, Neglén P. Analysis of 1,338 Patients with Acute Lower Limb Deep Venous Thrombosis (DVT) Supports the Inadequacy of the Term "proximal DVT." *Eur J Vasc Endovasc Surg* 2016;**51**(3):415–20. Doi: 10.1016/j.ejvs.2015.11.001.

4 Heit JA, Spencer FA, White RH. The epidemiology of venous thromboembolism. *J Thromb Thrombolysis* 2016;**41**(1):3–14. Doi: 10.1007/s11239-015-1311-6.

5 Lee B, Nicolaides A, Myers K, Meissner M, Kalodiki E. Venous hemodynamic changes in lower limb venous disease: the UIP consensus according to scientific evidence. *Int Angiol* 2016;**35**(3):236–352.

6 Prandoni P, Lensing A, Prins M, Frulla M, Marchiori A, Bernardi E, et al. Below-Knee Elastic Compression Stockings To Prevent the Post-Thrombotic Syndrome. *Ann Intern Med* 2004;**141**:249–56.

7 Kahn SR, Shrier I, Julian JA, Ducruet T, Arsenault L, Miron MJ, et al. Determinants and time course of the postthrombotic syndrome after acute deep venous thrombosis. *Ann Intern Med* 2008;**149**(10):698–707. Doi: 10.7326/0003-4819-149-10-200811180-00004.

8 Prandoni P, Anthonie WA, Lensing AW, Cogo A, Cuppini S, Villalta S, et al. The long-term clinical course of acute deep vein thrombosis. *Ann Intern Med* 1996;**125**(1):1–7.

9 Saarinen J, Kallio T, Lehto M, Hiltunen S, Sisto T. The occurrence of the post-thrombotic changes after an acute deep venous thrombosis. A prospective two-year follow-up study. *J Cardiovasc Surg* n.d.;**41**(3):441–6.

10 Kahn SR, Comerota AJ, Cushman M, Evans NS, Ginsberg JS, Goldenberg NA, et al. The postthrombotic syndrome: Evidence-based prevention, diagnosis, and treatment strategies: A scientific statement from the American heart association. *Circulation* 2014;**130**(18):1636–61. Doi: 10.1161/CIR.0000000000000130.

11 Meissner MH, Gloviczki P, Comerota AJ, Dalsing MC, Eklof BG, Gillespie DL, et al. Early thrombus removal strategies for acute deep venous thrombosis: Clinical Practice Guidelines of the Society for Vascular Surgery and the American Venous Forum. *J Vasc Surg* 2012;**55**:1449–62. Doi: 10.1016/j.jvs.2011.12.081.

12 Foegh P, Jensen LP, Klitfod L, Broholm R, Bækgaard N. Editor's Choice – Factors Associated with Long-Term Outcome in 191 Patients with Ilio-Femoral DVT Treated With Catheter-Directed Thrombolysis. *Eur J Vasc Endovasc Surg* 2017;**53**(3):419–24. Doi: 10.1016/j.ejvs.2016.12.023.

13 Dharmarajah B, Sounderajah V, Rowland S, Leen E, Davies A. Aging techniques for deep vein thrombosis: a systematic review. *Phlebology* 2015;**30**(2):77–84. Doi: 10.1177/0268355514528691.

14 Hoang P, Wallace A, Sugi M, Fleck A, Pershad Y, Dahiya N, et al. Elastography techniques in the evaluation of deep vein thrombosis. *Cardiovasc Diagn Ther* 2017;**7**(Suppl 3):S238–45. Doi: 10.21037/cdt.2017.10.04.

15 Arnoldussen C, Strijkers R, Lambregts D, Lahaye M, de Graaf R, Wittens C. Feasibility of identifying deep vein thrombosis characteristics with contrast enhanced MR-Venography.

Phlebology 2014;**29**(1 suppl):119–24. Doi: 10.1177/0268355514529697.
16 Phinikaridou A, Andia ME, Saha P, Modarai B, Smith A, Botnar RM. In Vivo Magnetization Transfer and Diffusion-Weighted Magnetic Resonance Imaging Detects Thrombus Composition in a Mouse Model of Deep Vein Thrombosis 2013;**6**(3):433–40. Doi: 10.1161/CIRCIMAGING.112.000077.
17 Saha P, Andia ME, Modarai B, Blume U, Humphries J, Patel AS, et al. Magnetic resonance T1 relaxation time of venous thrombus is determined by iron processing and predicts susceptibility to lysis. *Circulation* 2013;**128**(7):729–36. Doi: 10.1161/CIRCULATIONAHA.113.001371.
18 Kumar V, Abbas A, Fausto N, Aster JC. Robbins and Cotran Pathologic Basis of Disease 8th edition. Philadelphia, PA; 2010.
19 Boron WF, Boulpaep EL. Medical physiology : a cellular and molecular approach. 2nd ed. Philadelphia, PA: Saunders/Elsevier; 2009.
20 Marieb EN. Human Anatomy & Physiology. San Francisco: Pearson Benjamin Cummings; 2007.
21 Silver FH, Snowhill PB, Foran DJ. Mechanical behavior of vessel wall: A comparative study of aorta, vena cava, and carotid artery. *Ann Biomed Eng* 2003;**31**(7):793–803. Doi: 10.1114/1.1581287.
22 McGilvray KC, Sarkar R, Nguyen K, Puttlitz CM. A biomechanical analysis of venous tissue in its normal and post-phlebitic conditions. *J Biomech* 2010;**43**(15):2941–7. Doi: 10.1016/j.jbiomech.2010.07.012.
23 Deatrick KB, Elfline M, Baker N, Luke CE, Susan B, Stabler C, et al. Post Thrombotic Vein Wall Remodeling. *J Vasc Surg* 2011;**53**(1):139–46. Doi: 10.1016/j.immuni.2010.12.017.Two-stage.
24 Wang X, Li G, Chen B, Pu Y, Nie P, Li X, et al. Numerical Simulation of Hemodynamics in Portal Vein With Thrombosis By Computational Fluid Dynamics. *J Mech Med Biol* 2014;**14**(06):1440006. Doi: 10.1142/S0219519414400065.

Adeline SCHWEIN

MISE AU POINT ET APPLICATIONS D'UN MODELE PORCIN DE THROMBOSE VEINEUSE PROFONDE

RESUME

Bien que la thrombose veineuse profonde (TVP) soit un problème de santé majeur, de nombreuses inconnues persistent quant à son histoire naturelle et sa prise en charge optimale.
Dans ce travail, nous avons développé un modèle endovasculaire mini-invasif de TVP iliocave aiguë et subaiguë, qui est efficace chez les animaux de 60 kg, sûr, reproductible et qui respecte l'intégrité du système vasculaire.
L'étude des résultats obtenus par imagerie multimodale devrait mettre l'accent sur l'utilisation de séquences d'imagerie par résonance magnétique spécifiques comme technique d'imagerie non invasive pour évaluer le contenu structurel de la TVP dans le but de guider une prise en charge optimale spécifique à chaque patient.
L'analyse des propriétés mécaniques de la veine thrombosée a montré que la TVP induisait une augmentation progressive de l'épaisseur et de la rigidité longitudinale de la paroi veineuse, même après résolution du thrombus. Ces données devraient permettre d'améliorer le développement de matériel endoveineux dédié à la prise en charge de la maladie veineuse occlusive.

Mots-clés : Modèle animal, thrombose veineuse profonde, imagerie par résonance magnétique, traitement endovasculaire.

ABSTRACT

Although deep venous thrombosis (DVT) is a major healthcare issue, many unknowns persist regarding its natural history and optimal management.
In this work, we developed a minimally invasive endovascular model of acute and subacute iliocaval DVT, which is effective in 60 kg animals, safe, reproducible and which respects the integrity of the vascular system.
The analysis of the results obtained by multimodal imaging should emphasize the use of specific magnetic resonance imaging sequences as a non-invasive imaging technique to assess the structural content of DVT with the aim of guiding an optimal management specific to each patient.
Analysis of the mechanical properties of the thrombosed vein showed that DVT induced a progressive increase in the thickness and longitudinal stiffness of the vein wall, even after resolution of the thrombus. These data should improve the development of endovenous material dedicated to the management of venous occlusive disease.

Key words: Animal model, deep venous thrombosis, magnetic resonance imaging, endovascular treatment.